Sheffield Hallam University

A Sheffield Hallam University thesis

12011 12010
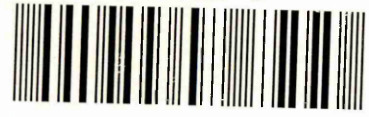
ProQuest Number: 10700919

ProQuest 10700919

DIGITAL ANISOCHRONOUS

PULSE TIME MODULATION TECHNIQUES

by

Ralph U. Reyher

A thesis submitted to the

Sheffield Hallam University

for the degree of

MASTER OF PHILOSOPHY

School of Engineering Information Technology

Sheffield Hallam University

Electronics and Communication Engineering Research Group

4 December 1995

ABSTRACT

Digital anisochronous pulse time modulation (PTM) techniques are alternative schemes for transmission of signals over optical fibre communication links. Modulation is simple and low cost and has the ability to trade performance with bandwidth overhead. Pulse interval width code modulation (PIWCM) and pulse interval code modulation (PICM) belong to the category of schemes where the former offers built in frame synchronisation capability and the latter offers improved receiver sensitivity.

This thesis is concerned with analysis, design, simulation and physical implementation of PIWCM and PICM for a single channel system. Original mathematical expressions are given for code characteristics, transmission capacity and power spectral density for both schemes, which explain the the anisochronous nature of the code formats. A simulation model based upon Matlab has been developed for both schemes to assist the development of the implementation process. Analytical and simulated results are presented along with the evaluation of error sources and their impact upon the system performance.

The PIWCM and PICM modulators/demodulators are formulated around analogue-to-digital converters and purpose designed Moore state machines, in order to generate the code formats and timing information needed to synchronise transmitter and receiver modules. Depending on source connection, the system is capable of transmitting PCM coded parallel binary information or directly sampled analogue message signals.

A complete system operating at 1 Mb/s has been designed, constructed and analysed. The results obtained are in close agreement with predicted and simulated data, indicating the potential of such schemes for wide-band transmission.

ACKNOWLEDGEMENTS

GLOSSARY OF ABBREVIATIONS

Abbreviation	Description
APD	Avalanche photo diode
APWM	Analogue pulse width modulation
ATM	Asynchronous transfer mode
DPPM	Digital pulse position modulation
DPWM	Digital pulse width modulation
EDI	Electronic data interchange
FDM	Frequency division multiplexing
FM	Frequency modulation
HDTV	High definition television
ISDN	Integrated services digital network
LAN	Local area network
LED	Light emitting diode
NRZ	Nonreturn-to-zero
PCM	Pulse code modulation
PFM	Pulse frequency modulation
PICM	Digital pulse interval modulation
PIM	Pulse interval modulation
PIN	P-N photodiode
PIWCM	Digital pulse interval width modulation
PIWM	Pulse interval width modulation
PPM	Pulse position modulation
PTM	Pulse time modulation
PWM	Pulse width modulation
SWFM	Square wave frequency modulation

TDM	Time division multiplexing
VCO	Voltage controlled oscillator
WDM	Wavelength division multiplexing

GLOSSARY OF SYMBOLS

Symbol	Definition
β_0	shift of sampling frequency
δ_1, δ_2, δ_b	sidetones in frequency spectrum
δ_a	random time delay
$\kappa_{g(t)}$	constant depending on the pulse shape
τ	pulse width
ν	time constant
ω_c, f_c	clock frequency
ω_m, f_m	modulating frequency
a, b, c, i	variables
A	amplitude, magnitude
B, B_N, B_U	bandwidth occupancy, N-naturally sampled, U-uniformly sampled
C	capacity of transmission channel
C/N, C/N_N, C/N_U	carrier-to-noise ratio, N-naturally sampled, U-uniformly sampled
D	duty cycle
f	fibre bandwidth
$F(t)$	frequency spectrum
f_g	guard band
f_s	sampling frequency
$g'(t)$	slope of rising pulse edge
$G(f)$	pulse shape transform
$g(t)$	pulse shape
$J_0(x)$, $J_a(x)$, $J_b(x)$	Bessel function
k	length of high or low-word

L	frame length
L_{avg}	average frame length
L_{max}	maximum frame length
L_{min}	minimum frame length
m	mark
M	modulation index
n	number of quantisation levels
N	length of truncated sequence
p	bit-resolution
Q	error function
r	Nyquist rate
R	transmission rate
s	space
S/N, S/N_N, S/N_U	signal-to-noise ratio, N-naturally sampled, U-uniformly sampled
$S(t)$	power spectral density
T	sampling period
t_0	maximum pulse width change or peak-to-peak deviation
t_a	stochastic pulse position
T_n	frame duration
t_r	rise time
T_s	time slot duration
W	channel bandwidth
X	decimal equivalent value
$x(t)$	pulse train
$X_T(f)$	Fourier transform of truncated pulse train $x(t)$

TABLE OF CONTENTS

viii

LIST OF TABLES

LIST OF FIGURES

CHAPTER 1

INTRODUCTION

1. INTRODUCTION

Currently, communication authorities provide a number of voice and data services (telephone, facsimile, teletex, etc.) over various public or private networks. These networks are specialised to provide one type of service only, and have therefore different transmission rates and characteristics. Some of the data services are provided in two or more networks, but the terminal equipment is not the same, nor is the modulation or coding of data. Internetworking can only be achieved using specialised gateway exchanges that convert from one form of transmission to the other [1].

The need to provide higher speed data rates results from the ever increasing processing power, storage capacity and transfer rate capability of modern data processing equipment. New communication services such as electronic data interchange (EDI), on-line airline travel and reservations, etc. are already integrated in private networks and will soon be available for a wide range of users. In the future, users will be faced with the interconnection of telecommunication networks and data networks through ISDN. The ultimate target for network operators is the integration of digital broadband services into the public networks. To fulfil this objective, much work has been done in defining new protocols such as asynchronous transfer mode (ATM) to capitalise on broadband-ISDN [2].

Market factors point towards an increase in telecommunication needs for both video and data as well as other novel applications. Services which are rapidly gaining importance are the multimedia services which include the basic components of the future broadband service: voice, data, video. However, such services require substantially more bandwidth capability in the access network than the existing copper pairs can provide. Consequently,

telecom operators are replacing large parts of their access networks at present with optical fibre, thus reducing the network operating costs and improving the quality of services to the end user [3]. Furthermore, the network operators need the services of other telecom operators or long distance carriers to support the growing number of interactive services beyond the boundaries of their cable franchise territory.

Originally, voice was carried as analogue information but, with the advent of digital transmission media, voice is now more often digitised — the analogue voice signal is sampled 8000 times per second and digitised with 8-bits, thus giving a data rate of 64 kb/s. The advantages of digital modulation techniques, in particular pulse code modulation (PCM) have been well defined. The most important advantages of digital transmission are its good signal-to-noise performance and system linearity which, to a great extent, is independent of transmission channel quality. Video signals have generally been carried in analogue form over wireless or cable TV systems, requiring only a few mega Hertz of bandwidth. However, when digitised the bandwidth requirement of an uncompressed video signal increases to 270 Mb/s [4]. To avoid the bandwidth overhead, video compression techniques are used to bring down the data rate to 3 Mb/s [4]. Data files such as computer files, graphic files or other application program data files, are usually transferred through purpose designed local area networks (LANs) at rates of between 10 Mb/s and 156 Mb/s [4].

At the physical level modulation techniques are employed to convey the original signal. The modulation formats fully utilise the given practical channel characteristics and provide relevant performance to a specific end user or network operator. Here, two digital modulation techniques will be investigated for transmission of voice or data over an electrical or optical link.

2

1.1. Objectives and Plan of Text

In this study the digital transmission of a single voice or data channel is presented. Theoretical characterisation and practical evaluation of the effectiveness of the digital pulse interval width code modulation (PIWCM) and digital pulse interval code modulation (PICM) system are described, along with the design and development of the system.

PICM and PIWCM are closely related to each other and can be easily transformed from one form to the other. They exhibit different characteristics and are therefore intended for different applications. The main advantage of PICM is its narrow pulse width, providing a high peak optical power level and low average optical power, ideal for optical sources. The use of PICM is intended for fibre-based long-haul transmission links. On the other hand, PIWCM has higher average power, but its average bandwidth occupancy is much lower than PICM. It is also self synchronised, since each frame is initiated with a rising edge, unlike PICM where frame synchronisation is essential. PICM and PIWCM code properties with their associated system requirements are examined and the system performances are compared with existing digital modulation methods. Software simulation of both modulation techniques was also carried out. A practical system, operating at a data rate of 1 Mb/s was designed, constructed and tested.

Digital modulation under the constraints of disturbances in the optical channel are the subject of Chapter 2. The characterisation and performance of existing continuous and discrete pulse time modulation techniques may be assessed in terms of spectral analysis and signal-to-noise performance. Furthermore, principal methods of modulation and demodulation of these techniques are explained with their advantages and disadvantages in Chapter 3.

Chapter 4 describes the code properties of PIWCM and PICM, together with mathematical models which are used to represent the codes in the time as well as in the frequency domain. Furthermore, error sources inherent to these modulation techniques are also given.

Chapter 5 looks at the system design which is based on conventional analogue-to-digital data conversion techniques and a synchronous modulator and demodulator. Either the PIWCM or PICM outputs can be transmitted via the optical or electrical link. By employing synchronous circuit design through state machines — implemented in programmable macro logic (PML) devices — the resulting process of modulation and demodulation could be kept compact.

A comprehensive software simulation package for the whole system has been developed in order to predict the system performance; it is described in Chapter 6. Finally, theoretical and practical results are given in Chapter 7 and conclusions are drawn in Chapters 8 and 9.

1.2. Published Papers

1) U. SCHILLER, R.U. REYHER, Z. GHASSEMLOOY, A.J. SIMMONDS and J.M. HOLDING: 'Modelling of baseband data transmission system in hardware and software', *IEEE Transactions on Education*, submitted: July 1993, reviewed: Feb. 1994, scheduled for publication: autumn 1996.

2) R.U. REYHER, U. SCHILLER and Z. GHASSEMLOOY: 'Modelling of baseband data transmission system in hardware and software', *Matlab User Group Meeting: 1994 Annual Meeting, 12. October 1994*, Hilton International Hotel Milton Keynes.

4

3) Z. GHASSEMLOOY, E.D. KALUARACHCHI, R.U. REYHER and A.J. SIMMONDS: 'A new modulation technique based on digital pulse interval modulation (DPIM) for optical-fiber communication', *Microwave and Optical Technology Letters*, Vol. 10, No. 1, Sep. 1995, pp. 1-4.

4) Z. GHASSEMLOOY, R.U. REYHER, A.J. SIMMONDS and E.D KALUARACHCHI: 'Digital pulse interval width modulation', *Microwave and Electronic Letters*, submitted: August 1995, accepted for publication: Vol. 11, No. 4, March 1996.

5) Z. GHASSEMLOOY, R.U. REYHER, A.J. SIMMONDS and R. SAATCHI: 'A novel digital modulation system using pulse interval code modulation (PICM) and pulse interval width code modulation (PIWCM)', *3rd International Symposium on Communication Theory and Applications*: 10-14 July 1995 Charlotte Mason College Lake District UK, pp 403-404.

6) R. U. REYHER, Z. GHASSEMLOOY, A.J. SIMMONDS and E.D. KALUARACHCHI: 'Digital pulse interval width code modulation (PIWCM) for optical fibre communication', *SPIE Photonics East: 1st International Symposium on Photonics Technologies and Systems for Voice, Video and Data Communications*, 23-26 Oct 1995 Pennsylvania Convention Center, Philadelphia USA, SPIE 2641-08.

CHAPTER 2

TRANSMISSION AND MODULATION

2. TRANSMISSION AND MODULATION

Communications refers to the electronic transmission of any type of information. The information may be encoded and then modulated before it is transmitted over the transmission channel, which may be a coaxial cable, a microwave link or an optical fibre cable. The primary factors to be considered when selecting a particular modulation technique are transmission bandwidth, signal-to-noise performance, bit-error rate, cost and complexity.

```
                          ┌─────────────┐
                          │  Modulation │
                          └─────────────┘
              ┌──────────────────┼──────────────────┐
       ┌────────────┐    ┌────────────────┐    ┌────────────┐
       │  Analogue  │    │ Pulse Analogue │    │   Digital  │
       └────────────┘    └────────────────┘    └────────────┘
          ├ AM             ├ Pulse Time            ├ PCM
          ├ FM             │    ├ Isochronous       └ Pulse Time
          └ PM             │    │    ├ PPM                ├ DPPM
                           │    │    └ PWM                ├ PICM
                           │    └ Anisochronous           └ PIWCM
                           │         ├ PIM
                           │         ├ PIWM
                           │         └ PFM, SWFM
                           └ Pulse Shape
                                ├ PAM
                                └ PSM
```
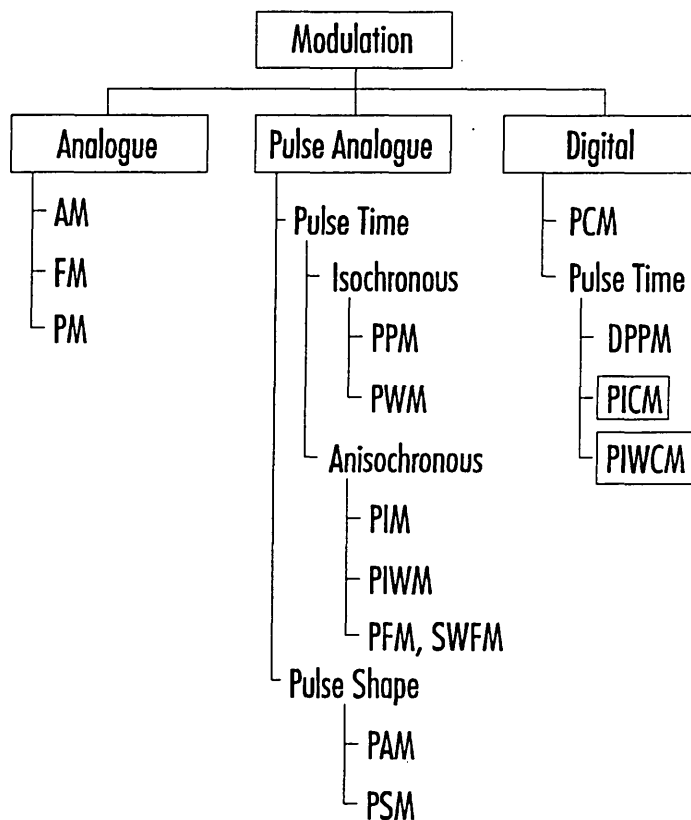
Figure 2.1 Modulation tree.

Figure 2.1 illustrates a modulation tree. The advantages and disadvantages of some of the wide range of modulation techniques will be discussed in the following sections.

2.1. Binary Transmission Channel

For a type of channel over which communication is desired, physical limitations determine the principal factors that affect the transmission of the message signal. These factors refer to sampling, channel capacity, signal power and noise distortion and consequently the bit-error rate [5].

The main objective when transmitting information over any communication channel is reliability, which is measured by the probability of errors in the recovered information. Fundamentally, reliable transmission is possible even over noisy channels as long as the transmission rate R is less than or equal to a maximum data rate, called the channel capacity C. This remarkable result, first shown by C.E. Shannon (1948), is known as the 'noisy channel coding theorem' which states that 'the basic limitation that noise causes in a communication channel is not on the reliability of communication but on the speed of communication'.

The capacity of an additive white Gaussian noise channel is given by Shannon's [6] formula as:

$$C = W \log_2 (1 + S/N) \tag{2.1}$$

where W is the channel bandwidth and S/N is the signal-to-noise ratio. There exists a trade-off between W and S in the sense that one can compensate for the other. Increasing the input signal power obviously increases the channel capacity C. However, the increase in C as a function of S is logarithmic and slow. Increasing W has two contrasting effects: on one hand, with a higher value of W one can transmit more samples per second and therefore increase the transmission rate R; on the other hand, a higher channel bandwidth means higher input noise to the receiver and this degrades the system performance. In all

7

practical systems one must have a transmission rate $R < C$ in order to achieve fewer errors during transmission in the presence of noise.

The minimum message rate r is equal to the Nyquist sampling rate $r = 2f_m$ and the information rate R can be measured in terms of bandwidth of the message signal f_m and independent levels n:

$$R = 2f_m \log_2 n \tag{2.2}$$

2.2. Optical Fibre Communications

Optical fibre communications is a transmission system employing a light source, turned on and off very rapidly by electrical pulses, whose emissions are sent through an optical fibre to a light sensitive receiver in order to convert the changing light intensity back into electrical pulses. While electrical transmission has limited application for high data rates as it suffers from attenuation and electromagnetic interference, optical transmission has advantages in high data rate and long-haul transmission, as it decreases the number of cables and reduces the number of repeaters needed for transmission. Optical fibres also offer increased security of communication due to very low fibre-to-fibre cross talk. Furthermore, optical fibres have smaller dimensions and are cheaper to produce, since the primary material of optical fibres is sand [7].

Although the intrinsic transmission capacity of optical fibres has been seen as virtually unlimited, with the increase of bit rates and progress in electronic circuits and optoelectronic components the span of ultra-high bit rates is now limited by fibre properties: dispersion and attenuation of standard optical fibres in terrestrial networks, optical fibre non-linearity especially for transoceanic transmission, optical noise or

8

bandwidth in optical amplifiers [3].

Dispersion limits the maximum rate at which information can be transmitted through a form of signal degradation that causes light pulses to spread in time. The relationship between bandwidth and dispersion is determined by the characteristics of the optical fibre cable. This relation depends principally on the numerical aperture (ability of the cable to collect light), the core diameter and the wavelength. Multimode fibre cores have the ability to gather more power but induce more reflections that reduce the data rate — single mode fibres have a lower efficiency of collecting light by small numerical aperture and smaller core but allow higher data rates due to fewer reflections in the core and little material dispersion.

The attenuation limitation of a point-to-point optical transmission system is determined by the available output power of the transmitter, the attenuation of the fibre and the receiver sensitivity. In order to achieve the maximum transmission span, most optical fibres operate at a wavelength of either 1300 nm (typically 0.35 dB/km) or 1550 nm (typically 0.2 dB/km) where single mode fibres have lowest loss at these wavelengths [8]. In practical systems, splice and connector losses lead to further power losses.

Considerable improvement in S/N performance can be obtained by fully exploiting the wide bandwidth of fibres [9], thus allowing much narrower pulses to be transmitted [10]. However, when reducing the pulse width, the choice of optical sources will be limited to devices that can provide more concentrated light beams, ie. lasers [11]. Optical sources and fibres limit the quality of the received pulses in that the received pulse may be time spread or light coloured (a pulse of light that includes many wavelengths) or both. The optical power emitted from a laser diode or a light emitting diode (LED) contains a range

9

of wavelengths (the wavelength range emitted by an LED is much greater than for a laser diode). These various colours travel at different speeds when propagating through a fibre. Consequently, a range of wavelengths will therefore produce pulses arriving over a range of times. The receivers performance depends on the optical detector. Higher sensitivities can be produced with avalanche photo diodes (APDs) in comparison to PIN diodes.

Current intercity optical trunk links, installed in the mid-eighties, operate at data rates of 140 Mb/s [3] and are being upgraded to provide data rates of 2.5 Gb/s [12]. The first transoceanic optical system installed in 1988 was capable of transmitting data at a rate of 280 Mb/s. By using erbium doped amplifiers, the fibre optic span is increased dramatically. The new generation transoceanic 'first erbium doped amplified' fibre system appearing in 1995 will provide a high speed data link of 5 Gb/s [3]. Recent results have shown that total bit rates of up to 340 Gb/s can be successfully transmitted over a distance of 150 km by sharing seventeen wavelength division multiplexing (WDM) channels at 20 Gb/s [13]. One single channel could therefore accommodate a minimum of 1000 high definition TV (HDTV) channels at a bit rate of 20 Mb/s each [14].

2.3. Digital Modulation

Digital signal transmission is popular and is becoming even more popular due to the low cost of digital circuits. They are less subject to distortion and interference than analogue circuits. With their binary nature, digital waveforms are ideal for transmission over noisy channels or environments. However, digital transmission requires synchronisation in which the receiver must know the timing of each discrete instance with relevant accuracy and must be able to determine the signal state under noisy conditions correctly. The combination of digital signals using time division multiplexing (TDM) results in multichannel transmission over one line, thus utilising the channel bandwidth more

efficiently. The performance of a digital system is often a trade-off between bandwidth occupancy and complexity.

2.3.1. Pulse code modulation

In pulse code modulation (PCM) the analogue input signal is sampled, quantised and encoded in groups of pulses of a fixed frame length. For optical fibre systems, the pulse streams are used to intensity modulate an optical source [15, 16]. At the receiver, the optical pulse groups are converted back into electrical signals, amplified, filtered and then further processed by the demodulator. This results in a train of individual amplitude modulated pulses. After passing the pulse train through a low-pass filter, the original analogue signal is recovered, as illustrated in Figure 2.2.
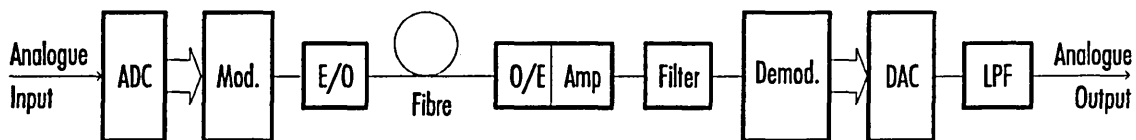
Figure 2.2 Block diagram of an optical PCM transmission system.

The analogue signal to be transmitted is sampled and quantised to the nearest of n quantisation levels; then each quantised sample is modulated into a $p = \log_2 n$ long pulse group. The difference between the analogue signal and the quantised signal levels — the uncertainty — is largely dependent on the resolution $n = 2^p$ or on the number of quantisation levels (uniform spacing). With a non-uniform spacing, quantisation noise can be made to be dependent on the signal size by providing fine quantisation of the weak signals and coarse quantisation of the strong signals. The effect is to improve the overall signal-to-noise ratio by reducing the noise for the predominant weak signals, at expense of the rarely occurring strong signals. With a greater number of levels, quantisation noise will be reduced, but at the cost of increased bandwidth.

11

The output signal-to-noise ratio of unipolar PCM with uniform quantisation can be expressed [17] as:

$$S/N = \frac{2^{2p}-1}{1 + 4(2^{2p}-1)P_e}$$

(2.3)

where p is the number of codeword bits and P_e is the error rate as:

$$P_e = Q\left(\sqrt{C/(2N)}\right)$$

(2.4)

Q is an error function of the carrier-to-noise ratio C/N at the input of the PCM demodulator. Where:

$$Q(x) = \frac{1}{\sqrt{2\pi}} \int_x^{\infty} \exp\left(-\frac{x^2}{2}\right) dz$$

(2.5)
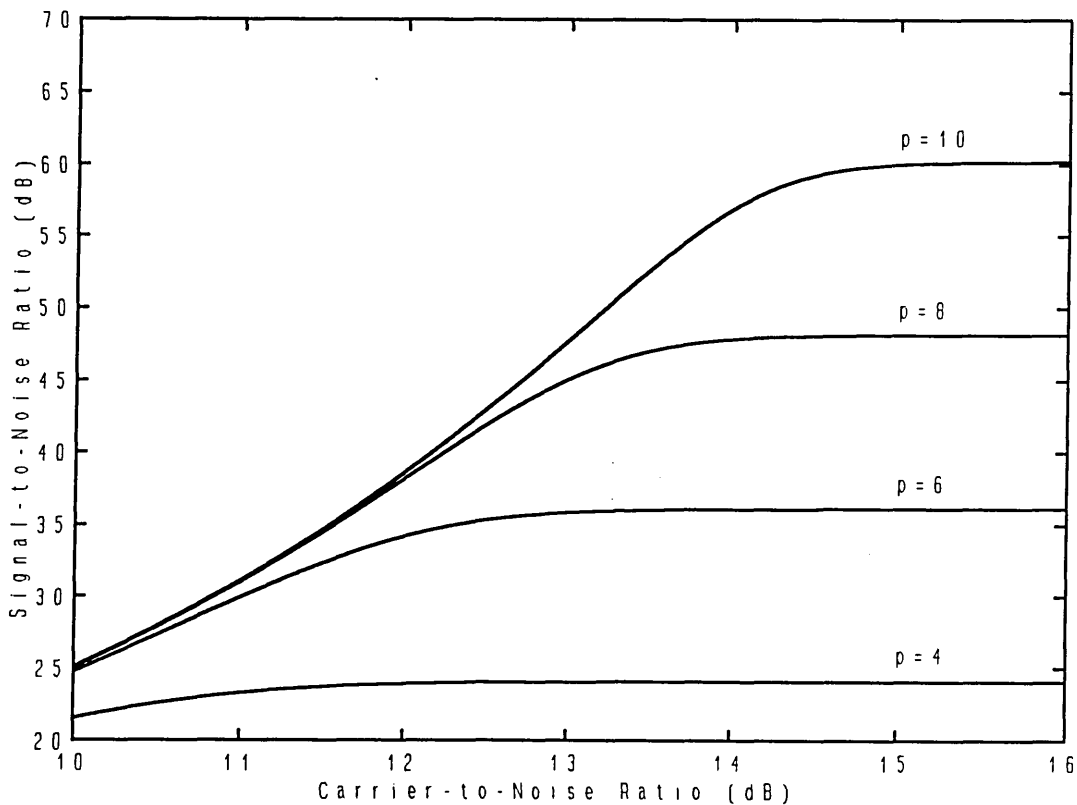
Figure 2.3 Performance of PCM in the presence of noise.

The performance of a PCM system as used for transmitting analogue signals is measured in terms of peak signal-to-noise ratio power at the receiver output. Carrier-to-noise ratio at the receiver input versus the signal-to-noise ratio at the demodulator output is plotted in Figure 2.3. This clearly shows that a PCM system exhibits a threshold effect beyond which S/N deteriorates rapidly. Above the threshold level, the dominant noise source is quantisation noise.

Figure 2.4.a. illustrates a nonreturn-to-zero (NRZ) PCM data with its spectral components shown in Figure 2.4.b. As can be seen from Figure 2.4.b, most of the signal energy is concentrated below $1/T_s$, thus the channel bandwidth required is equal to the bit-rate. The main limitations of NRZ signals are the presence of the dc component and the lack of synchronisation capability [18].
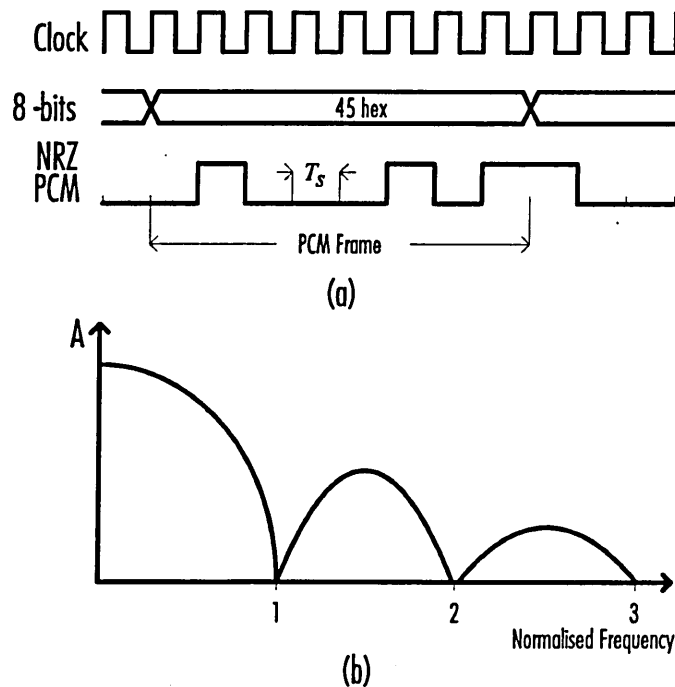
Figure 2.4 Example of an 8-bit NRZ PCM (a) waveform; (b) frequency spectrum.

2.3.2. Digital modulation in optical fibre communications

Currently, voice, data and video services are offered to customers through different network architectures [4]. In future these services will be provided to the end user by one single optical network [19]. A critical factor which will ensure reliable transmission of such diverse services is the S/N and error rate performance.

The error performance of a classical PCM system depends only on the signal-to-noise ratio, whereas in optical systems the equivalent signal-to-noise ratio will be a function of the pulse width. Using short optical pulses suits the optical source, since it has essentially a longer time period to prepare for the following pulse and, furthermore, it has been shown that the error probability decreases for pulses with fixed energy as the pulse width reduces [20]. The traditional approach of increasing the optical launch power in order to compensate for limited receiver sensitivity may be overcome by adapting alternative modulation formats to PCM. An increase of receiver sensitivity and increase of repeater spacing may be achieved by converting PCM into digital pulse position modulation (DPPM) before transmission [21-23], [57-70].

In DPPM the receiver sensitivity improves with increasing $n = 2^P$ because more bits are being conveyed by a single pulse. The improvement continues until the rise time of the pulse is comparable to the time slot duration. For this reason the optimum receiver sensitivity increases with the fibre bandwidth. Garrett [22, 23] has shown that digital PPM can offer a 10-12 dB improvement of receiver sensitivity over PCM. This represents an increase of regenerator spacing of 50-60 km [21]. If digital PPM is to be used in telecommunication links, it is essential that the slot rate is increased. The ultimate improvement offered by DPPM, however, depends on the optical source mean-to-peak power ratio — since the mean power of an optical PPM system must not exceed the mean

14

power of a PCM system — and the pulse width must not become smaller than the pulse rise time in the optical channel. A comprehensive description of DPPM is given in Section 3.3.1.

2.4. Summary

Practical reasons for modulation come from the necessity of preparing a message for transmission over a communications channel. Present trends in communications favour optical transmission systems due to the high information transfer rates and immunity to external disturbances. Optical links become more transparent through optical technology all along the transmission path. Future prospects indicate an all-optical communications network by the year 2005 [24]. PCM and PCM -related coding techniques represent a major contribution in digital communications but they have efficiency problems in optical communications. Alternative modulation techniques such as DPPM seek to capitalise upon the strengths of optical transmission.

CHAPTER 3

PULSE TIME MODULATION

3. PULSE TIME MODULATION

Pulse time modulation (PTM) [25] occupies an intermediate position between purely analogue and digital techniques, enabling beneficial trade-offs between fidelity and cost for specific applications. Modulation is simple, requiring no digital coding, while the pulse format of the modulated carrier renders the scheme largely immune to the channel non-linearity. Moreover, PTM is unique in its ability to trade signal-to-noise performance for bandwidth which is a particular exploitable feature in optical fibre systems. It is of particular interest where short pulses, such as solitons, may be employed which can yield further improvement in signal-to-noise ratio and bit-error-rate over PCM systems [26].

3.1. Continuous Pulse Time Modulation

Continuous PTM techniques represent an alternative approach to digital modulation and have been proposed for the economic short haul point-to-point distribution of video [27, 28], audio, data, or control and instrumentation signals over optical fibre [29, 30]. All PTM methods use a constant amplitude binary pulse carrier, where a range of time dependent features is used to convey the information [31, 32] as shown in Table 3.1.

PTM Type	Variable	Category
PPM	Position	Isochronous
PWM	Width (duration)	Isochronous
PIM	Interval (space)	Anisochronous
PIWM	Interval and width	Anisochronous
PFM	Frequency	Anisochronous
SWFM	Frequency	Anisochronous

Table 3.1 Continuous PTM schemes.

16

PTM may be classified in two categories: isochronous and anisochronous. Depending on the sampling nature. In the isochronous category the sampling takes place within a fixed time-frame, as shown in Figure 3.1.
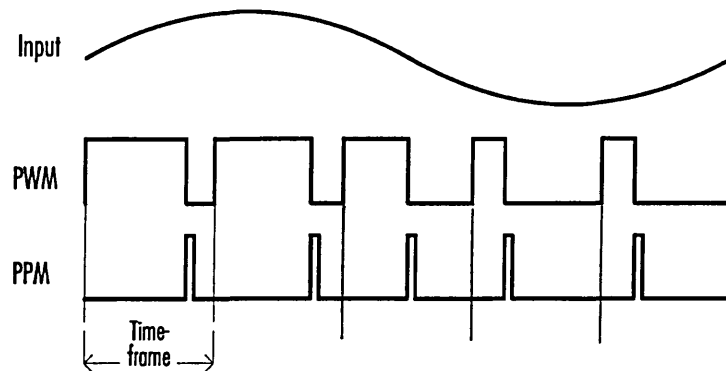
Figure 3.1 Isochronous PTM techniques.

In anisochronous systems each successive time frame commences immediately after the preceding pulse, thus resulting in a variable frame, shown in Figure 3.2.
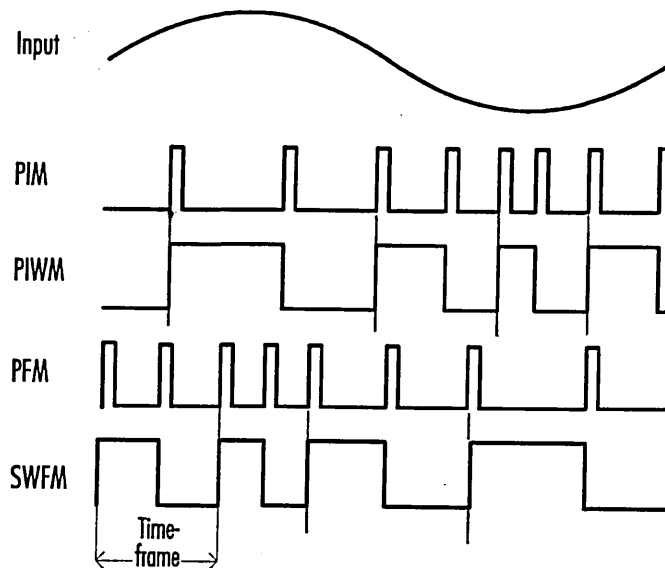
Figure 3.2 Anisochronous PTM techniques.

All PTM techniques produce modulation spectra that share a common set of features. In each case, modulation gives rise to diminishing sets of sidetones centred around the carrier

(sampling) frequency and its harmonics. Sidetones are separated in frequency by an amount equal to the modulating frequency [25], as illustrated in Figure 3.3. The sidetone profile is characteristic and unique to each PTM technique. In addition, a baseband component is also present for some PTM methods along with its harmonics depending upon the form of sampling employed in the modulator.
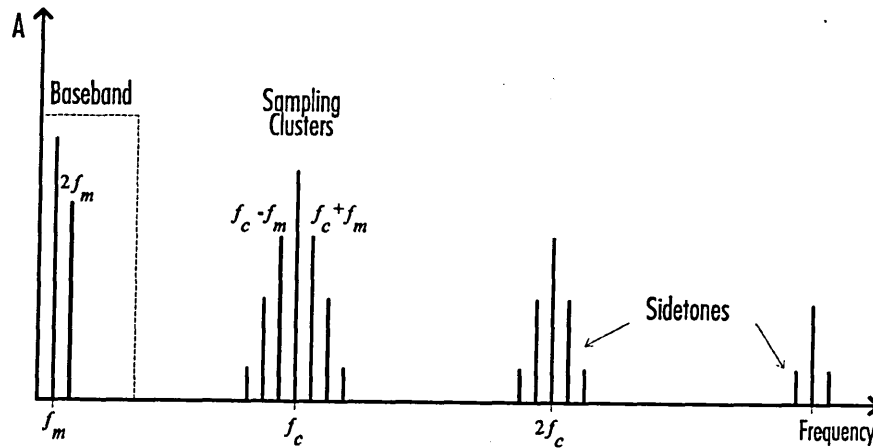
Figure 3.3 Typical PTM frequency spectrum.

Either natural or uniform sampling of the modulating signal may be adopted for PTM. The choice between natural sampling and uniform sampling is essentially a performance-cost trade-off. Naturally sampled modulators operate on the principle of direct comparison of modulating signal and sampling instances. Uniformly sampled modulators route the modulating signal through a sample and hold circuit and then compare the flat-topped amplitude modulated pulses with constant amplitude and frequency carrier signals. Uniformly sampled PTM schemes allow the transmitter to operate at much higher modulation indices than natural sampling, resulting in a greater modulating power to be transmitted and hence a better signal-to-noise performance.

In all PTM techniques noise affects the leading/trailing or both edges of the received pulses and manifests itself as timing jitter (dt, see Figure 3.4) in the regenerated pulse train, and

18
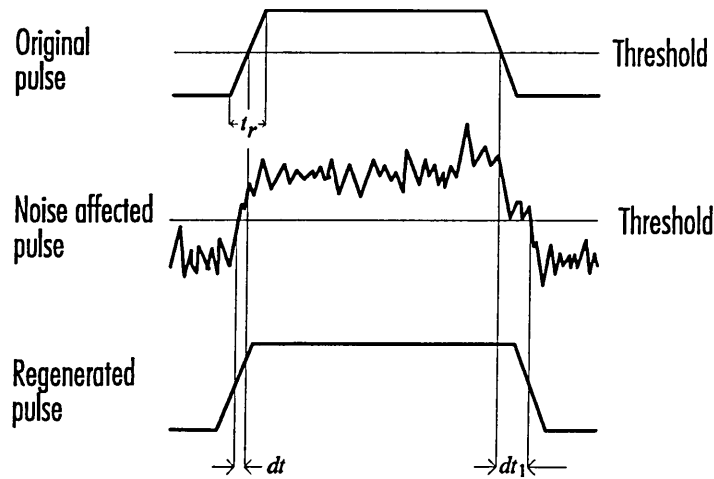
Figure 3.4 Noise contribution to PTM pulses.

hence as amplitude noise at the output of the demodulator. The slope of the received PTM pulse determines the period in which noise is able to influence the decoding [17, 33] and therefore the quality of the recovered signal. This phenomenon results in the demodulated S/N being [34]:

$$S/N \propto \left(\frac{W}{f_c}\right)^2 C/N \qquad (3.1)$$

This is a very useful characteristic of all PTM techniques, enabling them to trade-off channel bandwidth against signal-to-noise ratio.

3.1.1. Pulse width modulation

In pulse width modulation (PWM) [29], the width (or duration) of the pulsed carrier is changed according to the sample value of the modulating signal. Single edge modulated PWM may be generated by comparison of the modulating signal with a constant amplitude linear ramp waveform. The frequency of the ramp signal must be constant and equal to or greater than twice the modulating signal, see Figure 3.5.a. Double-edge modulated

19

PWM may be generated with a triangular waveform instead of a ramp. For a naturally sampled waveform this comparison is directly carried out at the comparator, whereas in uniformly sampled PWM the dc shifted input signal is routed first through a sample and hold circuit where samples are equally spaced in time irrespective of the input signal amplitude as shown in Figure 3.5.b. Single edge modulated PWM is self synchronised since the carrier (or clock) information is carried in the leading or trailing edge, unlike double edge modulated PWM where both edges are modulated by the input signal.
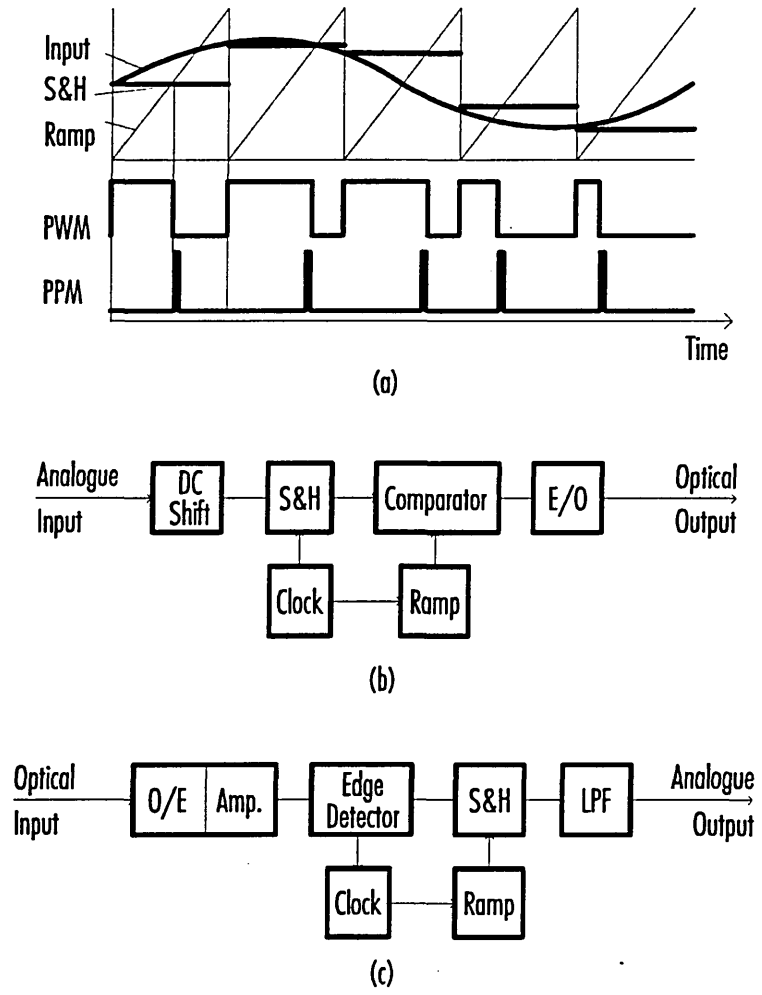
Figure 3.5 Uniformly sampled PWM: (a) modulator; (b) demodulator.

The spectrum of naturally sampled PWM shows an isolated baseband component at the frequency of the modulated signal f_m and rapidly diminishing series of sidetones spaced

on either side of the sampling frequency f_c and its harmonics. Additional harmonic components in the baseband are encountered in uniformly sampled PWM [35, 36]. A comprehensive treatment of the Fourier structure applicable to PWM has been given by Black [37] and Stuart [38]. The trailing edge modulated naturally sampled PWM pulse train may be expressed as [25]:

$$F(t) = \frac{1}{2} - \frac{M}{2}\sin(\omega_m t) + \sum_{a=1}^{\infty} \frac{\sin(a\omega_c t)}{a\pi} - \sum_{a=1}^{\infty} \frac{J_0(a\pi M)}{a\pi} \sin(a\omega_c t - a\pi)$$

$$- \sum_{a=1}^{\infty} \sum_{b=\pm 1}^{\pm\infty} \frac{J_b(a\pi M)}{a\pi} \sin(a\omega_c t + b\omega_m t - a\pi)$$

(3.2)

The modulating wave is $M\sin(\omega_m t)$, M is the modulation index $(0 < M < 1)$ and ω_m and ω_c are the modulating and carrier frequency respectively. $J_b(x)$ is the Bessel function of the first kind of order b. The combination of the third and fourth term from Eq. (3.2) creates the components around the carrier frequency and its harmonics. Term five represents the series of diminishing sidetones around the carrier and its harmonic
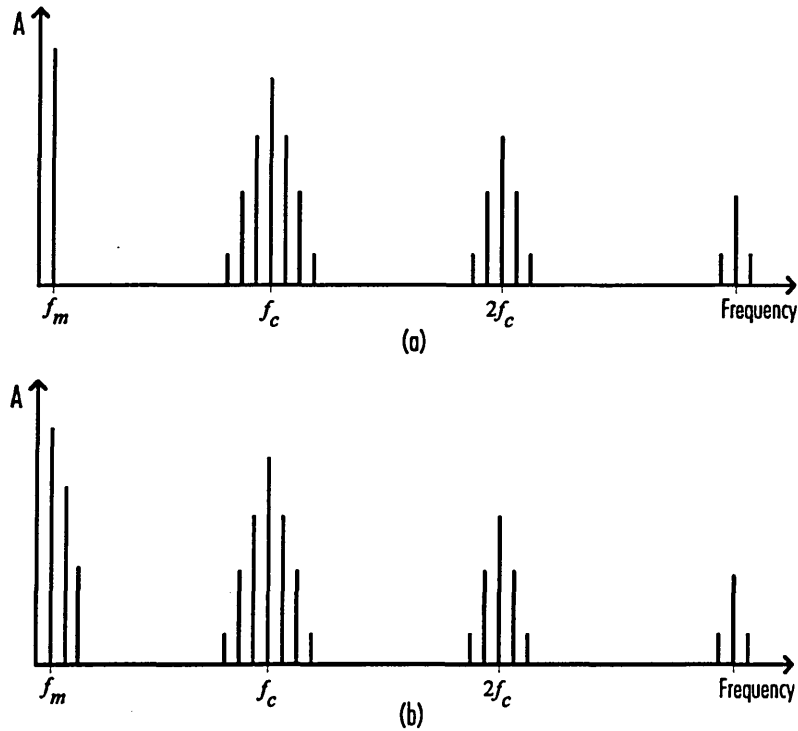
Figure 3.6 Power spectral density: (a) naturally sampled; (b) uniformly sampled PWM.

components, characteristic of PTM. When uniform sampling is employed, the resulting PWM spectrum is very similar to naturally sampled PWM [37], except that the baseband region also shows harmonics of the modulating frequency. The principal spectra for naturally sampled and uniformly sampled PWM are displayed in Figure 3.6.

At the receiving end, demodulation of naturally sampled PWM is accomplished by threshold detection and simple low-pass filtering to recover the baseband component directly. When transmitting uniformly sampled PWM, the baseband component and its harmonics require conversion into pulse amplitude modulation before low-pass filtering, see Figure 3.5.c. Because of the reconstruction process , uniformly sampled PWM can operate at higher modulation indices than naturally sampled PWM and it also gives lower harmonic distortion.

In analogue PWM the ramp linearity is usually found to limit the modulation index. Matching of both modulator and demodulator ramp profiles is desirable for lowest harmonic distortion at the system output. As a result of this, analogue PWM may be best operated with a modulation index lower than 50%. Digitally generated PWM will inherently improve the system linearity by allowing an increase of the modulation index to as high as 90%, but at an increased circuit complexity and cost [39]. For analogue PWM the modulation index is given by:

$$M = 2\frac{t_0}{T}100 \quad \% \tag{3.3}$$

where t_0 is the maximum pulse width change. The unmodulated pulse width is assumed to be $T/2$, i.e. a square wave. $T = 1/f_c$ and f_c is the carrier frequency. For the short distance fibre link, the channel bandwidth B_N required for naturally sampled PWM can be expressed as:

$$B_N = f_m \tag{3.4}$$

and the bandwidth B_U for uniformly sampled PWM is:

$$B_U = f_m (\pi M + 3) + 2f_g \tag{3.5}$$

where f_m is the baseband signal and f_g is the guardband (f_g is often equal to f_m).

The signal-to-noise ratio for naturally sampled PWM is given by [29]:

$$(S/N)_N = \left(\frac{M}{2}\right)^2 C/N \tag{3.6}$$

and the signal-to-noise ratio for uniformly sampled PWM is given by:

$$(S/N)_U = \frac{1}{2} \left(\frac{M \pi B_U}{2f_c}\right)^2 C/N \tag{3.7}$$

Equations (3.6) and (3.7) show that S/N of naturally sampled PWM is solely dependent upon the modulation index, whereas uniformly sampled PWM takes the bandwidth expansion as well as the sampling frequency f_c into account. For both cases of PWM the signal-to-noise ratio is proportional to M^2 [40]. For the same C/N, the enhancement for uniformly sampled PWM over naturally sampled PWM is as follows:

$$(S/N)_U = \frac{1}{2} \left(\frac{\pi B_U}{f_c}\right)^2 (S/N)_N \tag{3.8}$$

3.1.2. Pulse position modulation

Pulse position modulation (PPM) [41, 42] may be considered as differentiated PWM which carries information by virtue of the position of a narrow pulse within a given fixed time frame. The narrow pulse represents a power saving element that results in improved receiver sensitivity in optical communication systems [43]. This power saving represents

23

the fundamental advantage of PPM over PWM. PPM is generated by differentiating and rectifying the PWM waveform, see Figure 3.5.a. and Figure 3.7.a.

Analogue Input → DC Shift → S&H → Comparator →(PWM)→ d/dt →(PPM)→ E/O → Optical Output

Clock → Ramp

(a)

Optical Input → O/E | Amp. →(PPM)→ PPM to PWM →(PWM)→ LPF → Analogue Output

(b)
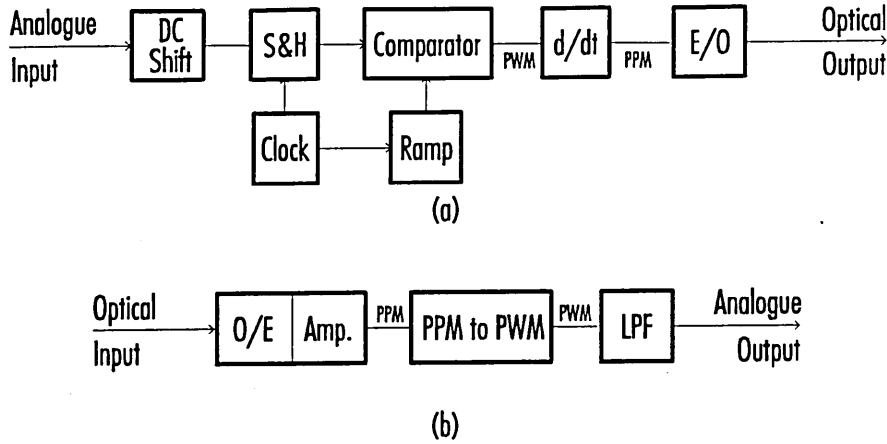
Figure 3.7 Uniformly sampled PPM: (a) modulator; (b) demodulator.

A method to evaluate the frequency spectrum of naturally sampled PPM was given by Stuart [38] and may be represented as [44]:

$$F(t) = \frac{A\omega_c \tau}{2\pi} + AM\cos(\omega_m t)\sin(\omega_m \tau/2)$$
$$+ \frac{2A}{\pi}\sum_{a=-\infty}^{\infty}\sum_{b=1}^{\infty}J_a(b\pi M)\frac{\sin[(a\omega_m + b\omega_c)\tau/2]}{a}\cos[(a\omega_m + b\omega_c)t]$$

(3.9)

where τ represents the pulse width of PPM pulses with amplitude A. The first term in Eq. (3.9) is the dc component of the unmodulated pulse carrier wave, while the last term is the phase modulated carrier signal producing the spectral components at the carrier frequency ω_c and all its harmonic frequencies, plus a cluster of sidetones separated by an amount equal to the modulating frequency ω_m. The second term of Eq. (3.9) represents the baseband component. This component is a differential version of the input signal. Because of this, PPM is usually converted into PWM after threshold detection. The baseband component depends on the duration of the PPM pulse. In the ideal case, when the PPM pulse is an impulse or a delta function, the PPM spectrum will have no baseband

component, see Figure 3.8. However, in real systems, the pulse width will be of finite

length, thus resulting in a baseband component being present in the PPM spectrum [45].
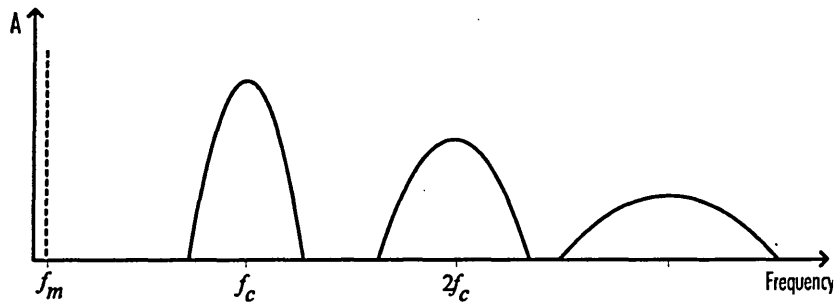
Figure 3.8 Frequency spectrum of PPM.

Demodulation of PPM at the receiving end is analogous to demodulation of PWM. Conversion from PPM to PWM is achieved with a combination of a bistable and a monostable, to obtain the PWM waveform as shown in Figure 3.7.b. Timing synchronisation between transmitter and receiver may be accomplished by transmitting the clock signal with the PPM waveform or by generating it at the receiver by using a clock recovery technique.

The modulation index M for PPM is similar to PWM and can be defined as:

$$M = 2\frac{t_0}{T} \qquad (3.10)$$

where t_0 is the maximum pulse position deviation and $T = 1/f_c$. The optical system bandwidth should be wide enough to preserve pulse position information. The required bandwidth can thus be estimated by the reciprocal of the pulse width τ:

$$B = \frac{1}{\tau} \qquad (3.11)$$

The choice of B decides the maximum modulation index that might be used. The signal-to-noise ratio in PPM systems is largely dependent on the time displacement t_0. Noise

25

. affects the time displacement by a fraction of the time displacement of the modulated pulse and is given by [46]:

$$(S/N)_N = \frac{1}{2}\left(\frac{MB}{f_c}\right)^2 C/N \qquad (3.12)$$

and for uniformly sampled PPM it can be shown to be [39]:

$$(S/N)_U = \left(\frac{M\pi B}{2f_c}\right)^2 C/N \qquad (3.13)$$

A comparison between the signal-to-noise ratios of PPM and of PWM shows that S/N for PPM is double that of PWM. The difference is that the noise error pulse train has only one edge pulse modulated, but the noise error pulse train for PWM contains a double edge. The enhancement for uniformly sampled PPM over naturally sampled PPM in terms of signal-to-noise ratio is as follows:

$$(S/N)_U = \frac{\pi^2}{2}(S/N)_N \qquad (3.14)$$

3.1.3. Pulse interval modulation

This modulation format falls into the category of anisochronous PTM techniques. In pulse interval modulation (PIM) [47], the interval between adjacent pulses is determined by the amplitude of the modulating signal. Moreover, PIM may be considered as conventional PPM except that it has a self generated carrier.

The PIM pulse train is generated by comparing the dc shifted modulating signal with a constant slope ramp. When amplitude equivalence is detected between the input signal and the ramp a short pulse is issued which constitutes a PIM version of the input signal, see Figure 3.9.a and Figure 3.11. On generation of the pulse the ramp is reset to its initial

zero value without being permitted to reach the ramp's final value. A sample and hold circuit for uniform sampling may be inserted at the modulator input.

Input

Ramp

PIM

PIWM

Time

(a)

Analogue
Input → DC Shift → Comp. → E/O → Optical Output

Ramp

(b)

Optical
Input → O/E | Amp → Ramp → LPF → Analogue Output

(c)
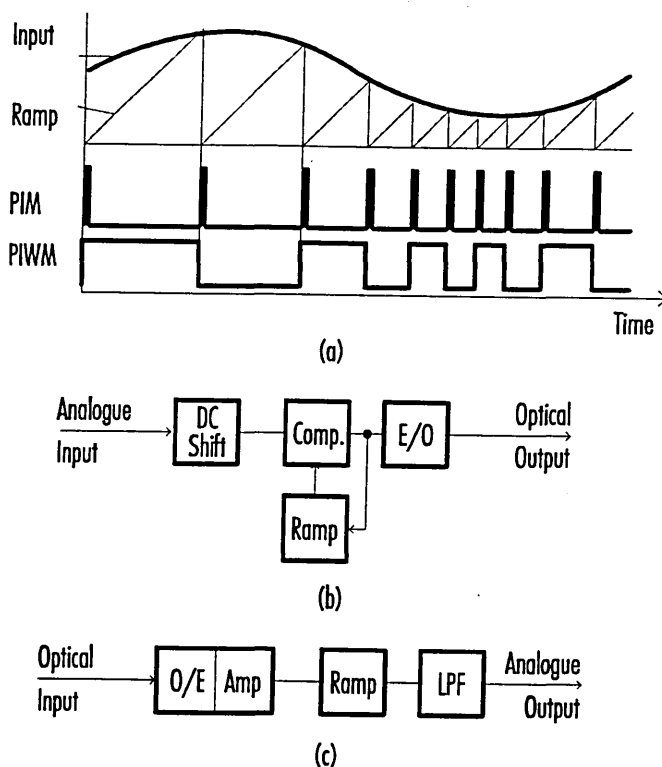
Figure 3.9 Naturally sampled PIM: (a) modulator; (b) demodulator.

Spectral measurements for PIM have been obtained by Tripathi [48] and an expression for the spectrum of PIM impulses was derived by Fyath [49] assuming a single tone modulating frequency signal. It can be written as follows:

$$F(t) = A\frac{\omega_c}{2\pi}\left[1 + \sum_{a=1}^{\infty} 2M^a \cos(a\omega_m t)\right] \cdot \left[1 + 2\sum_{a=1}^{\infty} \prod_{b=1}^{\infty} \sum_{c=-\infty}^{\infty} J_c(a\delta_b)\cos(a\omega_c t + bc\omega_m t)\right] \qquad (3.15)$$

in which the second term is the baseband component that represents the modulating signal along with its harmonics. The strength of these harmonics is a decaying function of the counting variable a since $0 < M < 1$. At low modulation indices these harmonic components become negligible, compared to the fundamental component and may be ignored. The fourth term in Eq. (3.15) referes to the spectral components generated slightly

asymmetrically around the sampling frequency f_c with harmonics and diminishing sidetones, see Figure 3.10.
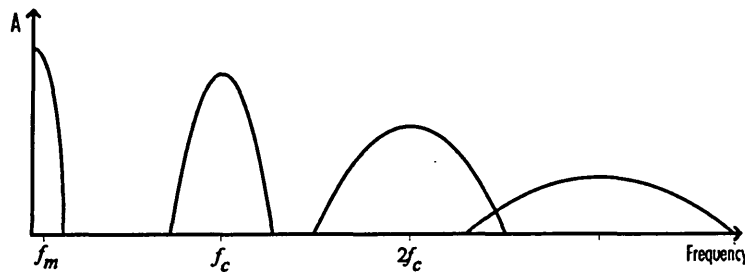
Figure 3.10 Frequency spectrum of PIM.

The receiver synchronises on every received pulse by initiating a ramp waveform, that is then reset immediately after a succeeding pulse is received. The maximum values of the ramp constitute the sampled points on the reconstructed waveform. Final filtering takes place by a low-pass filter or a combination of sample and hold and low-pass filter if uniform sampling is adopted, see Figure 3.9.b. When a low modulation index is used for the PIM generation, the low-pass filter at the demodulator may be of low order. However, at higher modulation indices spectral overlap may take place in the baseband region, therefore a higher order low-pass filter is required to reduce the effects of spectral overlap. In contrast to isochronous PTM, the modulation index of anisochronous PTM depends on the input signal-to-ramp ratio, rather than on the time deviation-to-frame ratio. This may be seen from Figure 3.11 in which the signal amplitude deviates between V_{min} and V_{max}. The maximum variation is t_0 and the average variation is around the dc level, hence T.
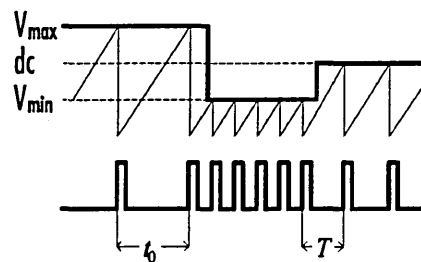
Figure 3.11 Modulation index for PIM and PIWM.

28

The modulation index for PIM can be defined as follows:

$$M = \frac{t_0}{2T}$$

(3.16)

where t_0 is the maximum pulse interval deviation and T is the non-modulated pulse interval. The system bandwidth B occupied by PIM is substantially dependent on the constant pulse width τ so that:

$$B = \frac{1}{\tau}$$

(3.17)

Both the channel and receiver must provide the required bandwidth $W \geq B$ to preserve the pulse information. Also, the sampling interval should be large enough so that the minimum pulse interval between two pulses is large enough to avoid inter-symbol interference (where energy from one pulse is transferred to the adjacent pulses). In PIM the noise in the demodulator output shows different characteristics than from those of PPM.

Ueno [50, 51] has developed a signal-to-noise analysis for a PIM system transmitting a colour TV signal f_m and a system bandwidth B for the PIM system. This approach assumes, that PIM pulses (of width τ) are spaced widely apart, neglecting inter-symbol interference, and also the limitation of noise to bandwidth f_m. The shape of the PIM pulse may be expressed as $g(t)$, and at time of threshold detection this pulse may be differentiated which expresses the slope of the rising edge at threshold detection $g'(t) = dg(t)/dt$. This effectively expresses the gradient of the angle of carrier amplitude A and the pulse rise time t_r so that $g'(t) = A/t_r$ and the rise time can be substituted with $t_r = 2/(\pi W)$ [37]. After modifications of [50] the expression for the signal-to-noise ratio becomes:

$$S/N = \left(\frac{MB}{\kappa_{g(t)}}\right)^2 \frac{2}{f_m f_c} \frac{1}{1 - sinc(2\pi f_m / f_c)} C/N$$

(3.18)

where $\kappa_{g(t)} = (A\ W)/g'(t)$ is a constant which depends on the pulse shape $g(t)$ and substitution gives $\kappa_{g(t)} = 2/\pi$. The second term in Eq. (3.18) displays the relation between the bandlimited noise signal of bandwidth f_m and the sampling signal. Assuming wideband noise, ie. $f_m \gg f_c$, Eq. (3.18) may be written as:

$$S/N = \frac{(\pi M B)^2}{2}\frac{1}{f_m f_c} C/N \qquad (3.19)$$

3.1.4. Pulse interval width modulation

Pulse interval width modulation (PIWM) [27] is derived from its counterpart PIM by passing a train of PIM pulses through a bistable (Figure 3.12.a.) to produce a waveform in which both mark and space convey the information. As with PIM, the anisochronous nature of PIWM arises because the modulator ramp is reset at the point when equivalence of ramp and input signal is detected and not by a predetermined interval controlled by the choice of the carrier (sampling) frequency, see Figure 3.9.a. Demodulation is achieved by converting PIWM into PIM pulses and then employing the standard PIM demodulation technique, see Figure 3.12.b.
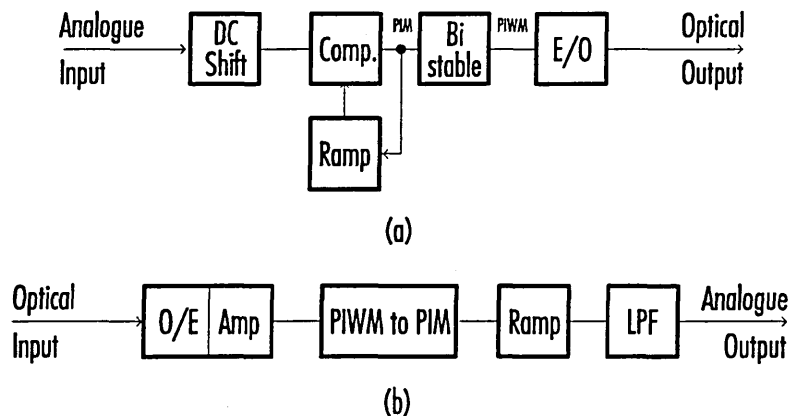
Figure 3.12 Naturally sampled PIWM: (a) modulator; (b) demodulator;

The modulation index for PIWM is analogous to PIM and is given by:

$$M = \frac{t_0}{2T}$$ (3.20)

Employing the same general approach as Fyath [49] for PIM, the expression for PIWM spectrum has been given by Wilson [52]:

$$F(t) = \frac{A}{2}\left[1 + \sum_{a=1}^{\infty} \sum_{b=-\infty}^{\infty} \sum_{c=-\infty}^{\infty} sinc(a\pi/2)\ J_b(a\delta_1)\ J_c(a\delta_2)\ \cos\left(\left[a\beta_0\omega_c + (b+2c)\omega_m\right]t\right)\right]$$ (3.21)

where A is the amplitude of the PIWM waveform. The PIWM spectral profile shown in Figure 3.13, resulting from Eq. (3.21) is slightly asymmetrical, unlike PWM, and contains no baseband components whatsoever, in contrast to PIM. Strong spectral components are generated around the sampling frequency ω_c and all its odd harmonics, surrounded by a diminishing series of sidetones, separated from each other by the modulating frequency ω_m. The profile of the sidetone structure changes considerably as a function of both the modulation index M and the sampling ratio ω_0/ω_m. The Bessel functions, J_b and J_c decrease rapidly for sidetones occurrences δ_1 and δ_2. The coefficient β_0 accounts for the shift of the sampling frequency and can be approximated for a modulation index $M < 0.5$ with $\beta_0 = 1 + M^2/2$.
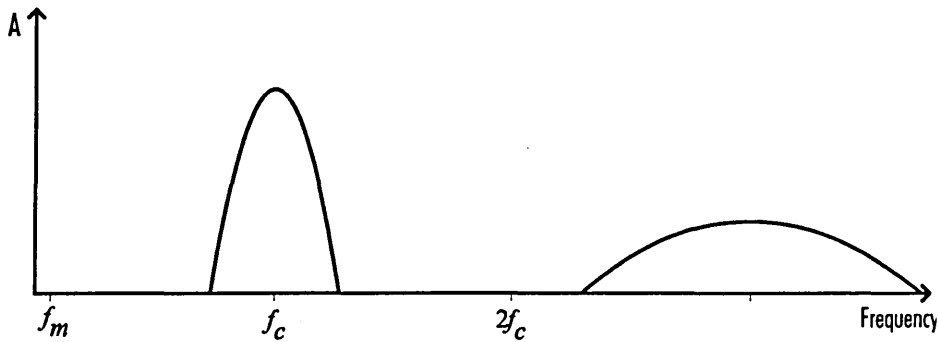
Figure 3.13 PIWM frequency spectrum.

For PIM the minimum permitted sampling ratio ω_0/ω_m is 2:1 in order to satisfy the sampling theory requirements. To generate PIWM, the PIM pulses are divided by two, reducing the minimum sampling ratio ω_0/ω_m to unity for PIWM. This does not violate the sampling theorem however, since the PIWM wave train carries information on both the rising and the falling edges, effectively taking two samples per cycle. The bandwidth occupancy B for PIWM may be approximated with reference to the average sampling frequency $1/T$ of the unmodulated signal, the dc shift, and the modulation index M:

$$B = \frac{1}{(1-M)T} \qquad (3.22)$$

For low modulation indices $M < 0.1$ this approximation may become $B = 1/T$ since the variation of the pulse width is relatively small, ie. the modulating signal swings around the dc shift with very low peak-to-peak amplitude. With larger pulse width variations however, the average transmission bandwidth of PIWM may be expressed as $B = 1/T_{min}$, see Figure 3.14.
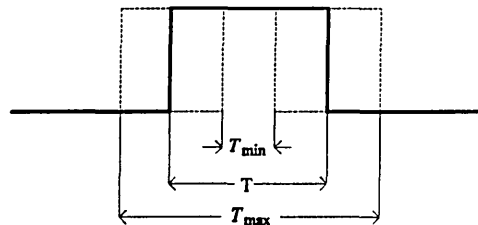
Figure 3.14 Change of pulse width in PIWM.

Signal-to-noise ratio analysis for PIWM is very similar to that of PIM since PIWM is converted into PIM in the demodulator, except that the noise affects both the leading edge and the trailing edge. Following a similar approach as in the previous section, the signal-to-noise ratio for PIWM at a sampling ratio of ω_0/ω_m is 2:1 can be expressed as [53]:

$$S/N = \frac{(\pi MB)^2}{4} \frac{1}{f_m f_c} \, C/N \qquad (3.23)$$

As expected, the signal-to-noise ratio for PIWM from Eq. (3.23) is very similar to PIM from Eq. (3.19).

3.1.5. Square wave frequency modulation

Square wave frequency modulation (SWFM) [54] and pulse frequency modulation (PFM) are of anisochronous nature and are very closely related., see Figure 3.15 In PFM the modulating signal modifies the pulse repetition rate according to the amplitude of the modulating signal. It is usually produced by directly modulating a voltage controlled oscillator (VCO). PFM is a differentiated version of SWFM, indicating every transition with a short pulse, see Figure 3.2. SWFM and PFM compare favourably with PCM performance.
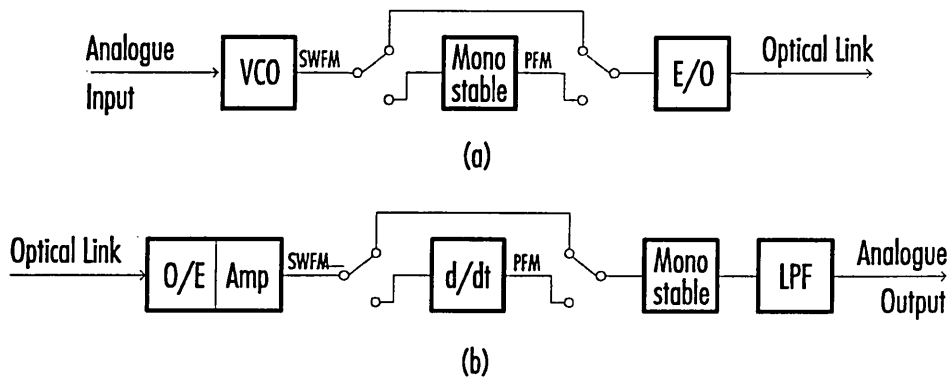
Figure 3.15 SWFM and PFM: (a) modulator; (b) demodulator.

The modulation index can be defined as follows:

$$M = \frac{\Delta f}{f_m} \qquad (3.24)$$

where Δf is the pulse frequency deviation and f_m is the modulating signal bandwidth. The spectrum of a single tone modulated PFM pulse train is given next [25]:

$$F(t)=\frac{A\omega_c\tau}{2\pi}\left[1+\frac{2M}{\omega_c\tau}\sin(\omega_m\tau/2)\cos(\omega_m t-\omega_m\tau/2)+2\sum_{a=1}^{\infty}\sum_{b=-\infty}^{\infty}J_b(aM)\frac{\sin(a\omega_c+b\omega_m)}{a\omega_c}\right.$$
$$\left.\cdot\cos[(a\omega_c+b\omega_m)t-b\omega_m\tau/2]\right]\qquad(3.25)$$

Neglecting the dc term, an unmodulated pulse carrier consists of the fundamental and harmonic components whose amplitudes follow a $\sin(x)/x$ envelope determined by the pulse width τ. Under modulation conditions, the PFM spectrum consists of a baseband component along with the sidetone structures set around the carrier frequency and all its harmonics. This sidetone pattern is slightly asymmetrical, with the upper sidetones being stronger than their lower sidetone counterparts, Figure 3.16.a. Unlike PWM and PPM, the number of sidetones appearing around any particular carrier harmonic is not determined solely by the amplitude of the input signal but also by its frequency.
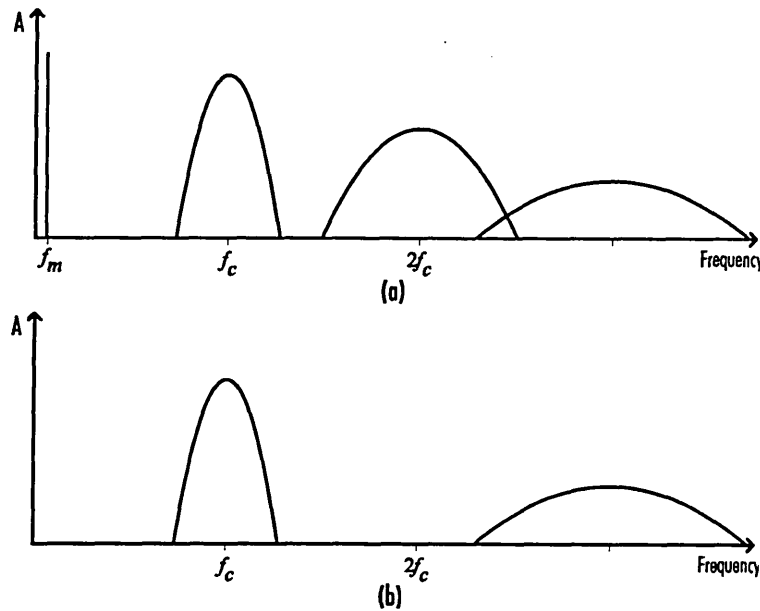
Figure 3.16 Frequency spectrum of (a) PFM; (b) SWFM.

In the case of SWFM, the frequency spectrum for a single tone modulated signal is [54]:

$$F(t)=AD\sum_{a=-\infty}^{\infty}\text{sinc}(a\pi D)\sum_{b=-\infty}^{\infty}J_a(aM)\exp[j(a\omega_c+b\omega_m)t]\qquad(3.26)$$

where D is the duty cycle. When the carrier is a perfect square wave, $D = 0.5$, the spectrum is made up of odd components and there is no baseband component, Figure 3.16.b. Deviation from 50% duty cycle will result in generation of a baseband component together with even harmonics. With a duty cycle of perhaps 5% to 10%, the SWFM spectrum becomes more and more that of PFM with baseband and all harmonics around ω_c. With narrower pulses, PFM occupies a larger bandwidth in the transmission channel:

$$B_{PFM} = 3f_m + 2(Mf_m + f_g) \tag{3.27}$$

than SWFM:

$$B_{SWFM} = 2(f_m + Mf_m + f_g) \tag{3.28}$$

at a modulation index of $M = 1$ and ignoring the guard band, PFM needs 1¼ more transmission bandwidth then SWFM. The associated signal-to-noise ratio for the PFM modulation format may be expressed as:

$$(S/N)_{PFM} = 3\left(\frac{MB_{PFM}}{2f_c}\right)^2 C/N \tag{3.29}$$

and for SWFM:

$$(S/N)_{SWFM} = \frac{3}{2}\left(\frac{MB_{SWFM}}{f_c}\right)^2 C/N \tag{3.30}$$

The improvement in S/N for SWFM over PFM and for the same transmission, ie. $B_{PFM} = B_{SWFM}$, $M = 1$ of the modulating signal and ignoring f_g follows from Eqs. (3.29) and (3.30):

$$(S/N)_{SWFM} = 2(S/N)_{PFM} \tag{3.31}$$

3.2. Performance of Continuous PTM

PIWM is suited for video and instrumentation signals over moderate length point-to-point optical fibre links without occurring the greater expense of PCM equipment. PIM has advantages in optical fibre transmission over PIWM due to its shorter pulses. The pulses may contain a higher optical peak level that allows an increase in the distance of transmission. With PIM and PIWM, weak signals are sampled at finer resolution and strong signals are sampled fewer times, hence providing non-linear sampling. PPM occupies the largest bandwidth of the discussed PTM schemes, which is traded for signal-to-noise performance. Its counterpart PWM is the most bandwidth efficient scheme among the discussed PTM techniques, but shows relatively poor signal to noise performance. PFM and SWFM modulating and demodulating circuits are simpler than the circuits of PIM and PIWM. Moreover, they offer a better signal-to-noise performance.

Table 3.2 compares PTM schemes with 8-bit PCM in terms of the bandwidth for a baseband frequency of 30 MHz [55, 56]:

	PCM	PWM	PPM	PIM	PIWM	PFM	SWFM
Used modulation Index	-	0.5	0.5	0.5	0.5	1.5	1.5
Sampling ratio	2.5	2.5	2.5	2.5	2.5	2.5	2.5
Carrier frequency (MHz)	600	75	75	75	75	75	75
Bandwidth occupancy (MHz)	600	197	400	200	150	240	210

Table 3.2 Comparison of various PTM to an 8-bit PCM at a sampling ratio of 2.5.

Using the parameters in Table 3.2 and Table 3.3, the signal-to-noise ratio versus the carrier-to-noise ratio characteristics of various PTM systems are illustrated in Figure 3.17 and Figure 3.18 respectively. The curves show that PCM has clear operating advantages over PTM techniques at low carrier-to-noise ratio. Among the PTM family SWFM, PPM

and PIM offer the best overall signal-to-noise performance at low sampling ratios, but the bandwidth occupancy for PPM is twice as large as the transmission bandwidth of PIM or SWFM.

	PCM	PWM	PPM	PIM	PIWM	PFM	SWFM
Used modulation index	-	0.5	0.5	0.5	0.5	1.5	1.5
Sampling ratio	5	5	5	5	5	5	5
Carrier frequency (MHz)	1200	150	150	150	150	150	150
Bandwidth occupancy (MHz)	1200	197	800	400	300	240	210

Table 3.3 Comparison of various PTM methods with 8-bit PCM at a sampling ratio of 5.

With the change of the sampling ratio, PPM maintains its position, displaying the best overall signal-to-noise performance, whereas PWM, PFM, SWFM deteriorate slightly at high sampling ratios, see Figure 3.18. The performance of each modulation scheme may be optimised for particular applications by selecting an appropriate sampling ratio and modulation index.

	PCM	PWM	PPM	PIM	PIWM	PFM	SWFM
Bandwidth occupancy	5	1	4.	3	3	2	2
Signal-to-noise performance	4	1	5	3	2	3	5
Signal power consumption	3	5	1	2	5	2	3
Complexity	5	3	3	3	4	2	1
Time multiplexing	Yes	Yes	Yes	Yes	No	Yes	No
Baseband signal	Yes	Yes	(Yes)	Yes	No	Yes	No

Table 3.4 PTM system comparison.

Table 3.4, summarises some important system parameters of various modulation techniques, ranging from 1 to 5, indicating very low or very simple to extremely high or extremely complex. The PCM format is NRZ, the PPM and PWM formats belong to the
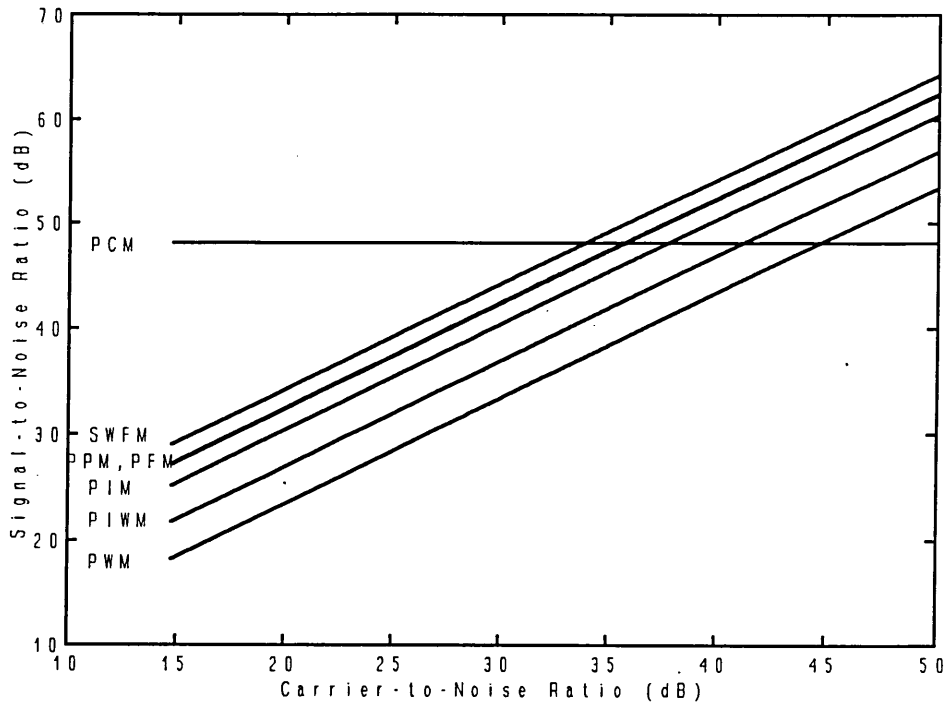
Figure 3.17 *S/N* vs *C/N* for various PTM at a sampling ratio of 2.5 and with 8-bit PCM.
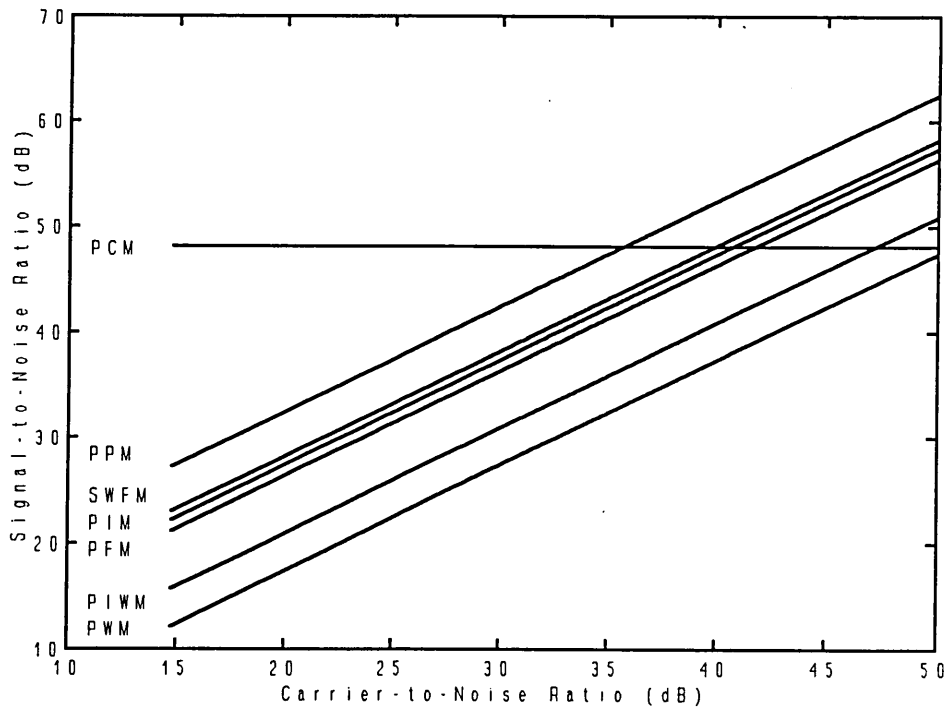
Figure 3.18 S/N vs *C/N* for various PTM at a sampling ratio of 5 and with 8-bit PCM.

category of uniform sampling whereas all other formats belong to the category of natural sampling.

3.3. Discrete Pulse Time Modulation

The previous sections indicate that present trends in transmission technology favour low-power optical systems. Advanced technology can improve the transmission system's performance, but the choice of the modulation format represents the fundamental factor for improvement. The ability to share a common medium for transmission of multiplexed signals, the bandwidth occupancy, the power necessary for transmission and the system complexity result in a number of widely used modulation methods.

3.3.1. Digital pulse position modulation

The digital pulse position modulation scheme has been suggested for long-haul data links over single-mode fibres [57]. Garrett [22, 23] has shown that bandwidth can be traded for signal-to-noise ratio. Martin and Hausien [58] applied DPPM to LANs and examined a broad number of PPM characteristics. Various other studies of digital PPM systems investigated the significance of the optical detector choice [59] and the influence of a dispersive optical channel with Gaussian shaped pulses [60, 61]. As indicated in Section 2.3.2, digital PPM can offer up to 12 dB [22] improvement of receiver sensitivity over PCM. This represents an increase of regenerator spacing of 60 km compared to PCM [21]. It would be nice to know this increase as a percentage.

Results obtained by Calvert [62] show an improvement of receiver sensitivity of 4.2 dB for DPPM instead of PCM. Further improvement in S/N of up to 7 dB in bandlimited systems employing pre-detection filtering has been demonstrated by Cryan [63, 64]. A block

· diagram of a digital PPM system is shown in Figure 3.19 and the digital PPM signal is illustrated in Figure 3.20.
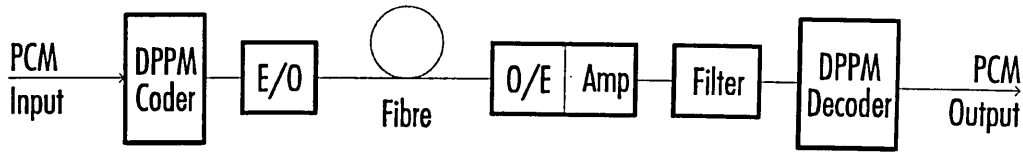
Figure 3.19 Simple DPPM system.
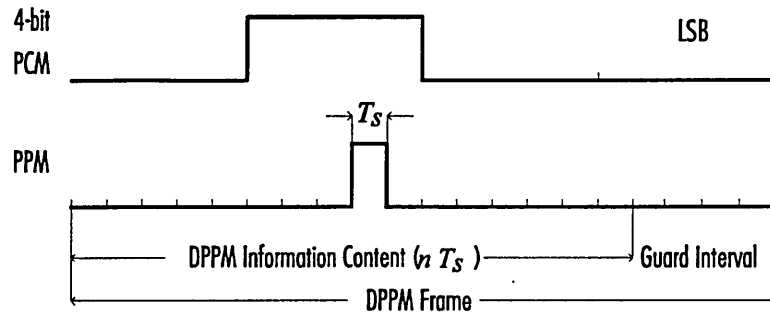
Figure 3.20 Digital PPM signal.

P-bits (termed the coding level) of binary PCM format are converted to DPPM, having a time frame of length T_n and transmitted by sending a single pulse in one of $n = 2^P$ time slots. According to Elmirghany [65] the mathematical expression for the digital PPM frame can be represented by:

$$x(t) = \sum_{a=-\infty}^{\infty} g(t - aT_n - t_a)$$

(3.32)

where $g(t)$ is the DPPM pulse shape, T_n is the frame duration and t_a is the stochastic wide-sense stationary sequence representing the data encoded into DPPM. The expression for the time slot duration T_s in DPPM in terms of sampling frequency f_s, modulation index M and number of time slots n can be written as:

$$T_s(DPPM) = \frac{M}{f_s n} \qquad\qquad (3.33)$$

Thus the clock frequency for DPPM will be higher than that of PCM by the ratio of $n/\log_2 n$. The associated bandwidth occupancy is just the reciprocal of the duration of one time slot, $B = 1 \ /T_s$.

Optimum pre-detection filtering though a matched filter could be used to recover a signal contaminated with additional Gaussian noise [21]. DPPM decision errors will occur due to receiver noise and will be of three types [23].

1) Erasures: failure to detect the pulse in the signalling slot.

2) False alarm errors: violation by noise that causes the receiver to detect a pulse.

3) Wrong slot errors: noise on the leading pulse edge produces a detection immediately preceding or following the containing pulse.

With reference to Cryan [21] the receiver sensitivity for DPPM is relatively poor for low fibre bandwidth. For a fixed value of n there is an optimum fibre bandwidth f, normalised to the pulse width, where no further improvement is obtained beyond this optimum, see Figure 3.21.a. The effect of improved receiver sensitivity arises due to the fact that with increasing n the mean-to-peak power increases, since the average optical power is maintained constant. With an increase of the number of time slots n, the probability of erasures and false alarm errors decreases. Eventually, a point is reached when the slot duration is comparable to the rise time of the pulse and wrong slot errors predominate [21, 66]. Optimum receiver sensitivity occurs when all three error categories contribute an equal amount of errors [57], see Figure 3.21.b (for $f = 10$).
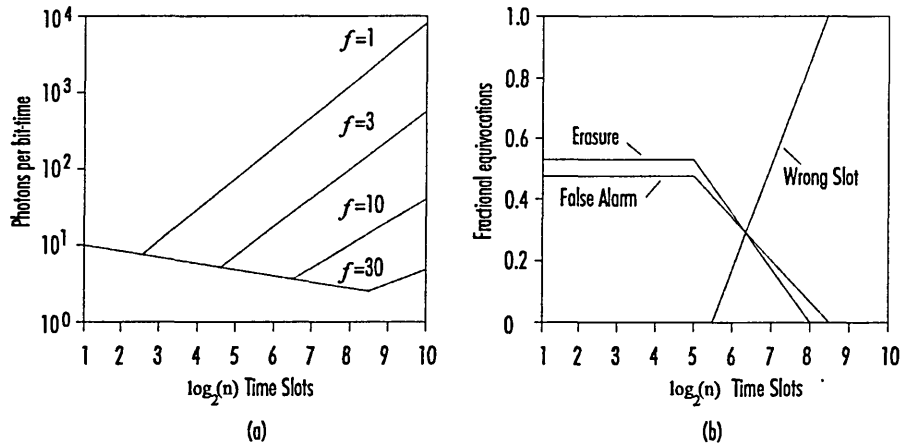
Figure 3.21 (a) DPPM receiver sensitivity for various fibre bandwidths; (b) trade-off between DPPM error sources as a function of time slots.

A numerical spectral model for DPPM composed of the sum of contributions from a set of delayed pulses has been obtained by Elmirghany [65]. The given spectral characterisation of a DPPM is given as:

$$S(f) = \frac{1}{NT_s(n/M)} \left| G(f) \sum_{a=0}^{N} \exp\left(-j2\pi fT_s\left[a(n/M)+n_a\right]\right) \right|^2 \tag{3.34}$$

where $G(f)$ is the DPPM pulse shape transform and $n_a = t_d/T_s$ is a random number between 0 and $(n\text{-}1)$ that gives the pulse position in the a-th frame. N gives the discrete length of the truncated sequence and must be such that $NT_s(n/M)$ is much greater than T_n. The DPPM spectrum displays distinctive frequency components at odd harmonics of the slot frequency that can be used for synchronisation at the receiving end, as shown in ?.
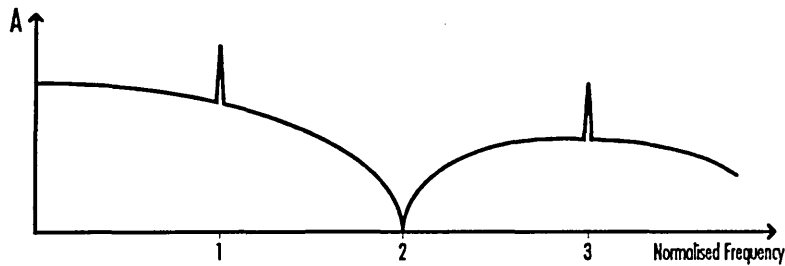
Figure 3.22 Analytical DPPM spectrum.

42

Digital PPM has been shown to offer better performance in terms of receiver sensitivity than PCM but at the cost of bandwidth expansion. Furthermore, several difficulties are associated with the transmission of high-speed digital PPM: the laser transmitter must be fast, the receiver must have a wide bandwidth and the digital coder/decoder must operate at the digital PPM clock rate, resulting in bandwidth expansion [67]. While PCM suffers from intersymbol and interframe interference, DPPM has very little intersymbol interference since there is only one pulse per frame. Interframe interference is minimised through a guard interval of relevant length. Synchronisation of DPPM systems, however, becomes more critical with a relatively large number of time slots per frame. It may be possible, as the position of the pulses may be significantly displaced from the centre, that the DPPM system may then fail to deliver reliable timing information at the receiver. To ease the task of the synchronisation circuits, line coding [68] or block synchronisation [69] may be employed for DPPM. Another method is the estimation of the optical DPPM frame phase by using naturally occurring sequences and avoiding sensitivity and bit rate penalties [70] associated with the previous methods.

3.3.2. Digital pulse width modulation

In the case of analogue PWM, the linearity of the analogue ramp has a significant influence on the overall system performance, since any non-linearity will result in harmonic distortion being generated at the output of the receiver. The problems associated with analogue PWM can be overcome by employing a digital technique to generate a PWM signal [71]. Here, the ramp generator, see Figure 3.5, is replaced with a p-bit counter, that counts from zero to 2^p-1, resetting to zero at every sampling interval.

This approach displays exceptional linearity since, except for the quantisation error, the system does not suffer from any harmonic distortion at higher values of the modulation

index. Digital PWM [72] systems are inherently superior to analogue PWM systems in terms of accuracy, linearity and stability. However, there is a disadvantage as an increase of clock speed for ramp generation by a factor 2^P over the sampling frequency is required, analogous to PPM. The overall DPWM sampling constraints are of course identical to analogue PWM, since the transmitted pulses are identical.

Results presented by Ghassemlooy [71] show, that digital PWM outperforms analogue PWM when operated at a modulation index of 50%, by up to 6-10 dB.

3.3.3. Digital pulse interval width modulation

A new optical communication system based on digital PIWM was proposed by Sato [73] where both mark and space of the signal are used to carry information. The overall aim was to provide good approximation of the amplitude probability of speech with an effective coder so that low level signals are sampled more often than the high amplitude signals.

The potential of digital PIWM lies in its transmission capacity and synchronisation ability. Because the PIWM code conveys the information in both mark and space, the overall transmission capacity is increased compared to DPPM. Simultaneously, receiver synchronisation is achieved with the PIWM code itself in which every PIWM frame is uniquely identified with a low-high transition.

The work described in the following chapters seeks to identify the potential of digital PIWM. This embraces solutions for code construction and their impact on the signalling format and is the subject of Chapter 4. System considerations and performance verification are the subject of Chapters 5, 6 and 7.

3.4. Summary

A review of principles of continuous and discrete optical pulse time modulation formats has been presented. Equations presented, describe the power spectral density of each method being proposed. Original signal-to-noise equations for various PTM techniques were presented.

Continuous PTM techniques are ideal for low bandwidth communication systems since they can operate at reduced sampling ratios. They are also suitable for high speed fibre communications. Overall, the compromise between bandwidth efficiency, signal-to-noise performance and cost is best traded with SWFM while PPM displays the best overall signal-to-noise performance.

In the digital PPM coding format, bandwidth may be traded for signal-to-noise performance due to an increase of optical peak power gaining high receiver sensitivity when compared to PCM. DPPM has been suggested for long-haul transmission.

CHAPTER 4

SYSTEM MODEL

4. SYSTEM MODEL

Digital pulse interval width code modulation (PIWCM) is a variation of Sato's anisochronous digital PIWM [73] that carries the information by varying both mark and space. Digital pulse interval code modulation (PICM) is the differentiated form of PIWCM and carries the information by varying the width of the space. The two codes can be easily converted from one form to the other. But they have different code characteristics and are therefore suitable for different applications. With PICM and PIWCM the modulated waveform is a discrete signal, consisting of time slots, unlike PIWM and PIM where the modulated waveform is continuous.

Code properties of PIWCM and PICM vary according to the frame length, resulting from non-perodic sampling intervals of the message signal. Mathematical models representing the codes both in time as well as in frequency domains are derived. Error sources inherent to these modulation techniques are also discussed.

4.1. Overall System Description

A block diagram of the digital PIWCM/PICM system is shown in Figure 4.1. An analogue signal is input to the analogue-to-digital converter (ADC) with p-bit resolution of which the
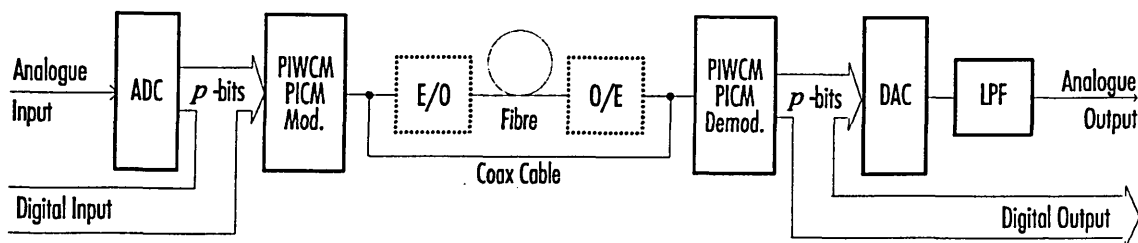
Figure 4.1 PIWCM and PICM system model.

output is fed into the PIWCM/PICM modulator; alternatively, a parallel bit stream of p-bits may be fed directly into the PIWCM/PICM modulator. Depending on source connection, PIWCM/PICM can carry encoded PCM signals or directly sampled signals. In either case p-bits of data are converted into frames of different frame length as shown in Figure 4.2.
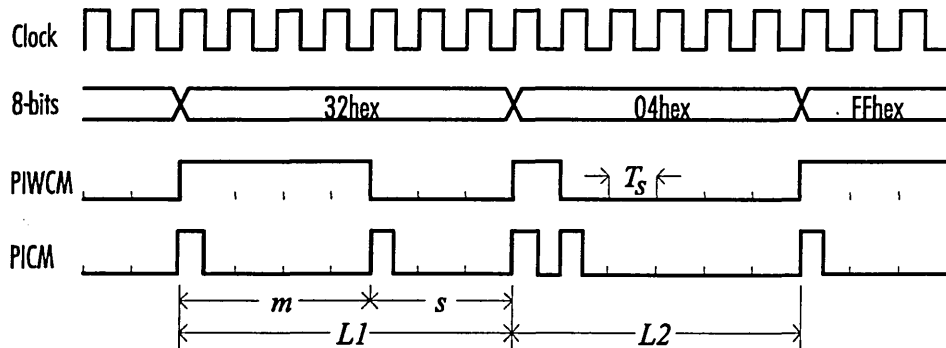
Figure 4.2 Digital PIWCM and PICM codes.

Figure 4.3 shows the particular mark-space combinations and frame length for given decimal equivalent values of p-bits binary data, whilst the resulting frame lengths is the sum of mark and space.

An optical source converts either of the electrical pulse trains into an optical signal which is then transmitted down an optical fibre cable. At the receiver, the optical signal is converted back into an electrical signal by an optical receiver. The regenerated PIWCM/PICM codes are then decoded into a parallel bit-stream using the PIWCM/PICM demodulator.

The DAC is followed by a low-pass filter that is employed to recover the original analogue signal and to filter out unwanted clock frequencies. Synchronisation is achieved by employing the same clock signal both at the transmitter and receiver.
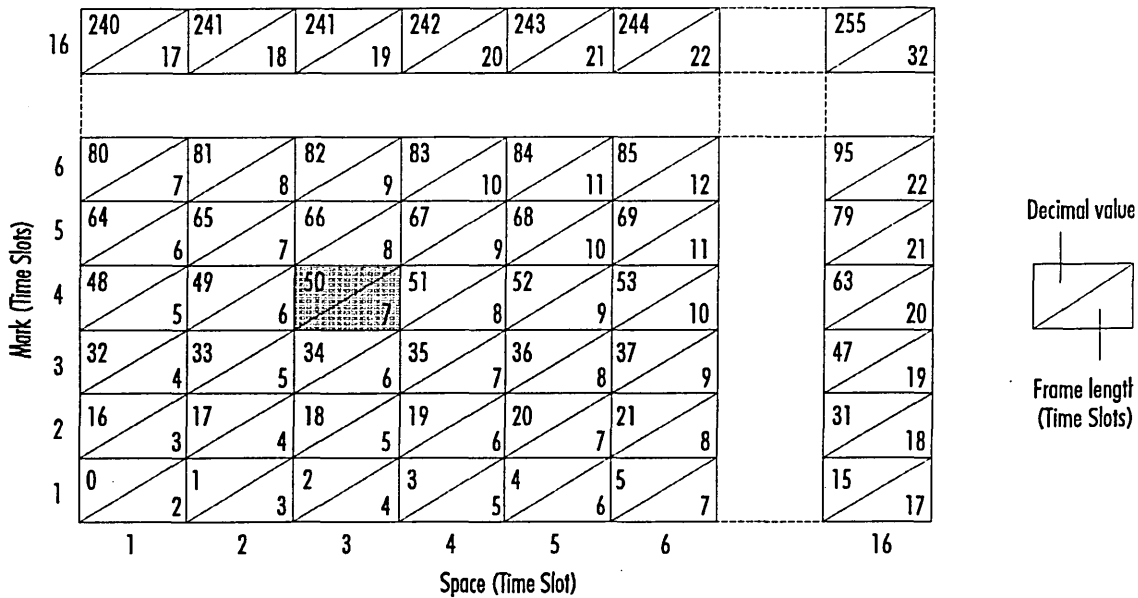
Figure 4.3 Decimal equivalent value with resulting mark-space combination and frame length.

The code generation principle of an 8-bit PIWCM/PICM system can be best described with reference to Figure 4.3. For example, taking the mark-space combination 4-3 as highlighted:

1) An analogue input signal may be divided into 256 discrete levels, eg. the 50th (decimal) level is equivalent to the p-bit binary set 0011 0010.

2) The digital information obtained is then divided into a high-word (0011) and a low-word (0010), corresponding to mark and space respectively. In this example, the number of time slots for mark and space would be 4 and 3 respectively. An additional time slot is introduced for mark and space to cater for zero level.

3) Finally, mark and space are combined together, resulting in a frame length of 7 time slots.

4.2. PIWCM Code Properties

Digital PIWCM is closely related to pulse analogue PIWM in that it employs a waveform in which both mark and space represent the sampled data [30]. Each successive frame length is different, being determined only by the sampled value of the modulating signal and not by the choice of the predetermined clock (sampling) period. As a consequence, receiver design problems are substantially reduced since there would be no requirement to introduce frame synchronisation bits in order to interpret the encoded sampled value correctly.

A p-bit digital signal is divided into two sets of k-bits (here k is chosen to be equal to half the p-bits), where the decimal equivalent of the binary combination in a given set determines the number of time slots for each frame, see Figure 4.3.

At time $t = 0$, conversion first takes place for mark followed by conversion for space. Finally, time slots for mark and space are combined together to produce the desired digital PIWCM signal. This new scheme offers higher transmission capacity by fully utilising the time slots for a given frame and eliminating unused time slots. Synchronisation is simple as each frame is initiated by a mark followed by space. The PIWCM frame length results from $L = m+s$, and is given by:

$$L = \left[Mod\left(\frac{X}{2^k}\right) + 1 \right] + \left[Rem\left(\frac{X}{2^k}\right) + 1 \right] \tag{4.1}$$

where X is the decimal equivalent of an p-bit binary data and $k = p/2$ bits. The first term represents the pulse width (mark) by taking the modulus of $X/2^k$ and the second term represents the pulse interval (space) by taking the remainder of $X/2^k$. Extra time slots are necessary to make sure that a zero level still has mark and space. The maximum frame length L_{max} for a p-bit system is therefore:

$$L_{max} = 2^{k+1} \qquad \textit{time slots} \qquad (4.2)$$

The average frame length L_{avg} expresses the average number of time slots to be issued and can be computed through:

$$L_{avg} = 2^k + 1 \qquad \textit{time slots} \qquad (4.3)$$

and the minimum frame length L_{min} is 2 time slots (for a decimal equivalent value of zero).

The expression for the duration of time slot T_s in PIWCM (corresponding to one clock interval) in terms of sampling frequency and maximum frame length is:

$$T_S(PIWCM) = \frac{1}{f_s \cdot L_{max}} = \frac{1}{f_s \cdot 2^{k+1}} \qquad (4.4)$$

ie. a PIWCM frame consisting of L_{max} time slots must be generated within the time of a time frame of a p-bit PCM data. Defining the transmission capacity as:

$$C = \frac{f_s \cdot maximum \ frame \ length}{average \ frame \ length} \log_2 (number \ of \ possible \ combinations) \qquad (4.5)$$

For PIWCM, the transmission capacity is:

$$C_{PIWCM} = \frac{f_s \cdot L_{max}}{L_{avg}} p = \frac{f_s \cdot 2^{k+1}}{2^k + 1} p \qquad \textit{bits/s} \qquad (4.6)$$

For comparison, the transmission capacity for PCM is $C_{PCM} = p f_s$. For large values of p the transmission capacity of PIWCM is twice that for PCM. This is as expected, since on average a PIWCM frame will be only half the length of a PCM frame, thus enabling twice the sampling frequency rate to be employed and permitting a signal of twice the bandwidth to be adequately sampled. In conjunction with increased bit-resolution, the clock frequency of PIWCM is increased with respect to PCM in the following manner:

4.3. PIWCM Power Spectral Density

A random process $x(t)$ can be written in terms of a waveform $g(t)$ of constant duration T_n and of amplitude A to form the random pulse train [74]:

$$x(t) = A \sum_{a=-\infty}^{\infty} g(t - aT_n - \delta_a) \qquad (4.9)$$

where δ_a is the random time delay valid within the interval $0 \le \delta_a \le T_n$. With reference to Figure 4.5, an infinite PIWCM pulse train $x_{PIWCM}(t)$ consisting of frames with different mark-space patterns can be mathematically represented as:

$$x_{PIWCM}(t) = \sum_{i=-\infty}^{\infty} g_{(m,s)i}\left[t - T_s\left(\sum_{a=-\infty}^{i-1} (m_a + s_a)\right)\right] \qquad (4.10)$$

where $g_{(m,s)i}$ represents the i-th PIWCM sample with m_i time-slots of mark and s_i time slots of space, m_a and s_a are the number of time-slots for mark and space at the a-th sample respectively, T_s is the duration of one time-slot is given by Eq. (4.4). Equation (4.10) indicates that PIWCM does not display a fixed periodic frame structure in the manner of PCM and DPPM, except in the absence of any incoming data where the result is an alternating mark and space pattern.
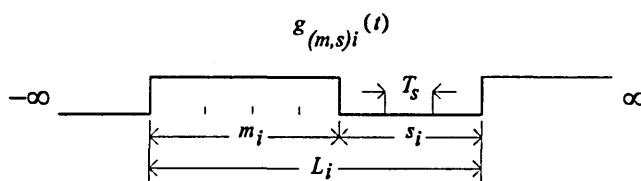
Figure 4.5 PIWCM time representation.

To be able to characterise the process practically it is beneficial to evaluate the power spectral density of a truncated realisation. Following the process similar to that obtained by Elmirghany [65], the power spectral density (PSD) function of the PIWCM process $x_{PIWCM}(t)$ truncated over a limited interval is given by:

$$S(f) = \lim_{T_n \to \infty} \frac{|X_T(f)|^2}{T_n} \qquad (4.11)$$

in which $X_T(f)$ is the Fourier transform of the finite energy pulse train $x_{PIWCM}(t)$ of length T_n. The length of the time window should be sufficiently large enough, so that the fluctuations due to the end effects of integration become small. For a p-bit system, 2^p possible frames may be generated. For an 8-bit system 256 frames, all with equal probability of occurrence, are generated, thus forming a long PIWCM pulse train $x_{PIWCM}(t)$. The Fourier transform of a given single frame with pulse width $T_s m$ is given by the Fourier integral:

$$G(f) = A \int_{-T_s(m/2)}^{T_s(m/2)} e^{-j2\pi f t} dt \qquad (4.12)$$

In Eq. (4.12) it is assumed that only a time shift of $t-T_s m$ is performed whilst the phase shift is neglected, since the function under the integral describes the distribution of the power with frequency:

$$G_{(m,s)}(f) = \frac{A}{\pi f} \sin(T_s m_a \pi f) \qquad (4.13)$$

Equation (4.13) fits into the spectral characterisation and the PSD for PIWCM becomes:

$$S(f) = \frac{1}{T_s \sum_{i=0}^{N} (m_i + s_i)} \left| \sum_{i=0}^{N} G_{(m+s)i}(f) \exp\left(-j2\pi T_s \sum_{a=0}^{i-1} (m_a + s_a)\right) \right|^2 \qquad (4.14)$$

where the variables m_i and s_i in the first term are the total number of time slots for mark and space accounted up to the i-th sample and N gives the length of the truncated data frame sequence. The second term, $G_{(m,s)i}(f)$ is the PIWCM pulse shape transform of the i-th and all preceding samples with the individual length $m_a + s_a$ of the i-th sample.

53

A typical PIWCM spectrum evaluated using Eq. (4.14) for random data taken over 4000 frames evaluated at 320 frequency points for 8-bit resolution is shown in Figure 4.6, with the frequency axis normalised to the slot frequency and power level over the frequency span to 0 dBm. The Matlab algorithm for evaluation of the PIWCM power spectral density is listed in Chapter 10.1.
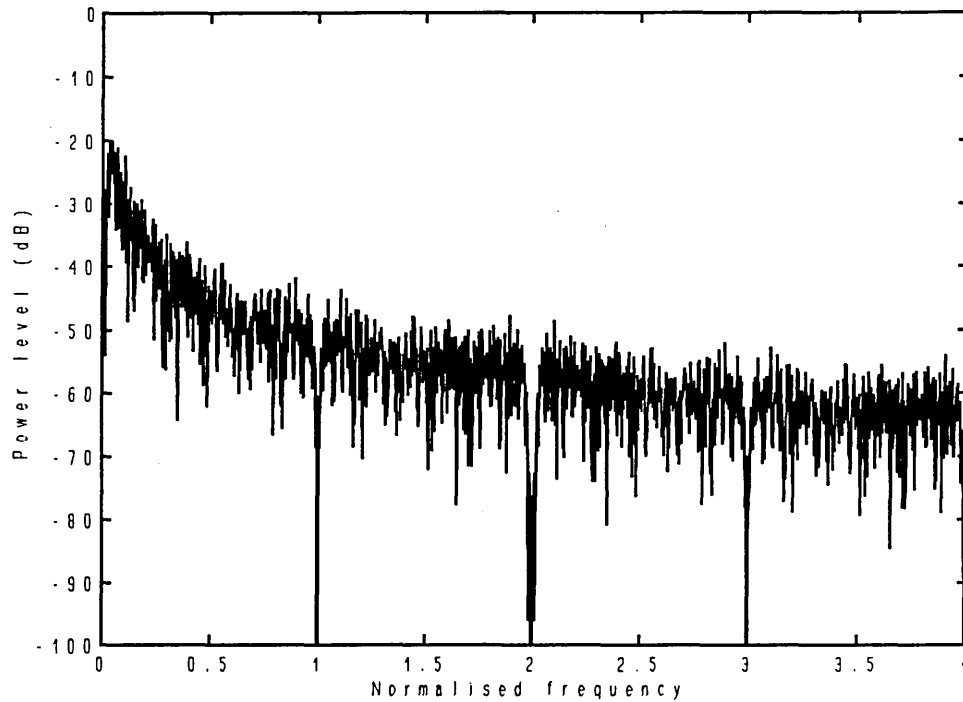
Figure 4.6 Predicted PIWCM power spectral density with $p = 8$.

4.4. PICM Code Properties

PICM is a differentiated version of PIWCM, where the transitions of each PIWCM frame are indicated with a short duration pulse (see Figure 4.2). Since PICM is generated from the PIWCM modulator, the frame length and slot rate are the same in both cases; hence the transmission capacity of PICM matches that of PIWCM. On the other hand the system bandwidth B is directly proportional to the pulse width τ. In the case of PICM, τ is assigned to be half the length of a time slot, $\tau = 0.5\ T_s$. The system bandwidth of PICM in

terms of time slots is therefore:

$$B_{PICM} = \frac{2}{T_s}$$

(4.15)

whilst for PIWCM the worst case system bandwidth is $B_{PIWCM} = 1/T_s$ and for comparison the worst case system bandwidth for PCM is $B_{PCM} = p/(2^{k+1} T_s)$.

4.5. PICM Power Spectral Density

Following a similar approach used for derivation of the mathematical model of the PIWCM pulse train $x_{PIWCM}(t)$, as in Section 4.3, the individual PICM frames $x_{PICM}(t)$ should now be considered as a construction of two mark-space sequences, $g_1(t)$ and $g_2(t)$, as illustrated in Figure 4.7. Here, only the space between constant duration pulses is modulated. The random process for PICM in terms of waveform $g_1(t)$ and $g_2(t)$ can be written as:

$$x_{PICM}(t) = A \sum_{i=-\infty}^{\infty} \left[g_1(t) \left(t - T_s \left(\sum_{a=-\infty}^{i-1} m_a + s_a \right) \right) + g_2(t) \left(t - T_s \left(\sum_{a=-\infty}^{i-1} m_a + s_a \right) - T_s m_i \right) \right]$$

(4.16)

where $g_1(t)$ and $g_2(t)$ represent the pulse shapes, placed at the beginning of mark and space respectively which compares closely to Eq. (4.9) and to the result given by Elmirghany [65].
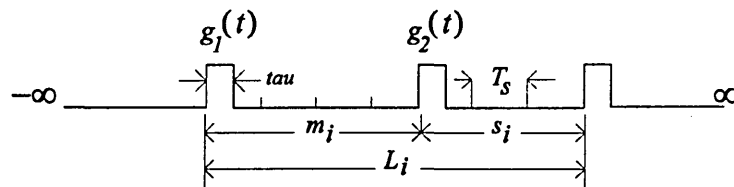
Figure 4.7 PICM pulse representation.

The spectral characterisation of a realisation of the PICM pulse train $x_{PICM}(t)$, given in Eq. (4.16), will be:

$$S(f) = \frac{1}{T_s \sum\limits_{i=0}^{N}(m_i + s_i)} \left| G_i(f) \sum_{i=0}^{N} \exp\left(-j2\pi T_s \sum_{a=0}^{i-1}(m_a + s_a)\right) \right|^2$$

$$+ \frac{1}{T_s \sum\limits_{i=0}^{N}(m_i + s_i)} \left| G_i(f) \sum_{i=0}^{N} \exp\left(-j2\pi T_s \sum_{a=0}^{i-1}(m_a + s_a) + m_i\right) \right|^2 \qquad (4.17)$$

where the pulse shape transform $G_i(f)$ for either of the mark or space sequences is:

$$G_i(f) = \frac{1}{\pi f} \sin(\pi f T_s D) \qquad (4.18)$$

where D is the duty cycle and T_s is the sampling period. With a duty cycle of 0.5, the odd harmonics of the slot frequency give inphase values to the PSD. The power spectral density obtained from Eq. (4.17) is illustrated in Figure 4.8, showing distinctive frequency components at odd harmonics of the slot frequency. Thus at the receiver, the slot rate can be extracted from the incoming data stream. The evaluated PSD of PICM using Eq. (4.17) was obtained by using random data taken over 4000 frames evaluated at 320 frequency
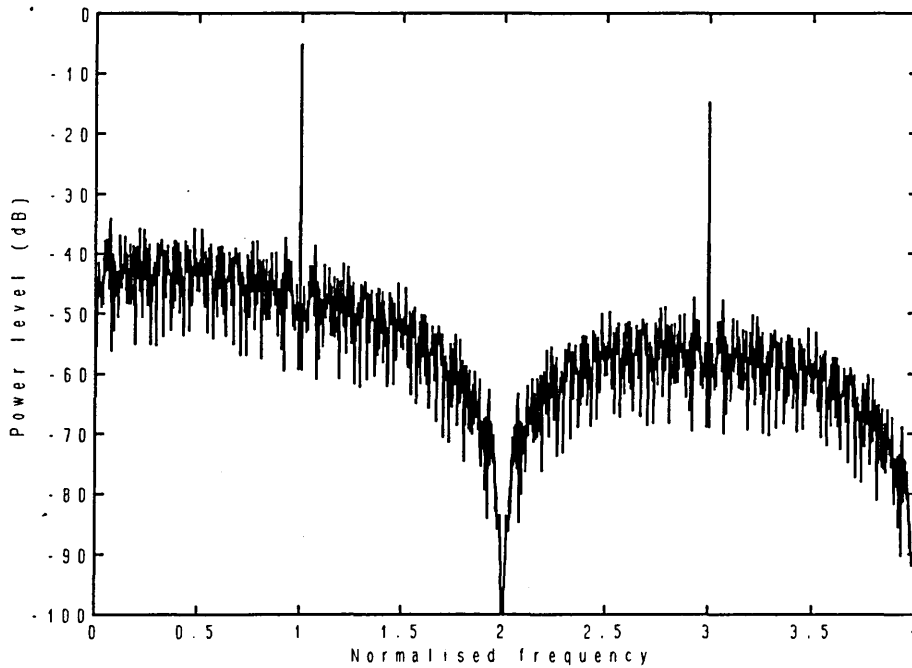
Figure 4.8 Predicted PICM power spectral density with $p = 8$.

points for 8-bit resolution, with the frequency axis normalised to the slot frequency and power level over the frequency span to 0 dBm. The Matlab algorithm for evaluation of the PIWCM power spectral density is listed in Chapter 10.1.

4.6. Error Sources

At the receiver errors occur when additive noise changes the level of the information data in the transmission channel, so that a wrong threshold decision is made at the sampling instant. The PIWCM code is recovered by determining the position of the pulse in each time frame relative to the clock interval. There are three sources of error for PIWCM:

1) Erasures: this occurs whenever noise destroys the pulse thus preventing detection. In PIWCM, this may result in change of mark and/or space, see Figure 4.9.a.

2) False alarm errors: in the interval between the start and arrival of the next rising or falling edge, the received output voltage may cross the threshold due to noise, see Figure 4.9.b.

3) Wrong slot errors: noise on the leading pulse or trailing by one time slot changes the width of mark, see Figure 4.9.c.

The effect of noise on the rising and falling edge (also known as wrong slot error) may be best explained in Figure 4.10.a where a frame may change by one or two time slots. A frame of combination (4,3), affected by wrong slot error, may be received as (4,4) or (4,5) etc., as shown in Figure 4.10.b, whilst false alarm and erasure errors may lead to a very different detected combination. For wrong slot errors the effect on the rising edge changes the length of the frame and may therefore extend or shorten the width of mark or the width of space. On the other hand, the falling edge does not influence the frame length but changes the mark-space ratio.
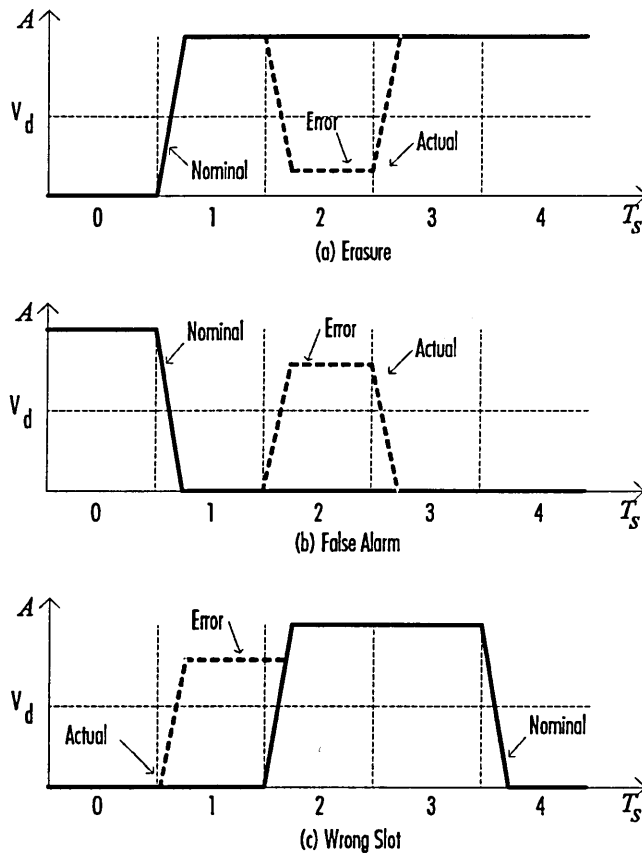
Figure 4.9 Error sources for PIWCM.

Combinations eg. (3,2) and (5,4) and those placed further away from the original frame due to very high noise levels, may not be considered, since they require errors on two edges and possibly an erasure or false alarm error in the same frame. The effect of the wrong slot changes for the code pattern (4, 3) may be summarised in Table 4.1.
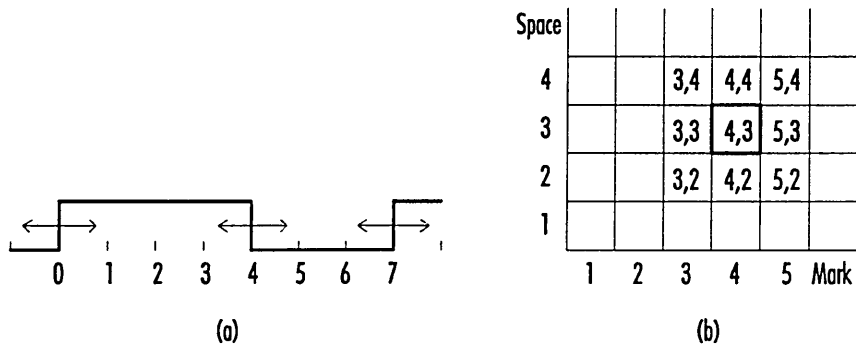
Figure 4.10 Changes in the mark-space (4,3) ratio due to noise: (a) frame; (b) coding scheme).

detected m, s	change of m, s	change of L	high-word	low-word	decimal value	level difference
3, 3	1, 0	-1	0010	0010	34	-16
3, 4	1, 1	0	0010	0011	35	-15
4, 2	0, 1	-1	0011	0001	49	-1
4, 3	0, 0	0	0011	0010	50	0
4, 4	0, 1	+1	0011	0011	51	+1
5, 2	1, 1	0	0100	0001	65	+15
5, 3	1, 0	+1	0100	0010	66	+16

Table 4.1 Effect of noise on the mark-space combination.

A change of mark by one time slot results in a level difference of ±16 quantisation levels, whereas a change of space by one time slot results in a level difference of only ±1 quantisation level. Again, this phenomenon is according to the coding rules, ie. the division into high-word and low-word where the difference of bit changes in the high-word is obviously more significant.

Error sources for PICM are similar to those of DPPM, see Page 41. Differences between PICM and DPPM error occurrences are that the PICM pulse train has two pulses per frame and these pulses are also longer than the DPPM pulses assuming the same data rate. In other words, the error rate for PICM may be twice as much as for DPPM. Furthermore, when transmitting PICM over a sufficiently long period, a point is reached where due to occurrence of erasure or a false alarm error the pulses are eventually swapped around. As a consequence, the detection of PICM forces the demodulator to convert first the low-word and then the high-word which inevitably leads to an indistinguishable recovered message signal. The error sources of PICM are of three kinds and can be described as follows:

1) Erasures: failure to detect the pulse in the signalling slot, see Figure 4.11.a

2) False alarm errors: violation by noise that causes the receiver to detect a pulse, see Figure 4.11.b.

3) Wrong slot errors: noise on the leading pulse edge produces a detection immediately preceding or following the containing pulse, see Figure 4.11.c.

(a) Erasure

(b) False Alarm

(c) Wrong Slot
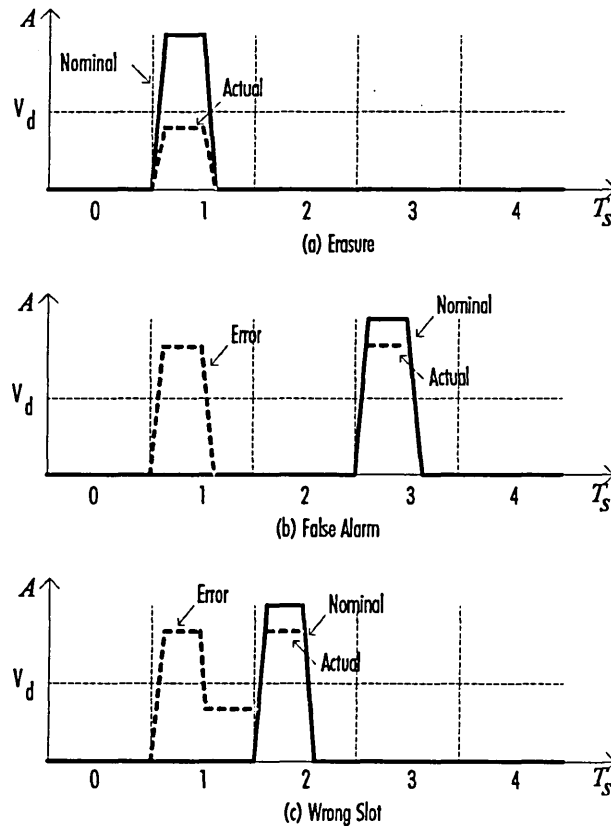
Figure 4.11 Error sources for PICM.

4.7. Summary

Theoretical properties of PIWCM and PICM techniques have been introduced in this chapter. It has been shown that the frame length varies according to the amplitude value of the modulating signal and consequently the sampling frequency varies according to the frame length. The average transmission capacity of PIWCM/PICM may be doubled compared to the fixed transmission capacity of PCM, but at the expense of increased clock

frequency and transmission bandwidth. Mathematical representations for both the PIWCM and PICM codes have been derived both in time and frequency domains. The frequency spectrum of PICM shows very distinctive peaks at the slot frequency, whereas these peaks are cancelled out in the PIWCM spectrum. Hence optimum timing extraction can be accomplished with PICM (compared to PIWCM and PCM).

Three different error sources, namely erasure, false alarm and wrong slot errors, that might affect the performance of PIWCM and PICM were introduced. Although PICM is better suited for optical transmission than PIWCM and PCM, only a single erasure or wrong slot error may have a hazardous effect on the recovered message signal. This indicates the need for a high-power drive for the optical source and/or highly sophisticated detection and filtering devices in conjunction with error correction schemes at the receiver. With PIWCM, the problem of errors is substantially less, since the receiver always synchronises on the rising edge and a frame containing an error may then be regarded as worthless. On arrival of the next correct frame, the PIWCM receiver is ready to receive the next correct sequence. Thus requiring less advanced equipment for transmission and detection compared to PICM and PCM.

CHAPTER 5

SYSTEM HARDWARE IMPLEMENTATION

5. SYSTEM HARDWARE IMPLEMENTATION

In Chapter 4, the coding rules of the PIWCM/PICM modulator were presented in which the digital input of p-bits was divided into two sets of $k = p/2$ bits. These two sets correspond to high-word (generating mark) and low-word (generating space). The design of transmitter and receiver is based upon 8-bit data converting circuits and the modulator and demodulator are implemented in programmable logic devices (PLDs).

5.1. Transmitter

Figure 5.1 shows the block diagram of the transmitter. Essentially, the analogue input signal is first buffered by an amplifier, used as an ADC driver. The ADC converts the analogue input signal into digital data at every clock interval and delivers the data to the input of the modulator. The modulator input is fitted with a D-latch. Its purpose is to take the data from the ADC one time slot before a new frame is started and to store this information until the arrival of the next instruction. Data from the output of the D-latch is fed into an 8 to 4-bit multiplexer (previously referred to the code splitter in Chapter 4) which issues first the high-word and then the low-word into the state machine. The state machine is a 4-bit counter and is based on the Moore algorithm [75]. It converts the binary information first into mark and then space producing the PIWCM frame. It is also capable of providing a short pulse at every transition within a PIWCM frame, thus generating the PICM pulse train. Furthermore, the start of frame (SOF) instruction enables the D-latch to take the next sample from the ADC just one time slot before end of frame. The transmitter circuit was implemented using a half flash ADC and an ADC driver amplifier circuit to provide low-impedance drive and capacitive load for the ADC [76].
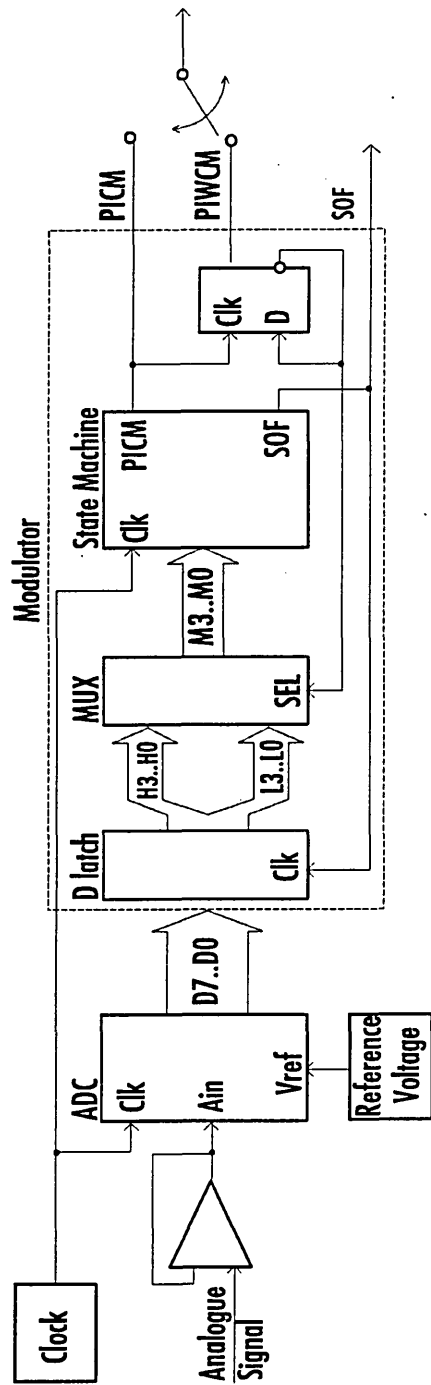
Figure 5.1 Digital PTM transmitter block diagram.

63

The 1 MHz clock input to the ADC and modulator is derived from an on board master clock generator, or alternatively, from an external frequency generator. To avoid clock or data edge crosstalk into the analogue input, or onto the ADC references, a single ground plane was used and the supply lines were heavily decoupled with good quality capacitors. All external inputs were terminated with 50 Ohm resistors.

5.1.1. Clock circuit

The master clock is used to provide overall synchronisation within the transmitter, and it also provides timing information to the receiver (clock recovery through phase locked loops may be used in future development). A 1 MHz clock is generated using a crystal controlled oscillator composed of 74LS04 [77] inverting gates, see Figure 5.2. To provide timing information for ADC, PLD and receiver, the clock signal is passed through separate buffers to supply a clean clock signal to the devices.
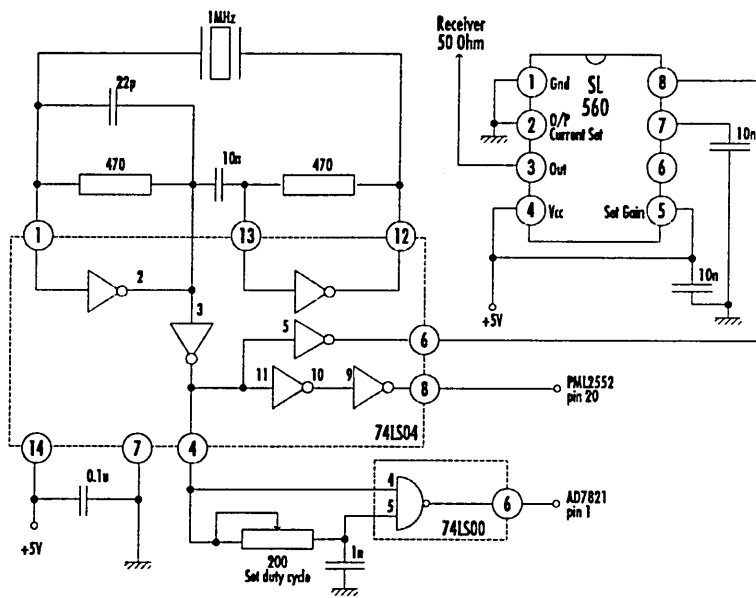
Figure 5.2 1 MHz clock generator circuit diagram.

The ADC requires a clock signal with a pulse width of greater than 530 ns, obtained through the low-pass filter 74LS00 [78] NAND gate combination. In order to connect the

receiver clock input to the transmitter, the *SL560* [79] low noise amplifier is used to provide 50 Ohm impedance drive for the clock line. Figure 5.3 shows the output of the clock generator running at 1 MHz at TTL levels.
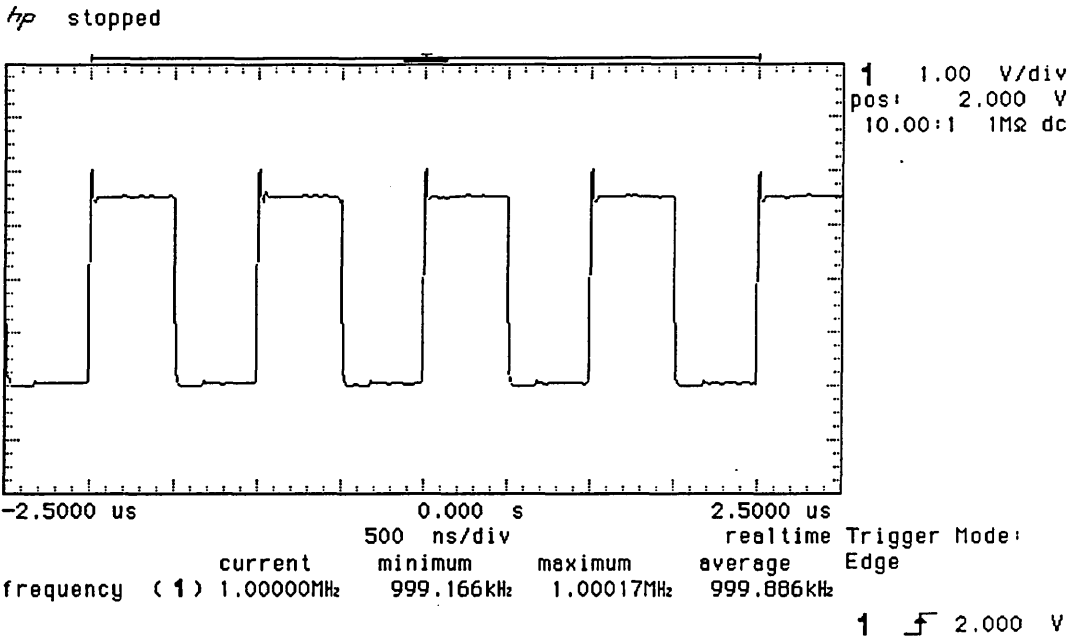
Figure 5.3 Output clock waveform.

5.1.2. ADC data conversion circuit

The requirement for a fast ADC is given by the minimum frame length of two time slots, as in the fastest case the ADC needs to sample the analogue signal every two time slots. For this task, a half flash ADC operating at half the clock frequency is required.

For the data conversion circuit in this study, the Analog Devices *AD7821* [80] 8-bit half flash ADC with TTL/CMOS outputs has been used. The AD7821 is an analogue-to-digital converter that utilises two 4-bit flash ADCs. The device contains a track and hold circuit that requires no external sampling devices, along with low power consumption and minimum package size. Figure 5.4 shows the configuration for the AD7821 in unipolar

conversion mode between zero and five volts maximum conversion range. The ADC is fed with the analogue signal at pin 1 through an amplifier circuit MAX492 and its conversion range is adjusted with the top reference to +5 V at pin 12 and the bottom reference voltage to ground at pin 11.
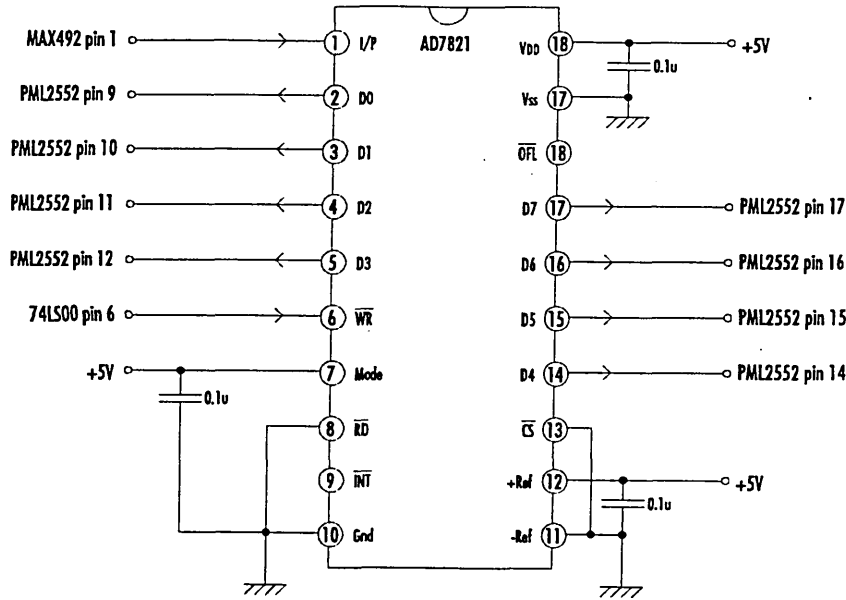
Figure 5.4 ADC circuit diagram.

The device operates in the stand alone mode, by which faster conversion times can be accomplished, since internal delay times through read-write (RD-WR) instructions are shortened. A TTL clock signal is passed into pin 6 while pin 7 is tied to high and pins 8 and 13 are tied to low. All data outputs (pins 2-5, 14-17) are fed directly into the modulating circuit PML2552. The output data are valid when pin 9 is held low. Although pin 9 is not connected to the PLD, Figure 5.5 shows the output at pin 9 (upper trace) and the PLDs inverted clock input (lower trace). This is to make sure that the modulator takes samples, at the rising clock edge, within that valid time interval. The ground layout is not separated into analogue and digital ground, thus the ADC's ground (pin 10) is connected to the solid ground plane. However, the ADC needs excellent and thorough supply

```
1   2.00  V/div
pos:    2.500  V
10.00:1   1MΩ dc


2   2.00  V/div
pos:    2.500  V
10.00:1   1MΩ dc
```

-2.5000 us   0.000 s   2.5000 us
                 500   ns/div   realtime Trigger Mode:
                                                          Edge

1 _f_ 2.500 V
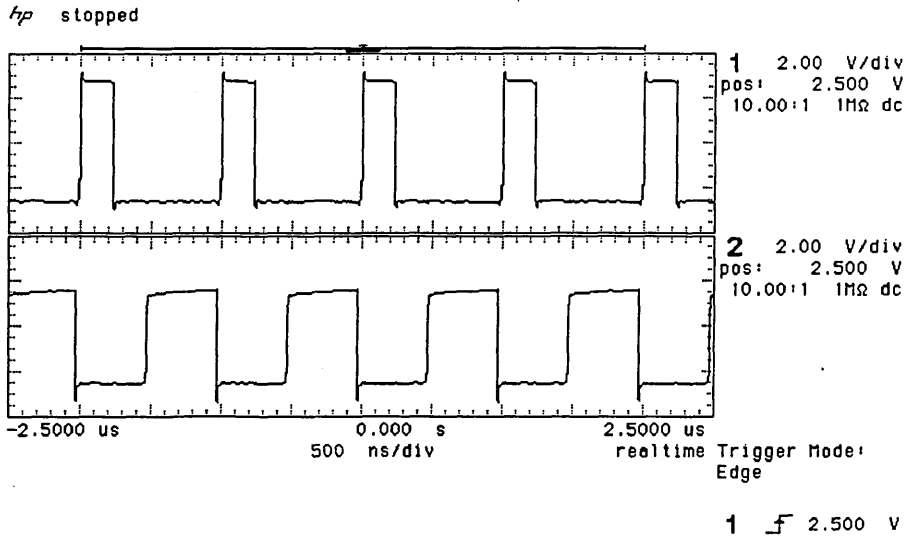
Figure 5.5 ADC and modulator clock synchronisation.

decoupling — electrolytic capacitors on the supply rail and smaller capacitors close to the

device pins.   Figure 5.6 illustrates the operation of the ADC for a 1 kHz sine wave of

maximum conversion range at pin 1 (upper trace) and the output D3, pin 5 (lower trace)

for a 1 MHz slot rate.

```
1   2.00  V/div
pos:    2.000  V
10.00:1   1MΩ dc


2   2.00  V/div
pos:    2.500  V
10.00:1   1MΩ dc
```

-1.00000 ms   0.000 s   1.00000 ms
                 200   us/div   realtime Trigger Mode:
            current   minimum   maximum   average   Edge
frequency (1) 1.00697kHz   1.00378kHz   1.01115kHz   1.00721kHz

1 _f_ 2.000 V
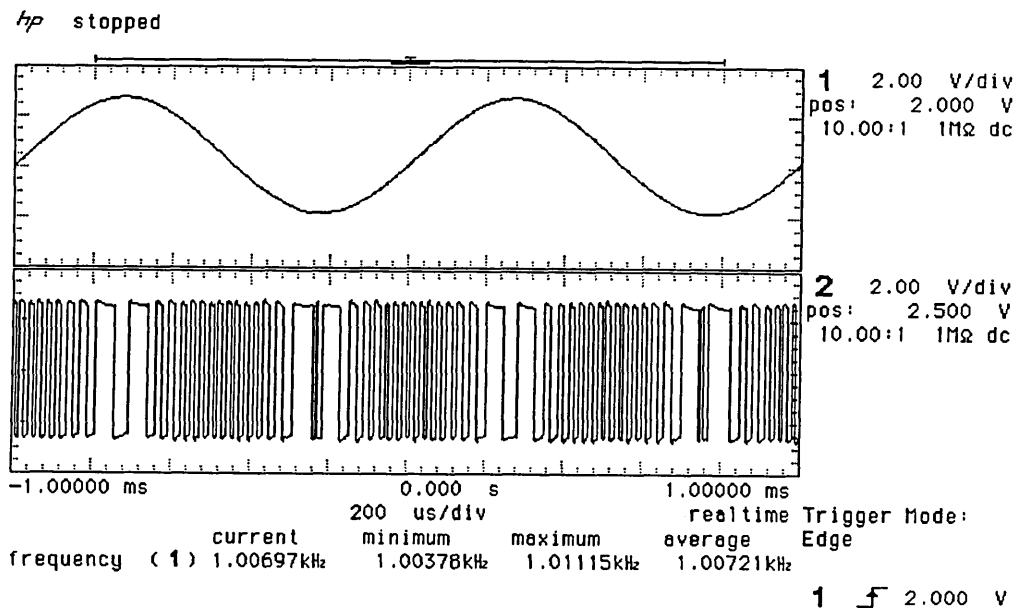
Figure 5.6 ADC operation for 1 kHz sine input and digital output D3.

5.1.3. ADC driver circuit

The analogue input of the AD7821 is connected to comparators and hence it has an input capacitance of a maximum of 55 pF. This capacitance is slightly voltage dependent and varies the ADCs input current; therefore it is important to provide a low impedance drive for the AD7821, which can be achieved with the *MAX492* [81] ADC driver amplifier. The MAX492 is an op-amp that can drive capacitive loads in excess of 1000 pF by altering the output current. The input signal is 5 V_{p-p} and is fed into a unity gain non-inverting buffer operated from a single +5 V supply, the input signal is centred at +2.5 V. Figure 5.7 shows the circuit diagram for the MAX492. The external input is terminated with 50 Ohms before being input to pin 3. Supply line decoupling is achieved with a 0.1 µF ceramic capacitor at pin 8 in conjunction with the on board decoupling electrolytic capacitors at the power supply.
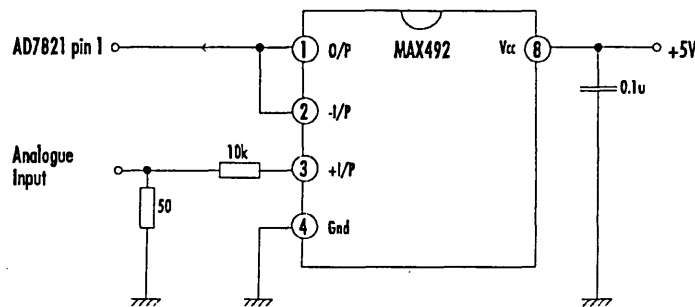
Figure 5.7 ADC driver circuit diagram.

5.1.4. Modulator

The modulator consists of four modules, see Figure 5.1. First, a D-latch, at the input of the modulator which samples the digital output of the ADC and stores it for the time duration that is required for generating the PIWCM/PICM frame. Second, an 8 to 4-bit multiplexer splits the 8-bit information sequentially into high-word and low-word. Third, a Moore state machine counts the number of time slots according to the binary information of either the low-word or the high-word issuing a pulse at the start of either word — thus forming the

PICM sequence. And, finally, the pulses from the Moore state machine are converted by a D-type flip-flop into the PIWCM sequence.

AD7821 pin 2	(9)	D0	PML2552	Vcc	(4)	o +5V
AD7821 pin 3	(10)	D1		Reset	(8)	
AD7821 pin 4	(11)	D2		Vcc	(21)	
AD7821 pin 5	(12)	D3		Vcc	(27)	
AD7821 pin 14	(13)	D4		Vcc	(38)	
AD7821 pin 15	(14)	D5		Vcc	(57)	
AD7821 pin 16	(16)	D6				10n
AD7821 pin 17	(17)	D7		Gnd	(15)	
74LS00 pin 6	(20)	Clock		Gnd	(32)	
	(22)	Disp0		Gnd	(37)	
	(23)	Disp1		Gnd	(49)	
	(40)	Disp2		Gnd	(66)	
	(41)	Disp3				
	(42)	Disp4		SOF	(46)	+5V
	(43)	Disp5		PICM	(47)	
	(44)	Disp6		PIWCM	(48)	Transmission channel 50 Ohm
	(45)	Disp7		Init	(50)	5k
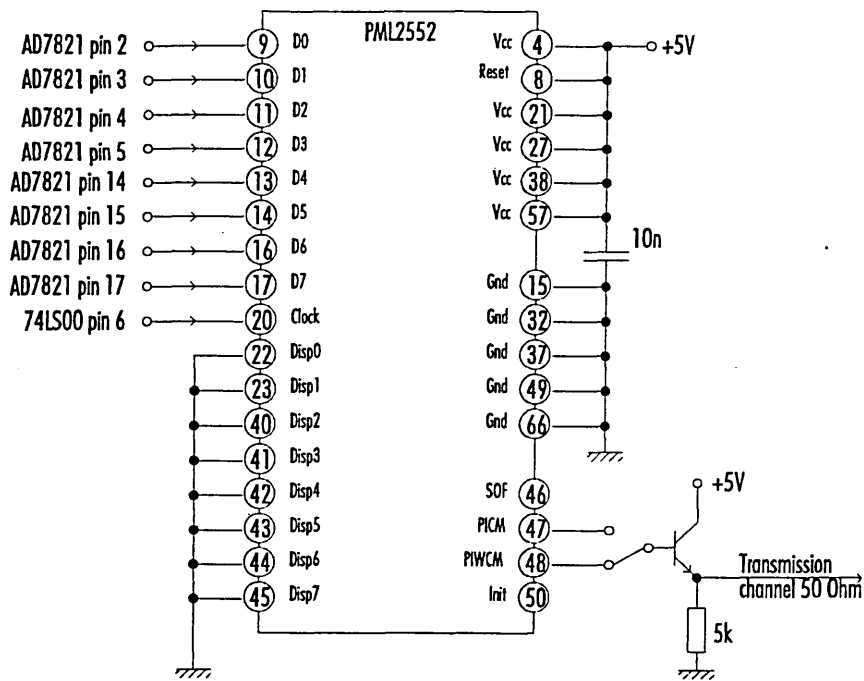
Figure 5.8 Modulator circuit diagram.

Figure 5.8 shows the pin layout of the modulator device *PML2552* [82]. The digital inputs from the AD7821 are fed directly into the PML2552 pins 9-14, 16-17. The TTL clock is input to pin 20. Displacement inputs Disp7..0, pins 22-23, 40-45 are connected to digital ground. Pin 8 is the designated reset input and is connected to the power supply Vcc. The reset function will be performed when power is switched off, so that a network of flip-flops will be reset to its initial states.

With reference to Figure 5.1 the process of enabling the D-latch is best illustrated in Figure 5.9. The D-latch samples the valid ADC outputs (D7..0) on receiving the start-of-frame (SOF) instruction (upper trace) from the modulator pin 46 and when AD7821 pin 9 is low (lower trace).

1   2.00 V/div
pos: 2.500 V
10.00:1   1MΩ dc

2   2.00 V/div
pos: 2.500 V
10.00:1   1MΩ dc

-2.5000 us   0.000 s   2.5000 us
                          500 ns/div   realtime Trigger Mode:
                                                                   Edge

1 _f 2.500 V
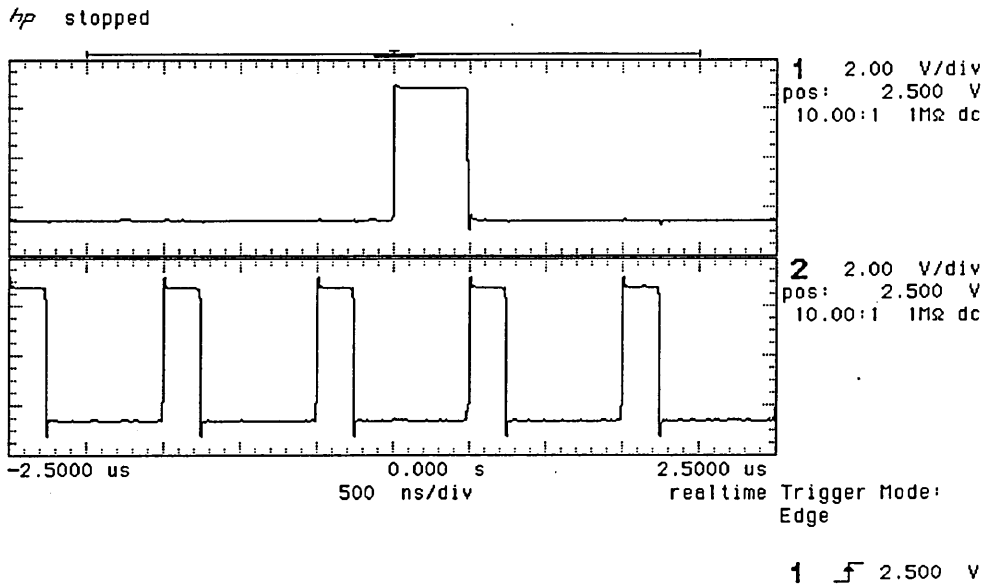
Figure 5.9 Modulator and ADC synchronisation.

The data input D7..0 is XORed with displacement data Disp7..0 which may be used for

the input of an offset or coded data, so that the D7..0 could be manipulated at every time

slot. For modulator PLD programming please refer to Section 5.4.

1   2.00 V/div
pos: 2.500 V
10.00:1   1MΩ dc

2   2.00 V/div
pos: 2.500 V
10.00:1   1MΩ dc

-25.000 us   0.000 s   25.000 us
                          5.00 us/div   realtime Trigger Mode:
+width   (1) 6.01190us   -width   (1) 5.00057us   Edge

1 _f 2.500 V
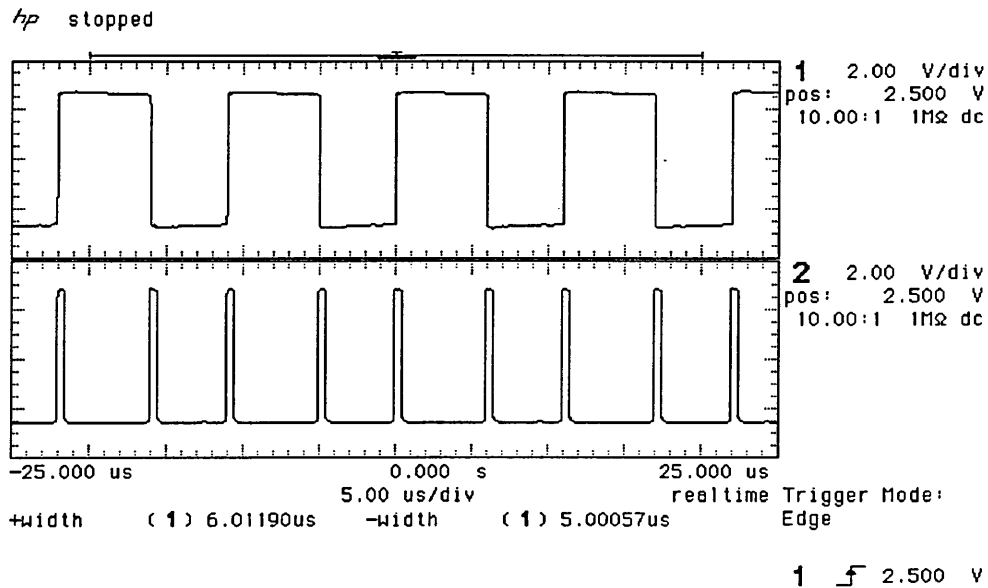
Figure 5.10 Modulator output.

The PIWCM (pin 48) or PICM (pin 47) outputs may be selected through a switch and directed into the 50 Ohm transmission channel. SOF, pin 46, and Init, pin 50, are used for reference only and are not connected. Figure 5.10 shows the observed output of the transmitter for a constant dc voltage level with a mark-space combination of 6,5; PIWCM (upper trace) and PICM (lower trace).

5.2. Transmission Channel

Either electrical or optical transmission of the PIWCM and PICM wave trains can be chosen. The electrical link is a coax cable of one meter length, connecting transmitter and receiver. In order to simulate the transmission channel, a noise signal is added to the transmitted signal. For measurements of the BER, a circuit for error detection has been implemented, see Figure 5.11.
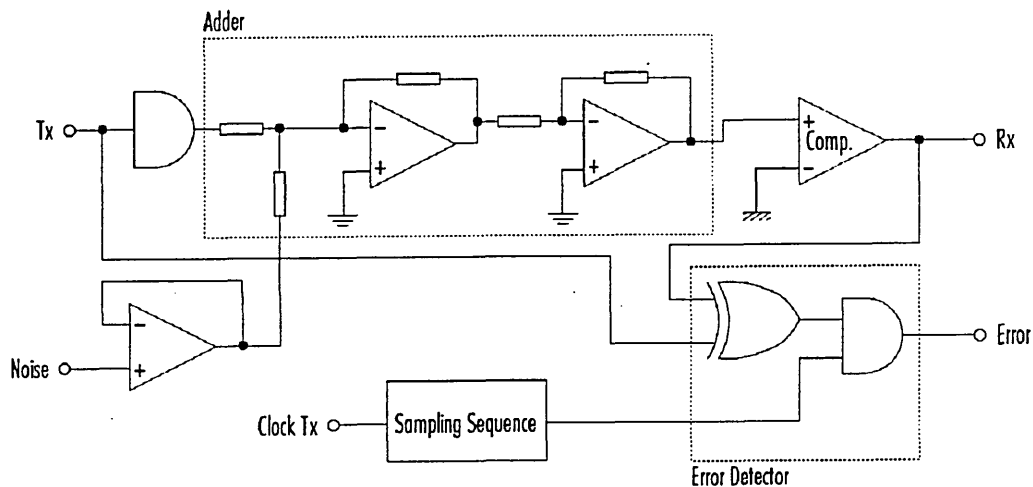
Figure 5.11 Transmission channel and error detector block diagram.

5.2.1. Signal and noise adder

Figure 5.12 shows the circuit diagram of the signal and noise adding circuit. Where necessary 50 Ohm termination impedance has been used. Both the modulated signal and
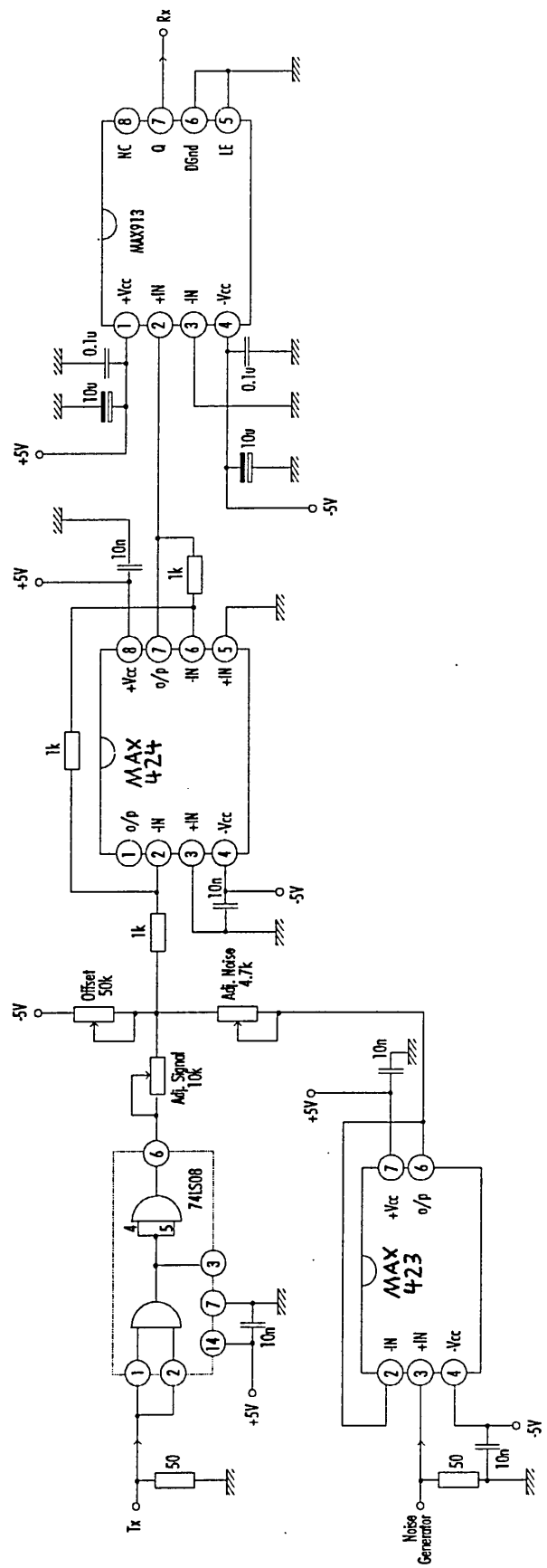
Figure 5.12 Signal and noise adding circuit.

72
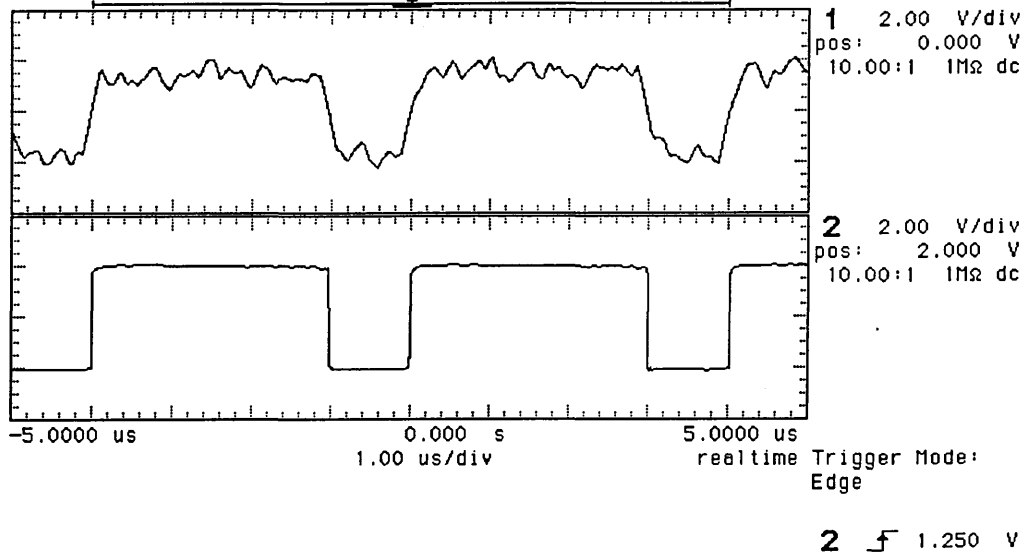
Figure 5.13 PIWCM waveform: (a) input and (b) output comparator.
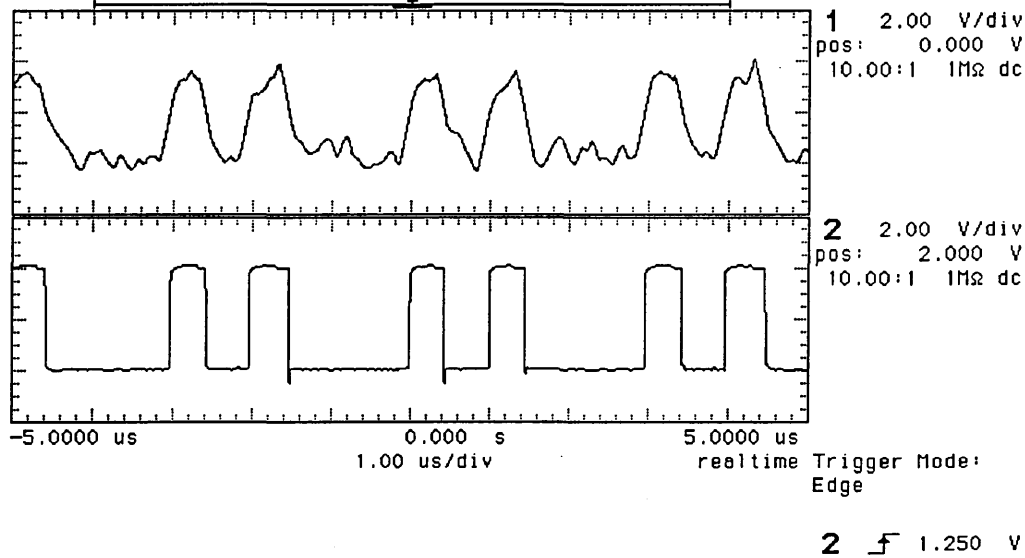
Figure 5.14 PICM waveform: (a) input and (b) output comparator.

the noise are buffered before being added with an AND gate *74LS08* [83] and with an amplifier *MAX423* [84]. A wide bandwidth amplifier *MAX424* [84] has been used, that basically determines the transmission bandwidth of the transmission channel.

The noise contaminated signal is then passed through a threshold detector, constructed of a fast comparator *MAX913* [85] with the threshold level set to half the peak amplitude of the received PIWCM/PICM pulse train. This eliminates the amplitude related noise of the pulse train and reproduces the PIWCM/PICM waveform. Pin 5 is connected to ground in order to make the comparator latch transparent. To minimise unwanted parasitic capacitances, the supply lines +Vcc and -Vcc were decoupled to the digital ground plane with 10 μF tantalum capacitors and with electrolytic 0.1 μF capacitors very close to the pins. Figure 5.13, illustrates the input and PIWCM output waveforms of the comparator, whilst Figure 5.14 shows the PICM input and output waveforms of the comparator.

5.2.2. Sampling instants and error detection

Having regenerated the digital PTM signal, it is then compared with the transmitted PTM signal. The resulting signal is then sampled at the optimum points in order to detect any error that might have resulted due to the presence of noise. In both cases (PIWCM/PICM), the sampling points were set at the middle of each bit, see Figure 5.15.
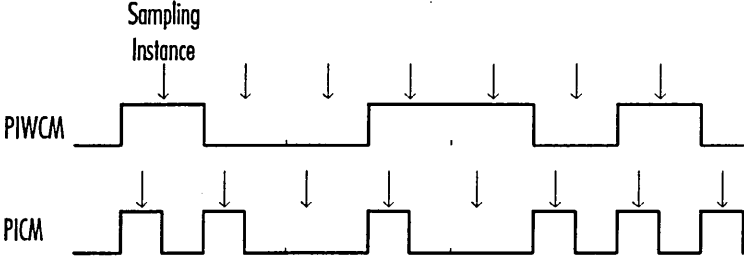
Figure 5.15 Sampling points for digital PTM.

Two monostable multivibrators with Schmitt-trigger inputs *SN74121* [86] were used to generate the sampling pulses. The first monostable shifts the sampling point along the time axis and the second monostable adjusts the duration of the sampling pulses. In order to detect fewer errors, the duration of the sampling pulses is kept very small, ie. 100 ns. Since the sampling pulse width may accommodate more than one error pulse, this pulse width should be small, eg. 100 ns. Figure 5.16 shows the circuit diagram of the sampling and error detection circuit.
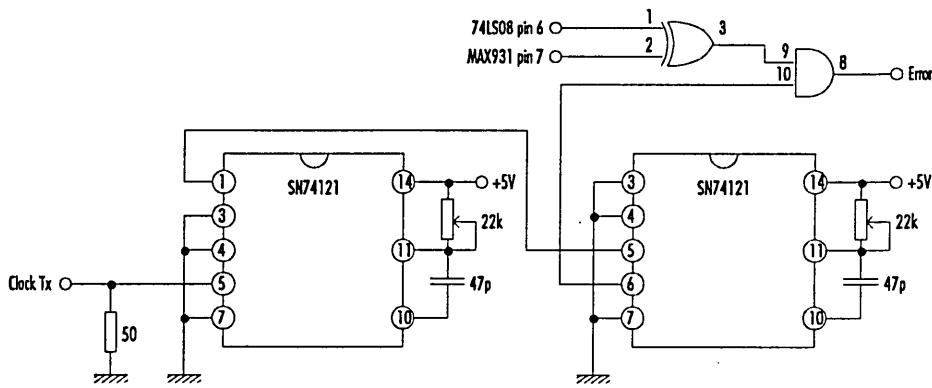
Figure 5.16 Sampling and error detection circuit.

5.2.3. Optical transmission

The optical transmission system being used was based upon the Hewlett Packard transmitter *HFBR-14X2* [87] and receiver *HFBR-24X4* [88], operating at a wavelength of 820 nm. The fibre being used was a two meter 50/123 μm graded index. Figure 5.17 shows the optical receiver output for PIWCM (upper trace) and PICM (lower trace).

5.3. Receiver

At the receiver, after electrical to optical conversion and threshold detection, once again a Moore state machine is employed to convert the PIWCM/PICM pulse trains into an 8-bit parallel word by counting ones and zeros. Two sets of D-latches were connected to the
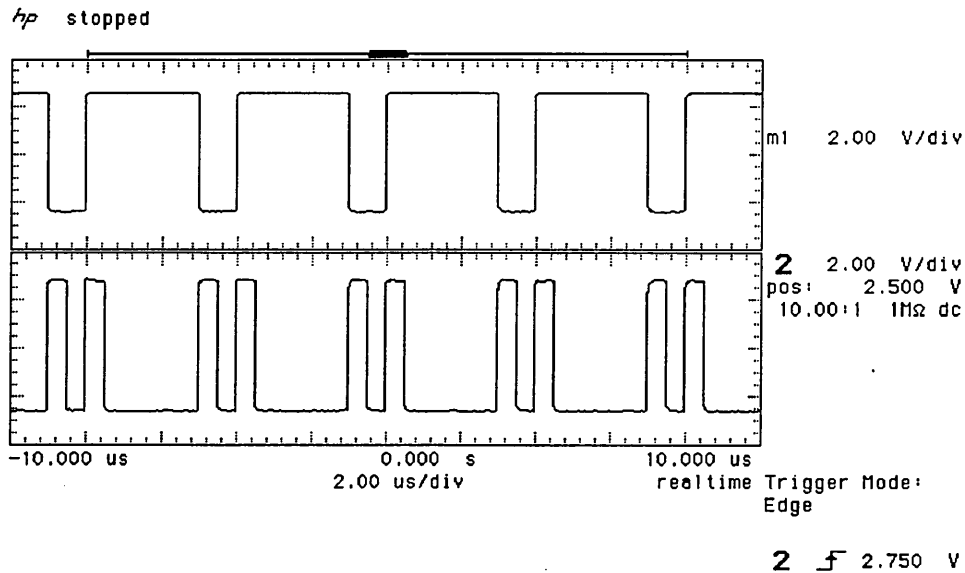
Figure 5.17 Optical receiver output waveforms.

output of the demodulator state machine; one for the high-word and one for the low-word, see Figure 5.18. Together they provide the recovered 8-bit word for the DAC. The DAC is clocked with a VALID pulse indicating the end of conversion which is issued by the state machine. The output stage of the transmitter is a 2nd order active Butterworth filter with cut-off frequency of 5 kHz. In this prototype system, synchronisation is simply achieved by deriving the master clock from the transmitter and delaying its pulses with a monostable. The demodulator is triggered with the rising edge of the delayed clock.

5.3.1. Demodulator

The operation of the demodulator is very similar to that of the modulator. Figure 5.19 shows the pin layout of the demodulator. It is capable of demodulating both PIWCM and PICM signals. However, the PICM pulse train is converted into PIWCM using a D-type flip-flop before being fed into the state machine see Figure 5.18. The clock is derived from the clock line driver circuit SL560 pin 3 (see also Figure 5.2) and is fed into the demodulating circuit PML2552 pin 20. The displacement inputs Disp7..0 between pins 9-14 and 16-17
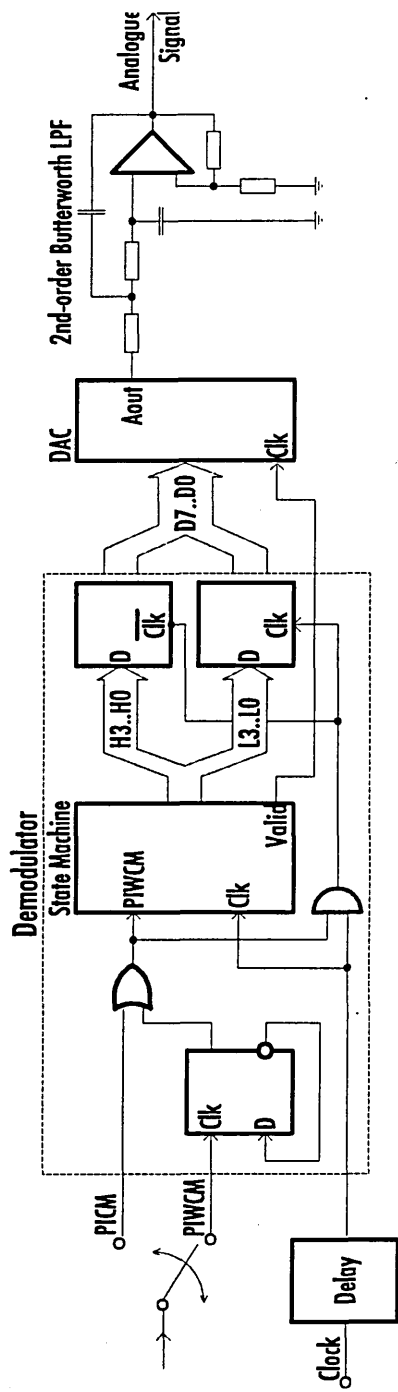
Figure 5.18 Digital PTM receiver block diagram

were directly connected to digital ground. The digital outputs D7..0, pins 54-50, 48-46 were directly input to the digital-to-analogue converter. A VALID pulse (pin 67) is issued when the frame sequence has been converted. Its negative complement (pin 68) initiates the conversion process of the DAC with its falling edge. If an error occurs (ie. mark or space is longer than 16 time slots) during transmission the output at pin 1 goes high and stays high until a correct frame pattern has been received. The demodulator PLD programming algorithm is further described in Section 5.4.
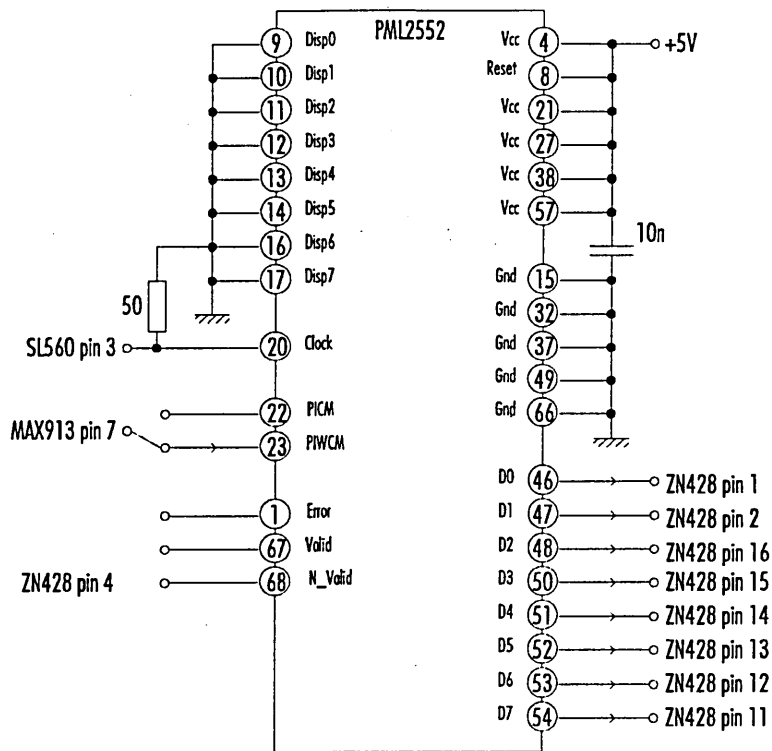
Figure 5.19 Demodulator circuit diagram

5.3.2. DAC data converting circuit

For digital-to-analogue conversion, the Plessey *ZN428E8* [89] monolithic 8-bit D-A converter with input latches in unipolar operation mode has been used. The ZN428E8 has a settling time of 800 ns which is less than the period of one time slot (T_s = 1 µs).

Figure 5.20 shows the circuit diagram for the data conversion circuit at the receiver. The input latches are controlled by the inverted Enable input at pin 4. Data from the demodulator are taken when the N_Valid (pin 68 PML2552) goes low and are held throughout the process of conversion until arrival of the next N_Valid instruction. The reference voltages between Vref In (pin 6) and analogue ground (pin 8) for the ZN428E8 are set by the 390 Ohm resistor placed between pins 6 and 10. A stabilising capacitor between pins 7 and 8 is required for the internal reference option, Vref Out being connected to Vref In. The analogue output (pin 5) is connected to the input of the low-
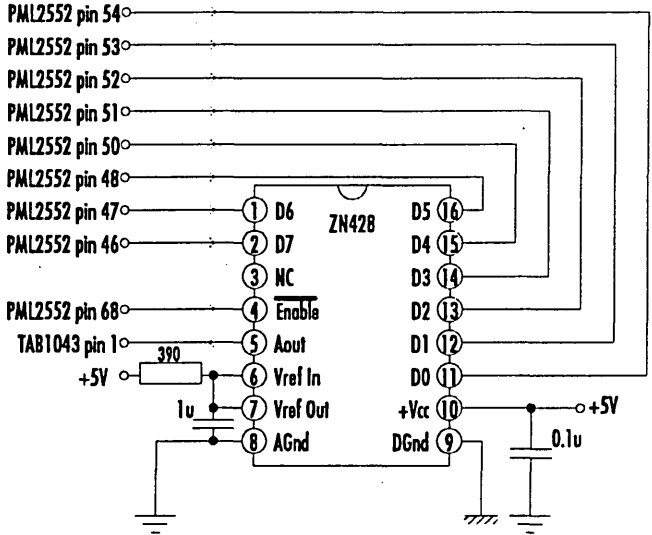
Figure 5.20 DAC circuit diagram

pass filter TAB1043 pin 1. Figure 5.21 compares the analogue input at the ADC with the output of the DAC, for a 1 kHz triangular waveform with an amplitude of 2 V_{p-p}, showing that the signal has been faithfully recovered.

5.3.3. Output low-pass filter and amplifier

A simple 2nd-order active Butterworth low-pass filter has been used. With a 2nd-order low-pass filter a roll-off of 40 dB per decade can be achieved, giving sufficient attenuation between the desired analogue signal of under 5 kHz and the 1 MHz clock signal.

79

```
1   2.02  V/div
pos:    2.529  V
10.00:1   1MΩ  dc


2   928  mV/div
pos:    1.256  V
10.00:1   1MΩ  dc
```

```
-290.00 us          -40.00 us          210.00 us
                   50.0 us/div                     realtime Trigger Mode:
                                                            Edge

                                        1  _ƒ  3.497  V
```
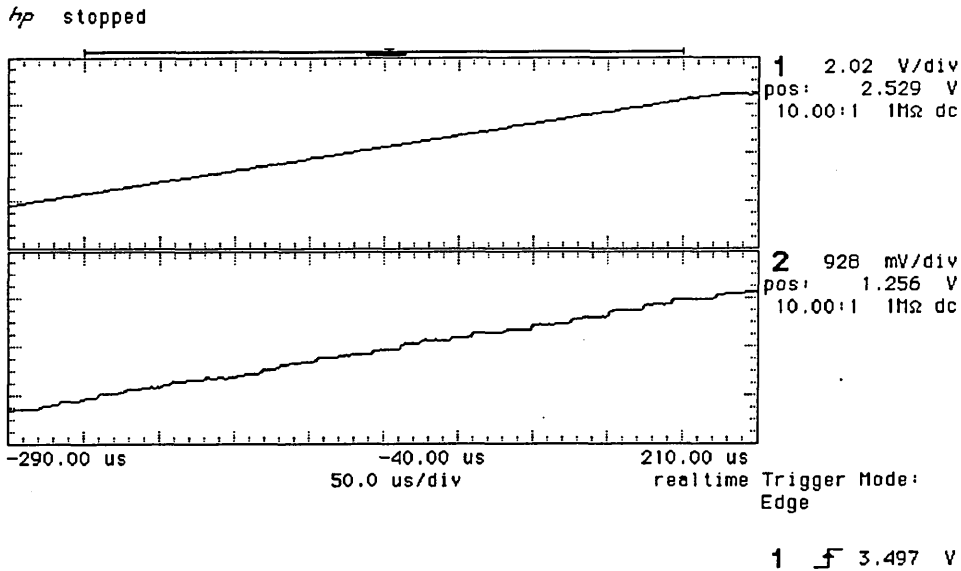
Figure 5.21 1 kHz triangular wave: (a) analogue input; (b) DAC output.

Figure 5.22 shows the circuit implementation of the receiver output stage using the Plessey *TAB1043* [90] operational amplifier. This device has an operating frequency range under 1 MHz, so the clock waveform is partly attenuated by the device itself and further attenuation for the analogue signal is accomplished with the filter design. The input bias for pin 16 is set by the 100 kOhm variable resistor which also determines the frequency response of TAB1043. The component values for the low-pass filter were calculated using a GW Basic based program given by Middlehurst [91].
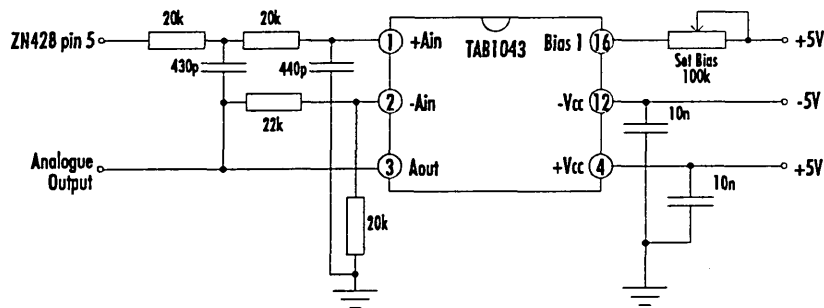
Figure 5.22 2nd-order active Butterworth filter circuit diagram

5.4. Modulator and Demodulator PLD Programming

Design details for modulator and demodulator were presented in the preceding sections. Here, the author wishes to give further details about in the PLD programming and the algorithms used to implement the design. Programmable logic devices (PLDs) were used to accommodate all logic circuits of the modulator in a single chip according to the specification given in Section 4.2., thus making the system layout simpler. Advantages of PLDs are [92]:

1) Simplified design because of large number of available gates.

2) Substitution of layout with an enhanced version without the need for changing the chips pin-layout.

3) Implementation of state machines in PLD devices.

The most important advantage is that digital circuits can be designed with state machines, rather than designing an equivalent circuit for the state machine at gate level and having to balance the timing with buffers as with asynchronous digital networks [75].

The modulator and demodulator are programmed in a Philips programmable macro logic *PML2552* [82] that provides gate arrays capabilities for general purpose logic integration. The PML2552 incorporates the PML folded NAND array architecture and flip-flop building blocks which provide 100% connectivity to eliminate routing restrictions. The devices have been programmed with the Snap [93] development software which gives easy access to the density and flexibility of the PML2552 through a variety of design entry formats, including schematic, logic equations and state equations in any combination. The PLD programming followed the approaches specified in Philips application notes [94, 95].

5.4.1. Modulator state algorithm

Figure 5.23 illustrates the circuit equivalent schematic for the modulator which has been translated into the Snap compatible equation (see Chapter 10.3) format suitable for programming the Philips PML2552. The heart of the modulator is a Moore state machine performing the transformation of parallel code into a sequence of pulses. Its design can be described in 18 states. After resetting all flip-flops to state zero (INI), the state machine performs the transformation of 4-bits parallel into sequential pulses. It converts first the high-word then the low-word.

Figure 5.24 represents the modulator state diagram where state zero (M0) and state sixteen (M16) are associated with the start of the high-word and start of the low-word respectively. The states in between represent the number of time slots to be counted. Having received the binary data (e.g. 1111) the state machine jumps from its present state (M0) to its new state S15 and sets a network of flip-flops in the state machine and performs the counting operation. Conversion of the high-word is completed when S1 is reached. On arrival of the low-word the state machine once again changes its state from present state to M16 and starts counting down to state S1. Whenever the states M0 and M16 are passed, the state machine issues a pulse which is then converted by a D-type flip-flop into the PIWCM sequence. Looking at the output of the flip flop, state M0 indicates the rising edge and state M16 indicates the falling edge of the PIWCM pulse train.

5.4.2. Demodulator state algorithm

A complementary Philips PML2552 is also used as a demodulator and it has been programmed with the Snap development software, as listed in Chapter 10.5. The demodulators circuit equivalent schematic is shown in Figure 5.25
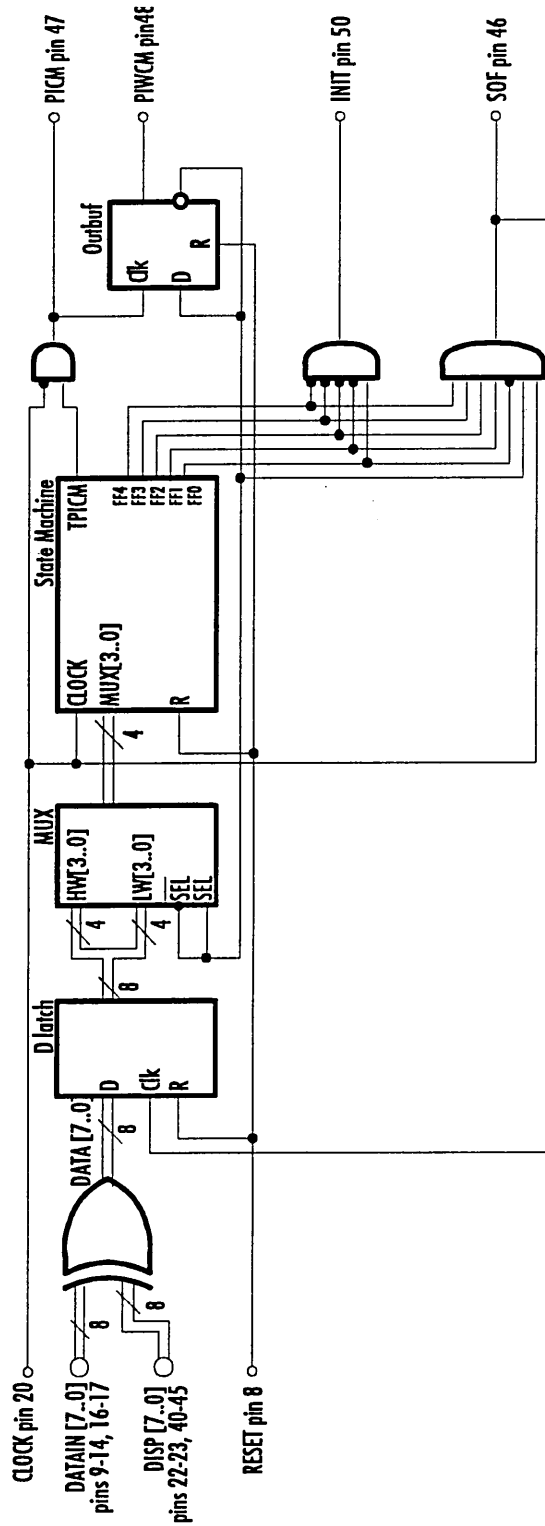
Figure 5.23 Modulator circuit equivalent schematics.

83
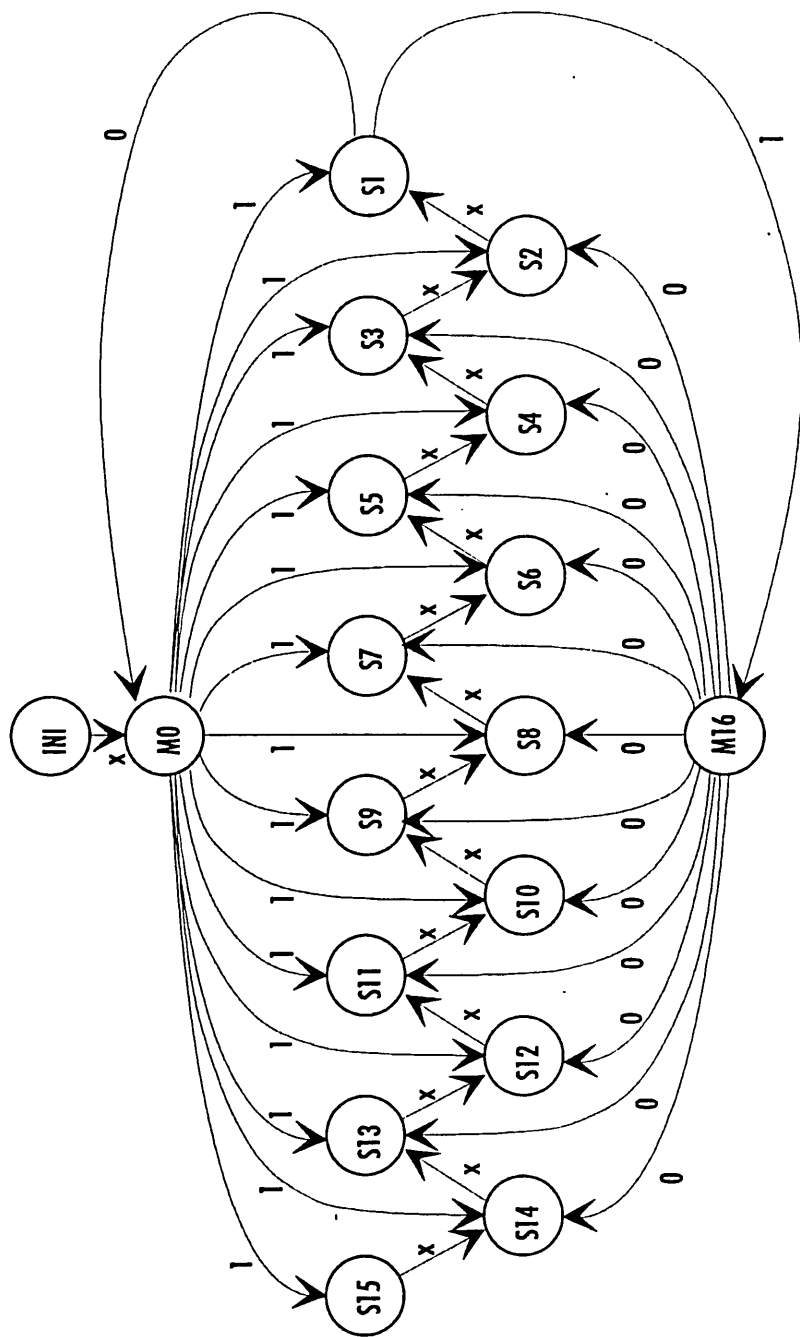
Figure 5.24 Modulator state algorithm

84

The receiver Moore state machine is illustrated in Figure 5.26. It converts the received sequential information of the PIWCM pulse train into an 8-bit parallel word by counting ones and zeros. The initial state of the state machine is M16 and it counts down at every clock cycle. Receiving a PIWCM frame of one mark and one space will result in jumps between the states M0 and M16. If a different code word is detected, for example sixteen marks and three spaces, the state machine counts upwards until state S15 is reached, returns back to M16 and counts to the new state of S18. Any sequence longer than sixteen time slots will result in an error until a transition in the opposite level is received. Two sets of D-latches are connected to the output of the demodulator state machine; one for the high-word and one for the low-word. Together they provide the recovered 8-bit word for the DAC. The DAC is clocked with a pulse indicating the end of conversion which is issued by the state machine.

5.5. Summary

In this Chapter, the design and implementation of the digital PTM systems have been discussed. Both the modulator and demodulator have been carried out using single chip programmable logic devices. Appropriate captured waveforms were also shown in order to confirm the operation of the system. The PLD implementation proved to be successful as the design was improved by reprogramming the devices and not changing the hardware layout. State machine algorithms for code generation and detection were presented through state diagrams. The hardware performance will be further discussed in Chapter 7.
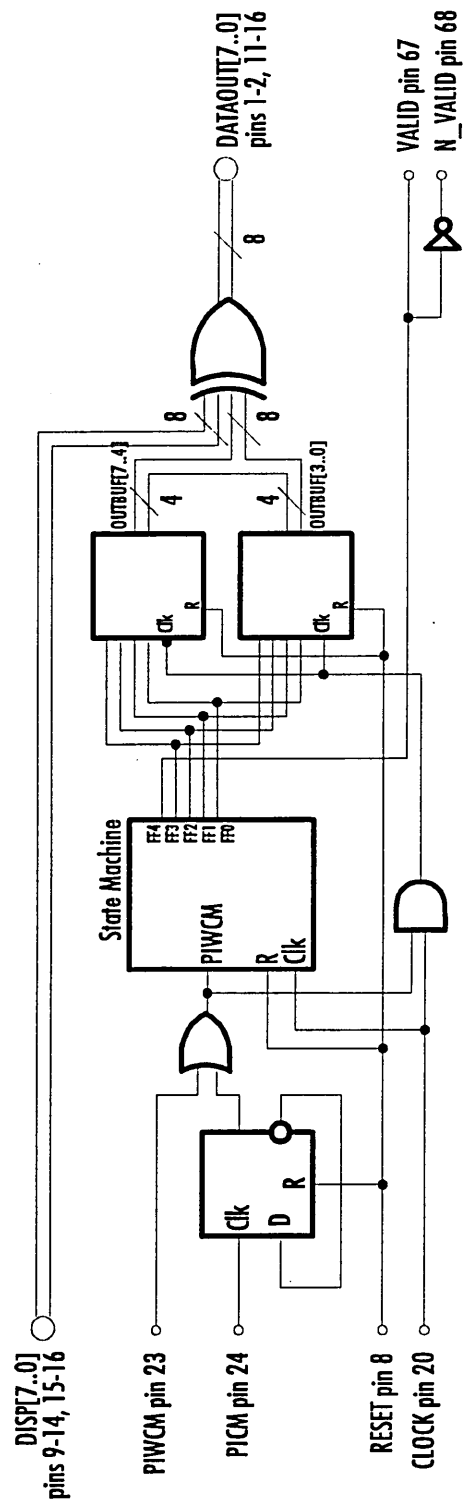
Figure 5.25 Demodulator circuit equivalent schematics.

86
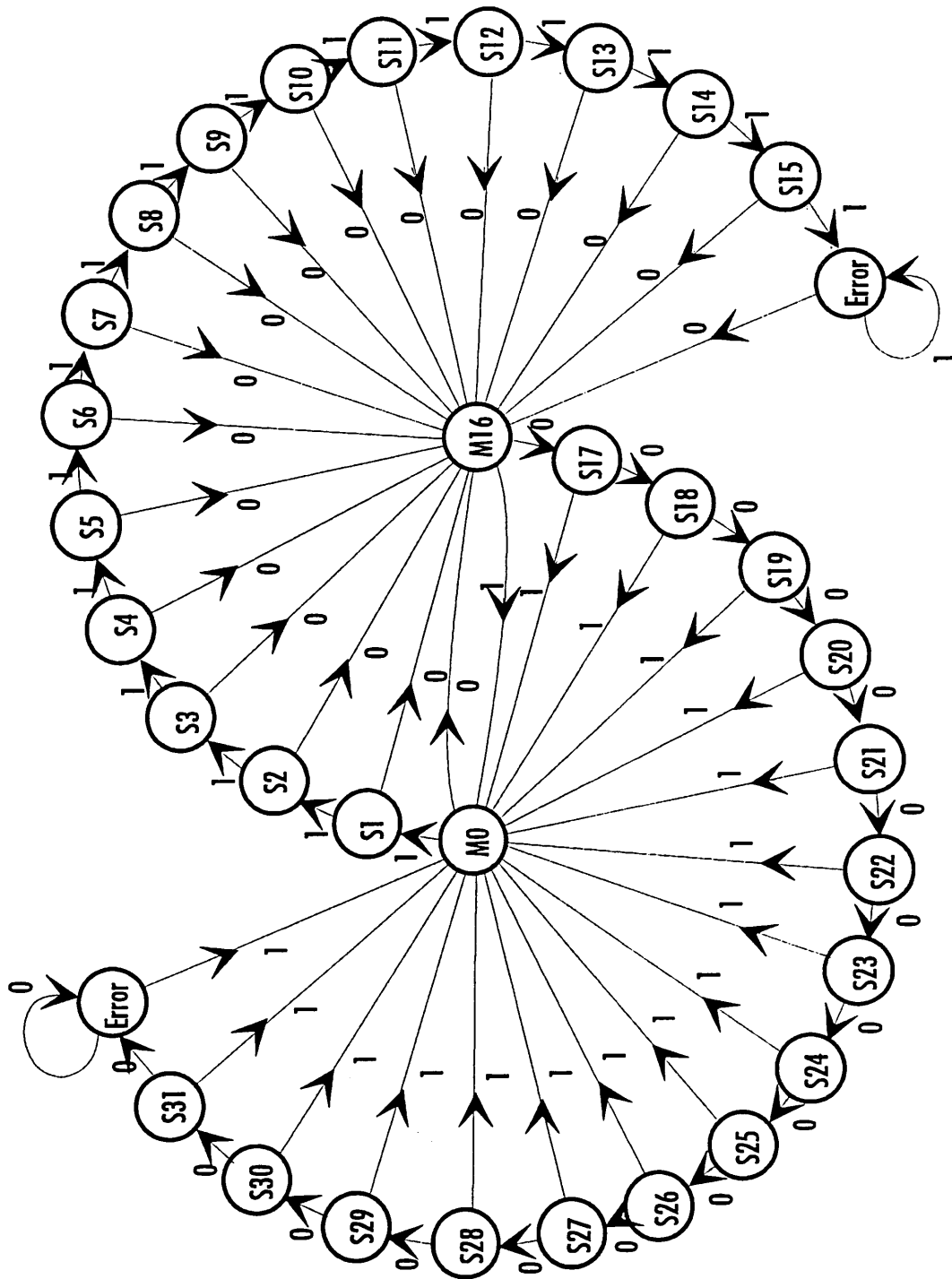
Figure 5.26 Demodulator state algorithm

87

CHAPTER 6

MATLAB SIMULATION PACKAGE

6. MATLAB SIMULATION PACKAGE

In conjunction with the hardware implementation of the digital PTM system, described in Chapter 5, a software simulation package based on Matlab has been developed.

Software simulation is a tool which may be used to help designers to analyse the system performance well in advance. Advantages of software simulation are:

1) Design changes can be made easily and results readily obtained which otherwise may take a significant amount of time in the real hardware system.

2) Several case studies could be carried out without the risk of destruction or damage to the hardware.

3) Has the possibility to vary all parameters of interest, thus allowing the designer to optimise the system prior to hardware realisation.

Although simulation adds another step in the developing process of the product, the overall task is speeded up and optimised [96].

The complete digital PTM system can be conveniently modeled with the Matlab software package, version 4.2 for MS-Windows [97]. Matlab stands for matrix laboratory and is a multipurpose scientific software package for numeric calculations. It allows expressions of a programming algorithm as in any other programming language. Macros and instructions can easily be written and tailored for specific needs. This makes Matlab applicable to many engineering problems [98]. Therefore, Matlab is the appropriate package to carry out the entire software simulation of the digital PTM system.

6.1. Overall Software Approach

In developing the software attention was paid to making the resulting software user friendly and easy to handle. Simulation is carried out in a number of consecutive steps. The software is divided into three basic sections (transmitter, channel, receiver) and their sub-sections. The simulation package can be accessed via graphical user interface (GUI) routines which provides the link between processes through commonly defined matrices. These matrices reside in Matlab's memory and their elements can be called on demand. This provides an efficient and clearly structured intercommunication process between the Matlab command window and the dialogue boxes.

Four menus are available in the Matlab based graphical user interface. They provide easy access to relevant dialogue boxes that enable the user to emulate the process of modulation and demodulation. The GUI is based upon a top-to-bottom and left-to-right pull-down menu structure.

6.2. Organisation of the Software

The software package is designed to model accurately the behaviour of the existent hardware system and includes the following features.

1) Input: analogue signal, digital code pattern or text string.

2) Sampling, analogue-to-digital convertor and modulator.

3) Channel bandwidth and noise.

4) Threshold and pre-detection filters.

5) Demodulator, digital-to-analogue convertor and filtering.

6) Time and frequency representation and error analysis.

The software package is organised in the command window which gives simple access to the system modules by providing hierarchally structured pull-down menus as shown in Figure 6.1. They prompt the user to the relevant dialogue boxes or to the Matlab prompt and hence to let the user to interact with the simulation package.
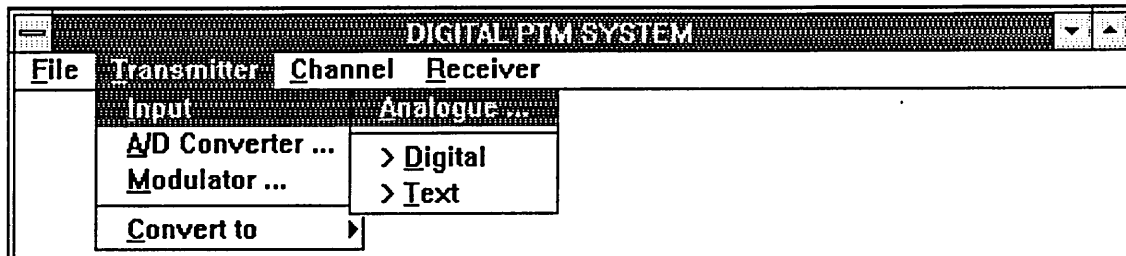
Figure 6.1 Command window menus.

File menu: allows the user to apply system functions during the Matlab session such as load and save workspace and frame construct.

Transmitter menu: allows the user to set-up the input format for transmission before being encoded and modulated. The structure of the transmitter menu is based upon the data exchange between the analogue input, the A/D conversion, the modulator dialogue boxes and the data entry through an 8-bit binary matrix or a text string. Figure 6.2 shows that the analogue input may be accessed through the ADC and the modulator dialogue boxes or, alternatively, it may be directly converted into binary format before being converted with the convert to digital menu option into the PIWCM/PICM pulse trains. When choosing digital or text string entry, the input data does not need to be processed since the binary matrix is already generated. The user may then return to the transmitter dialogue box in order to prepare the codes for transmission in different modes. The transmitter dialogue boxes allow the user to generate a particular code pattern of a given mark-space combination, for a specific amplitude. The number of frames generated is a function of bits used.

90
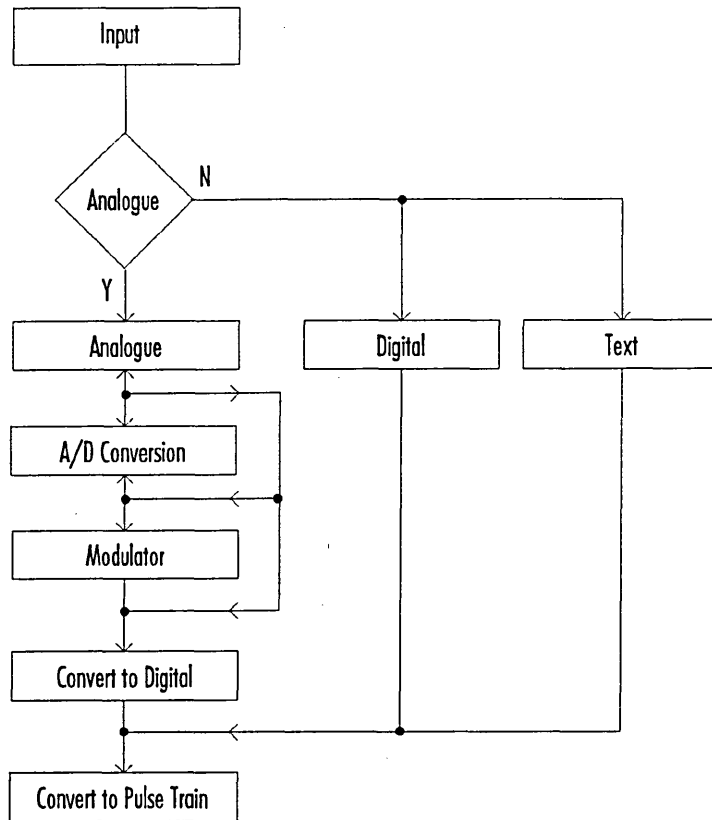
Figure 6.2 Transmitter input options.

In this study, the maximum number of frames generated is 256. This is independent of the shape and the number of oscillations of the input signal.

Channel menu: allows the user to select the appropriate code to be transmitted (PIWCM or PICM). It also defines the electrical channel bandwidth and sets the noise parameters. The limitation on the channel bandwidth will affect both the transmitted signal and the noise. Its influence on the overall code behaviour can be shown graphically in time or frequency domain as shown in Figure 6.3.

Receiver menu: incorporates signal slicing, pre-detection filtering, demodulation and final filtering along with the display of the recovered waveform. System performance
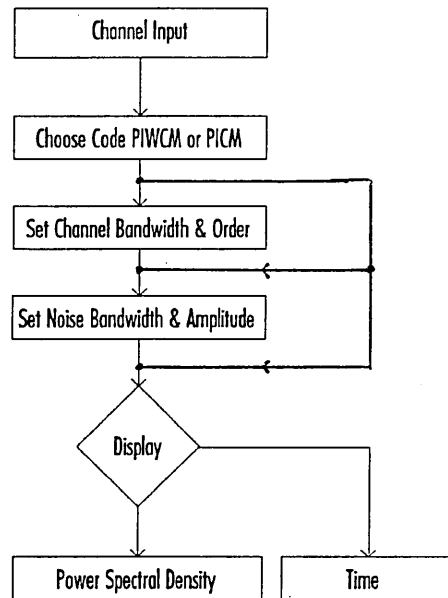
Figure 6.3 Transmission channel setup and display options.

indicators, such as probability of errors versus carrier-to-noise ratio are also carried out in this menu. Figure 6.4 shows the receiver menu structure.

6.3. Procedures of Simulation Routines

Most of the written m-files are functions used to automate long sequences of commands. The advantage of using functions in Matlab is that variables within the body of the function are all local variables and only occupy workspace memory when this particular function is called. Upon releasing the function from its computational process, memory space allocated for local variables is cleared and provided for other processes. Global variables are system variables that reside permanently in Matlab's memory.

Dialogue boxes have a number of check boxes, text edit fields, sliders and push buttons. The values of elements in dialogue boxes are stored in globally assigned variables, which represent the dialogue box in Matlab's workspace. Each of the variable's elements is called on demand, ie. when the corresponding (or a function related) dialogue box is
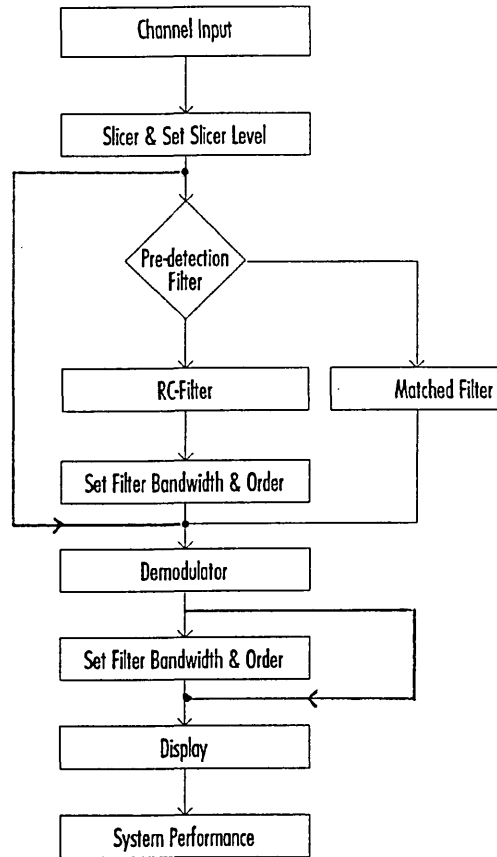
Figure 6.4 Receiver menu structure.

invoked via the command window. For example, the system variable PLOTPAR is generated by the chplot.m function, representing the channel display dialogue box. Within the simulation package, the global variables are written with capital letters thus: GLOBAL_VARIABLE and local variables are written with upper and lower case letters, thus: Local_Variable.

6.3.1. Frame construct

The function frame.m takes the user to the Matlab prompt and it generates a frame combination when a decimal value has been entered. It utilises the dec2bin.m function as illustrated for an 8-bit frame length code.

```
function [M, S, F]=frame(val,res)
%FRAME    returns the system's code construction according to the
%  decimal input value.
%  [M, S, F]=FRAME(VAL,RES);
%  M: mark, S: space, F: frame length
%  VAL: decimal value for 8 bit val is valid for within the
%      interval 0 <= VAL <= 255
%  RES: resolution of ADC, 8 for 8 bits, 12 for 12 bits
...
res=8;
...
if rem(res, 2)==0
    n=2^(res/2);
    if val <= 2^res-1
        M=floor(val/n)+1;
        S=rem(val,n)+1;
        F=M+S;
        Mbin=dec2bin(M-1, res/2);
        Sbin=dec2bin(S-1, res/2);
        ...
        disp(['I/P value: ',num2str(val)])
        disp([' (M,S)=F:   (',num2str(M),',',num2str(S),')=',...
            num2str(F),' TS'])
        disp(['Binary:     ',num2str(Mbin),' ',num2str(Sbin)])
        ...
    end
    ...
end
```

6.3.2. Decimal to binary conversion

This converts decimal values into binary by using the dec2bin.m function. The default

resolution is 8-bits, hence the decimal values will range between zero and 2^8-1.

```
function bin=dec2bin(dec, res);
%DEC2BIN is the decimal to binary conversion of a given decimal
%  value DEC that returns the corresponding binary value BIN.
%  The resolution of the conversion can be specified with RES.
%  Default usage 8-bit BIN=DEC2BIN(DEC);
%  assigning another resolution, eg. BIN=DEC2BIN(DEC, 12);

%check if i/p is integer
if any(dec ~= round(dec))
    dec=round(dec);
    disp('Requires integer argument. Use nearest value instead.')
end
...
%check for if input fits resolution
if 2^res-1 < dec
    dec=2^res-1;
    disp('Input exceeds resolution. Use maximum value instead.')
end
%start conversion
bin=[]; x=dec; i=0;
```

```
for i=1:res
    bin=[bin rem(x, 2)];
    x=floor(x/2);
end
bin=fliplr(bin);
```

6.3.3. Load initial screen

To load the initial screen, the file codepic.mat in the code directory is loaded,

containing the variables picture and map and deletes these variables after loading into

the command window in order to free some workspace memory while storing picture

and map in the figure handle.

```
%LOADSCR loads the initial screen
if exist('codepic.mat')
    load codepic
else
    disp('*.mat file not existent, check with ''what''')
end
colormap(map)
set(gca, 'position',[0 0 1 1])
image(picture)
axis off
clear map picture
```

6.3.4. Text string input

The input for the digital PTM system can be chosen according to the user specification.

One option is to select the text string input on the Matlab prompt. The ttext.m function

generates the binary equivalent of the text input string in the BINARY variable. Further

processing is necessary in order to generate the variable BINVAL that will be used by the

modulator.

```
function [BINARY, TSTRING]=ttext
%TTEXT enter text and convert digitally
%   [BINARY, TSTRING]=TTEXT;
...
disp('Enter string to be transmitted')
disp('for example: ''Hello World''')
binary=input('String= ');
TSTRING=binary;
binary=(binary-0);
if length(binary) >= 256
    disp('Data not valid.  String is reduced to 256 elements')
    binary=binary(1:256)';
```

```
else
    [a, b]=size(binary);
    binary=[binary zeros(a, 256-b)]';
end
%assign output parameter
BINARY=[];
for i=1:256
    BINARY=[BINARY dec2bin(binary(i))'];
end
BINVAL=binary;
BINARY=BINARY';
...
```

6.3.5. Sampling

Sampling of the analogue input signal is accomplished through equally spaced samples.

The anisochronous nature of PIWCM and PICM is not taken into account. The function

bin256.m generates a maximum of 256 samples independent of the number of cycles of

the input signal.

```
function [BINVAL,SAMPLE]=bin256
%BIN256 samples the analogue waveform at equally spaced
%    intervals for an 8-bit resolution, eg. 256 values.  If the
%    number of oscillations is large, the whole wave form is still
%    divided into 256 samples, but the space between them is wider
%    than for one oscillation. [BINVAL, SAMPLE]=BIN256;
...
spoint=(length(WAVE_FORM)-1)/256;
spoint=spoint:spoint:256*spoint;
time=1:length(WAVE_FORM);              %generate reference vector
Vq=(Vmax-Vmin)/255;                    %voltage of each level
...
%divide analogue signal into 256 equally spaced points
sample=interp1(time, WAVE_FORM, spoint);    %interpolate signal
...
%generate samples
for i=1:256
    if Vmin > sample(i), sample(i)=Vmin; end
    if Vmax < sample(i), sample(i)=Vmax; end
end
sample=round((sample-Vmin)/Vq);
BINVAL=dec2bin(sample);
SAMPLE=sample;
...
```

6.3.6. Analogue to digital conversion

Before modulation can take place, the input signal (analogue or text string) must be

converted into binary format. The adc8.m routine divides the analogue waveform

96

WAVE_FORM into 256 equally spaced quantisation levels representing the full amplitude

range. The algorithm for conversion utilises the dec2bin.m routine.

```
function [BINVAL, HEXVAL]=adc8(mode, n, Nmin, Nmax, display)
%ADC8    8-bit analogue-digital converter at clock speed
%  Conversion within 256 levels equally spaced in the specified
%  range or fixed automatically.
%  MODE: conversion mode 'A' best fit, 'N' for normal fit
%  N: decimal counter variable specified for real amplitude
%     range of ADC
%  NMIN: minimum amplitude value (must be greater than zero)
%  NMAX: maximum amplitude value
%  DISPLAY: include if display is desired
...
%sampled waveform must have 256 values
sig=WAVE_FORM(1:(length(TIME)-1)/255:length(TIME));
%best amplitude fit
if strcmp('A', mode)
    Nmax=max(WAVE_FORM); Nmin=min(WAVE_FORM);
    %make analogue signal positive
    sig=abs(Nmin)+sig;
    %fix extrema
    Nmax=max(sig); Nmin=min(sig);
end
%specified ADC amplitude range
if strcmp('N', mode)
    ...
    %fix amplitude range
    for j=1:length(sig)
        if sig(j) < Nmin, sig(j)=Nmin;
        elseif sig(j) > Nmax, sig(j)=Nmax; end
    end
end
%fit quantisation to amplitude range
q=(Nmax-Nmin)/255;
...
%find value of sig(n)th element
elseif (n >= 0) & (n <= 255)
    n=n+1;
    val=round((sig(n)-Nmin)/q);
    HEXVAL=dec2hex(val);
end
...
%perform A/D conversion
BINVAL=dec2bin(val);
...
```

6.3.7. Modulator

Modulation of the globally assigned binary matrix BINVAL is performed by the mod.m

function which generates the desired PIWCM and PICM pulse trains. The variable POINTS

is to the length of the fundamental time slot and the variable MODPAR is the system

variable of the modulator dialogue box.

```
function [PICM, PIWCM, DTIME]=mod
%MOD returns PICM & PIWCM modulated code
%   [PICM, PIWCM, DTIME]=MOD;
%   PICM: pulse interval code modulated signal
%   PIWCM: pulse interval code width modulated signal
%   DTIME: returns PICM's associated time vector
...
%get resolution
if ADCPAR(6)==1
    res=4;          %8-bits
    ...
end
%get pulsewidth for PICM
pw=POINTS*MODPAR(11);
%get r,c of BINVAL
[r,c]=size(BINVAL);
%get decimal value and assign high and low word
bin=BINVAL;
high=bin(:,1:res);
low=bin(:,res+1:2*res);
...
%count discrete states for word
mark=0; M=0;
space=0; S=0;
for i=1:r
    mark(i)=bin2dec(high(i,:))+1;
    M=linspace(1,1,mark(i)*POINTS);
    space(i)=bin2dec(low(i,:))+1;
    S=linspace(0,0,space(i)*POINTS);
    piwcm=[M S];
    PIWCM=[PIWCM piwcm];
    picm_m=zeros(1, mark(i)*POINTS);
    picm_m(1:pw)=linspace(1,1,pw);
    picm_s=zeros(1, space(i)*POINTS);
    picm_s(1:pw)=linspace(1,1,pw);
    picm=[picm_m picm_s];
    PICM=[PICM picm];
    ...
end
...
%generate associated time vector
DTIME=0:length(PIWCM)-1;
DTIME=DTIME./POINTS;
```

6.3.8. Channel properties

A Butterworth low-pass filter is employed to simulate the transmission channel. This is
carried out by using the channel.m function for a frequency range of 1 MHz to 10 MHz
and filter order of 1 to 7.

```
[c,d]=butter(filt_ord,Wchannel);
piwcm=filter(c,d,PIWCM);
picm=filter(c,d,PICM);
```

It is assumed that noise will affect the transmitted signal during transmission. Matlab provides various routines to generate noise. Here, white and Gaussian noise is used, generated with the Matlab function: `noise=namp*randn(size(PIWCM));`. Further filtering may be used in order to bandlimit the noise before it is added to the signal. A simple function of `CODE=piwcm+noise;` is used to simulate signal plus noise. The carrier and noise power are measured separately, and the signal-to-noise ratio is obtained accordingly by utilising the `signr.m` function:

```
%SIGNR   signal-to-noise ratio of 'Signal' and 'Noise'
%   [SigRMS, NoiseRMS, SNRdB]=SIGNR(S, N);
noisems=mean(N.^2); NoiseRMS=sqrt(noisems);
sigms=mean(S.^2); SigRMS=sqrt(sigms);
SNR=sigms/noisems;
SNRdB=10*log10(SNR);
```

6.3.9. X-Y scope

The time domain display of the signals at any point in the transmission system is catered for by the function `scope.m`. It has self-adjusting amplitude range capabilities and the it can sweep through the entire discrete time range, at a specified interval, read from the global system variable `PLOTPAR` and is being initiated through `chplot.m`.

```
function scope(X, Y)
%SCOPE   continuous display of a specified signal in time domain.
%   SCOPE(X, Y); displays the self-adjusting signal
%   X: x-vector, eg. time
%   Y: y-vector, eg. amplitude
...
if strcmp(action, 'start')
    figure
    set(gcf,'Color',[0 .7 0], 'MenuBar','none','Name',...
        'X-Y Scope','NumberTitle', 'off');
    set(gca, 'Position', [.1 .2 .85 .7]);
    axis off
    axes(gca)
    plot(X, Y, 'y', 'EraseMode', 'none')
    set(gca,'XGrid','on','YGrid','on');
    axis([0 PLOTPAR(17) ymin ymax]);
    %push button OK
    uicontrol('Style','PushButton','String','OK',...
        'Position',[.1 .05 .12 .08], 'Units', 'normalized',...
        'CallBack','close(gcf)');
    %define slider
    uicontrol(gcf,'Style','text',...
        'Position',[.4 .09 .25 .04],...
        'Units','normalized',...
```

```
        'Backgroundcolor',[0 .7 0],...
        'String','Sweep Time Slots');
    PLOTPAR(20)=uicontrol(gcf,'Style','slider',...
        'Position',[.35 .05 .35 .04],...
        'Units','normalized',...
        'Min', 0, 'Max', max(X), 'Value', 0,...
        'Callback',[...
            'PLOTPAR(19)=round(get(PLOTPAR(20),''Value''));',...
            'set(gca,''Xlim'',[PLOTPAR(19) PLOTPAR(19)
                +PLOTPAR(17)]),']);
    uicontrol(gcf,'Style','text',...
        'Position',[.3 .05 .05 .04],...
        'Units','normalized',...
        'Backgroundcolor',BG_COLOUR,...
        'String',num2str(get(PLOTPAR(20),'Min')));
    uicontrol(gcf,'Style','text',...
        'Position',[.7 .05 .1 .04],...
        'Units','normalized',...
        'Backgroundcolor',BG_COLOUR,...
        'String',num2str(get(PLOTPAR(20),'Max')));
    %set scale
    uicontrol(gcf,'Style','text',...
        'Position',[.85 .09 .1 .04],...
        'Units','normalized',...
        'Backgroundcolor',[0 .7 0],...
        'String','Scale');
    PLOTPAR(18)=uicontrol(gcf,'Style','edit',...
        'Position',[.85 .05 .1 .04],...
        'Units','normalized',...
        'Backgroundcolor',BG_COLOUR,...
        'String',num2str(PLOTPAR(17)),...
        'Callback',[...
            'set(gca,''Xlim'',[PLOTPAR(19) PLOTPAR(19)
                +PLOTPAR(17)]),',...
            'PLOTPAR(17)=str2num(get(PLOTPAR(18),''String''));']);
end
```

6.3.10. Power spectral density

This displays the spectral behaviour of the transmitted PIWCM and PICM using the
chplot.m function. It utilises the psd.m signal processing toolbox function according
to the user specified or self-adjusting PSD resolution nfft. Furthermore, it allows the user
to zoom in to the spectrum.

```
...
%include NFFT
if PLOTPAR(11)==1
    pow=str2num(get(PLOTPAR(14),'String'));
    nfft=2^pow;
else
    nfft=2^round(log2(length(CODE)));
end
```

```
. if PLOTPAR(9)==1
    ...
    [Pxx, F]=psd(CODE,nfft,freq,'none');
    Pxx=10*log10(Pxx/nfft);
    ...
    plot(F, Pxx)
    ...
    uicontrol('Style', 'PushButton', 'String', 'Zoom In',...
        'Position',[0.3 0.05 0.12 0.07], 'Units', 'normalized',...
        'CallBack','zoom on, set(gcf,''pointer'',''crosshair'')');
    uicontrol('Style', 'PushButton', 'String', 'Zoom Out',...
        'Position',[0.5 0.05 0.13 0.07], 'Units', 'normalized',...
        'CallBack','zoom out; set(gcf,''pointer'',''arrow'');');
...
```

6.3.11. Pre-detection filter

The receiver performance (in the sence of absence of errors) can be improved by incorporating a pre-detection filter instead of a simple threshold detector or slicer: `code=CODE-slicer_level;` The simulation package is capable of simulating both types of filters: RC-filter (of a specified order and cut-off frequency) and matched filter. For the RC-filter, the filter function from the Matlab signal processing toolbox is used within the `recgen.m` function.

```
[a,b]=butter(order,fco);
code=filter(a,b,code);
```

In contrast to the RC-filter, a matched filter is independent of any bandwidth, since it operates on the basis of integration. The data are changed from unipolar to bipolar before being integrated. Ideally, any positive or negative code level would result in a positive or negative slope ramp by which the noise level should be averaged to zero by the end of each bit period. However, in a real system, the integrator is reset to its initial value zero at the end of each bit period. The resetting times of PIWCM and 50% duty cycle of PICM are one and ½ time slot respectively. Therefore, the matched filter function `match.m` must be able to select between the integration time for PIWCM or PICM, represented by the local variable `points`:

```
function matched=match(Y);
%MATCH generates output of matched filter
%   MATCHED=MATCH(Y);
```

```
%  Y: signal to be filtered
...
begin=1;
matched=[];
n=length(Y);
if CHPAR(13)==1
    points=POINTS/2;            %PICM
else
    points=POINTS;             %PIWCM
end
stop=points;
while stop <= n,
    matched=[matched cumsum(Y(begin:stop))];
    matched(begin)=0;
    begin=begin+points;
    stop=stop+points;
end
%consider last sample
matched=[matched cumsum(Y(begin:n))];
```

6.3.12. Error detection

The quality of any digital transmission link is best judged by counting the number of errors

it may produce under noisy conditions. This simulation compares the original transmitted

pulse train with the recovered pulse train at the output of the regenerator device and

generates error pulses. These pulses are accumulated in err_pre(1) and the bit-error

rate is obtained from err_pre(2).

```
function err_pre=error1(X, Y)
%ERROR1 error detection for pre-detection method
%   ERR_PRE=ERROR1(X, Y);
%   X: original signal
%   Y: noise polluted signal
...
%find level
slicer_level=RECPAR(10);
n=length(Y);
X=X-slicer_level;
Y=Y-slicer_level;
%define sampling points
if CHPAR(13)==1
    points=POINTS/2;            %PICM
else
    points=POINTS;             %PIWCM
end
spoint=points:points:n;
%sample signals
sampleX=X(spoint);
preX=(sign(sampleX)); preX=sign(preX-0.1)+1;
sampleY=Y(spoint);
preY=(sign(sampleY)); preY=sign(preY-0.1)+1;
%count errors
```

```
err_pre(1)=sum(xor(ceil(preY),ceil(preX)));
err_pre(2)=err_pre/(length(preY));
```

6.3.13. Demodulator

The demodulator function demod.m is more complex than its counterpart mod.m. If PICM
is transmitted, it is first converted into PIWCM. The decision is taken, when
CHPAR(13)==1 for PICM or CHPAR(14)==1 for PIWCM. In the case of PICM, the
demodulator synchronises upon the first pair of pulses in order to identify a mark-space
sequence. Due to high noise levels, however, the first pair of pulses may be swapped
around so that the first pulse would correspond to space and the second pulse would
correspond to space. In any case, the first frame of the PICM sequence will be lost — this
is common in real-world applications as well. For a 50% duty cycle PICM, the pulse width
is half the slot duration. Mark and space durations are obtained by counting the number
of ones and zeros which are then assigned to the DEC output matrix.

```
function [BIN, DEC, F]=demod
%DEMOD   PICM & PIWCM demodulator, only one code can be
%   transmitted at one time.
%   [B, D, F]=DEMOD;
%   B: binary return value of demodulator
%   D: decimal return value
%   F: decimal description of successive frames
...
res=8;            %8-bit resolution
...
lvl=5;            %TTL
...
pw=MODPAR(11);    %get PICM pulse width
n=length(PRECODE);
precode=PRECODE;
if RECPAR(6) ~= 1, precode=precode-lvl/2; end
precode=sign(precode);
precode=sign(precode-0.1);
%Assign variables needed for demodulation
M=0; S=0; F=[];
Mbin=[]; Sbin=[]; BIN=[]; DEC=[];
if CHPAR(13)==1               %PICM is transmitted
    disp('Converting PICM into PIWCM');
    %define sampling instances
    spoint=POINTS*pw:POINTS*pw:n;
    sample=precode(spoint);
    index=1; start=2; stop=64; count=0; run=0;
    piwcm=[];
    i=2;
```

```matlab
    %synchronise; lose first frame
    for j=1:stop+1
        if sample(j)==1 & run~=3
            count=count+1;
            run=run+1;
        elseif sample(j)==1 & run==3
            start=count+1;
            break
        else
            count=count+1;
        end
    end
    %count marks and spaces
    for i=2:length(sample)
        %first pulse
        if sample(i-1)==-1 & sample(i)==1 & index==1
            index=0;
            piwcm=[piwcm 1];
        %second pulse
        elseif sample(i-1)==-1 & sample(i)==1 & index==0
            index=1;
            piwcm=[piwcm -1];
        %count mark
        elseif sample(i)==-1 & index==1 &
            rem(spoint(i)/(POINTS/2),2)==1
            piwcm=[piwcm 1];
        %count space
        elseif sample(i)==-1 & index==0 &
            rem(spoint(i)/(POINTS/2), 2)==1
            piwcm=[piwcm -1];
        end
        if rem(i,counter)==0
            disp([num2str(percent),' % done'])
            percent=percent+25;
        end
    end
    sample=piwcm(1:length(piwcm));
elseif CHPAR(14)==1   %PIWCM is transmitted
    %define sampling instances
    spoint=POINTS:POINTS:n;
    sample=precode(spoint);
end
disp('Now demodulating PIWCM')
%count marks and spaces
for i=2:length(sample)
    if sample(i)==1                 %count mark
        M=M+1;
    elseif sample(i)==-1            %count space
        S=S+1;
    end
    if sample(i-1)==-1 & sample(i)==1           %new frame
        F=[F [M S]'];
        Mbin=dec2bin(M-1, res/2);
        Sbin=dec2bin(S-1, res/2);
        BIN=[BIN [Mbin Sbin]'];
        M=0;
        S=0;
    end
end
F=F'-1;
```

```
BIN=BIN';
[r, c]=size(BIN);
for j=1:r
    D=bin2dec([BIN(j,:)]);
    DEC=[DEC D];
end
```

6.4. Summary

A software simulation package based on Matlab has been developed for the digital PTM system. Its structure and capabilities were discussed. Its aim is to give designers a tool for analysing and implementing the system before carrying out the hardware work. Limitations of the simulation package are basically determined by the available memory and the processor speed of the computer. Results obtained through software simulation are discussed and compared to the hardware results in Chapter 7.

CHAPTER 7

RESULTS AND ANALYSIS

7. RESULTS AND ANALYSIS

Previous Chapters have discussed the methods employed and the specific implementation of the digital PTM system. This Chapter deals with the results and analysis obtained for the complete system by means of theoretical comparisons and validation tests. Both practical and simulation results were taken for the electrical link.

7.1. Power Spectral Density

Spectral measurements were carried out for both PIWCM and PICM modulated waveforms under ideal-noiseless conditions to judge the system performance. A test signal of 1 kHz was used for this particular measurement in order to clearly show the characteristics of the signals, since it is a convenient sub-multiple of the clock frequency.

The point chosen for comparison of the theoretical spectral prediction, practical spectral measurement and spectral software simulation is the output of the transmitter. The digital PTM spectra are composed of the sum of contributions from a set of delayed pulses, describing the distribution of power versus frequency. This approach is equally valid for PIWCM (Section 4.3) and PICM (Section 4.5).

In the case of PIWCM, Eq. (4.14) characterises the associated PIWCM random pulse train given in Eq. (4.10). Its pulse train is composed of time slots of mark and space, with the signal energy stored in the mark only. From Eqs. (4.13) and (4.14) it can be seen that the Fourier transform depends on the pulse width and the preceding frame lengths.

106

The measured, calculated and simulated spectral behaviour of the PIWCM waveform for a slot rate of 1 MHz and an input frequency of 1 kHz is illustrated in Figure 7.1, showing close agreement in all cases. Due to the fundamental pulse width of one clock interval, the PIWCM PSD provides distinctive spectral components at the slot frequency. The spectral lines in between show the variation of mark and the frame length. As can be seen, the power spectral distribution is mainly concentrated at frequencies lower than the slot rate, decaying rapidly at frequencies above the slot frequency. This indicates that the PIWCM signal may be transmitted over channels having a bandwidth of less than the slot rate [99].

On the other hand, the PSD for PICM comprises a constant pulse width and a variable frame length. Equation (4.16) shows that the pulse train is constructed of two mark-space sequences. Again, the PSD from Eqs. (4.17) and (4.18) produces distinctive frequency components at odd harmonics of the slot frequency, as shown in Figure 7.2.b. Variation of this component with respect to the duty cycle has been analysed and it was observed that a 50% duty cycle is suitable for optimum timing extraction [100]. As a result of this component, at the receiver there is no requirement to extract frame frequency and phase from the received pulse train for synchronisation. It is sufficient to employ a PLL to extract the slot information directly from the received data stream. Its harmonics are placed between even multiples of the slot frequency, decaying with an increase of frequency. In comparison to the theoretical prediction Figures 7.2.a and 7.2.c show the measured and simulated PICM spectra respectively. In contrast to PIWCM, the bandwidth needed for PICM is at least twice as large and hence this scheme is only suitable for systems where the bandwidth is twice the slot rate.

(a)

f1   **1**   FFT
       10.0   dB/div
pos: -20.00   dBm

-25.000 us   0.000 s   25.000 us
             5.00 us/div   realtime Trigger Mode:
y2(f1)   0.00000 dBm   x2(f1) 2.00000 MHz   Edge
y1(f1)   0.00000 dBm   x1(f1) 1.00000 MHz
delta y 0.00000 dB   delta x 1.00000 MHz
                           1/delta x 1.00000 us   **1** _f_ 2.500 V

(b)

Level (dB) vs Normalised Frequency

(c)

Magnitude (dB) vs Frequency (Hz) x 10^6
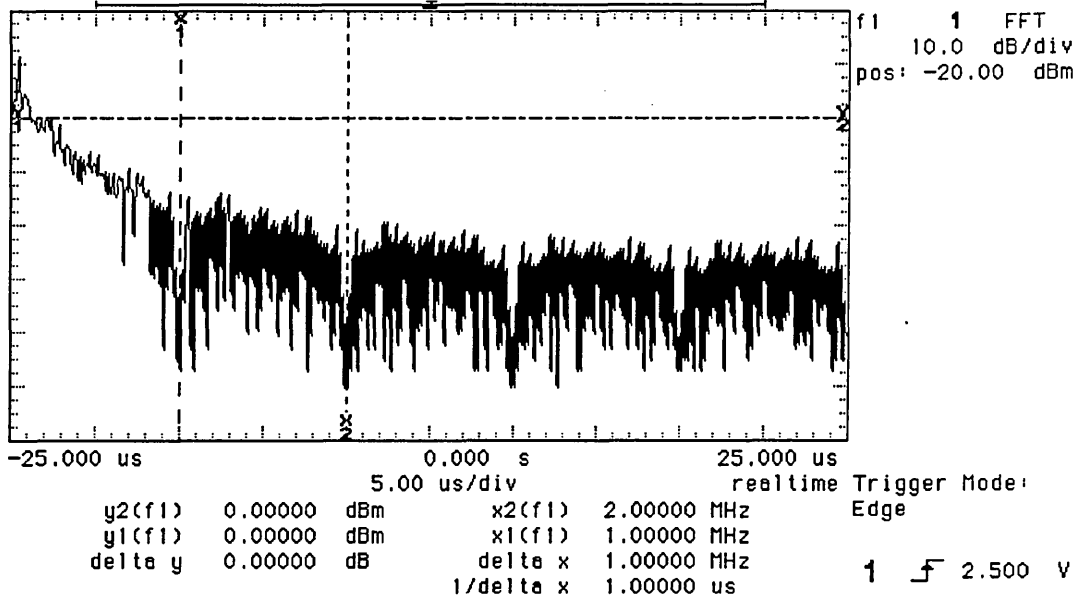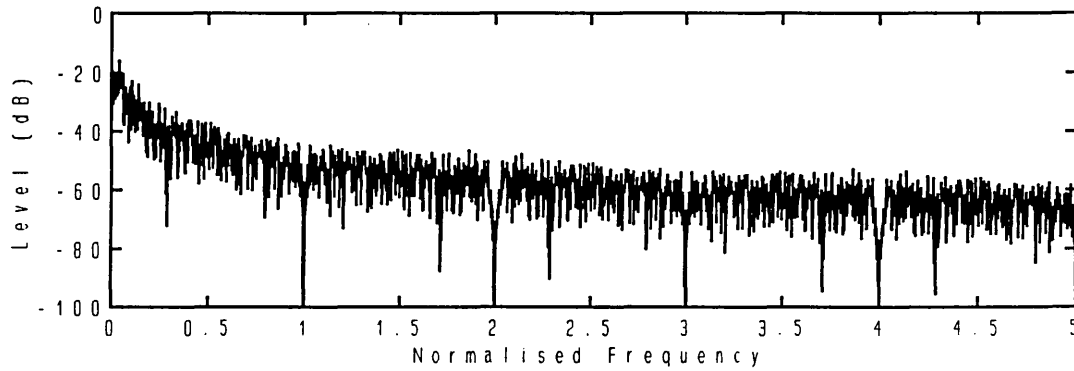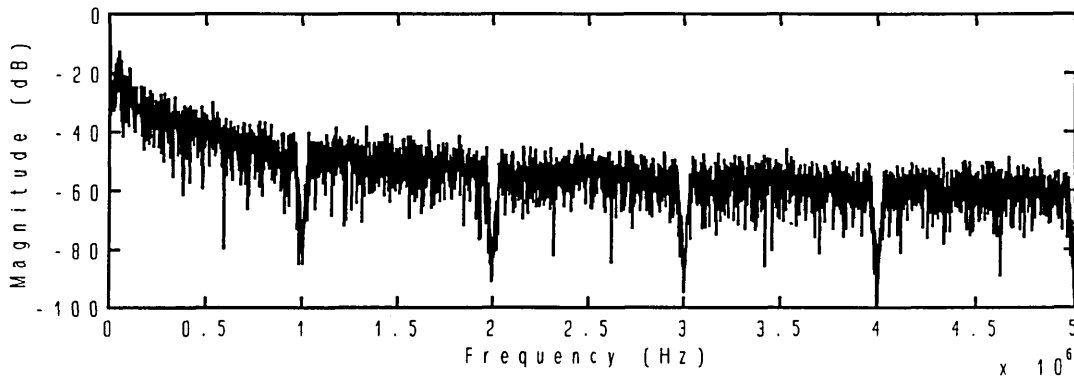
Figure 7.1 PSD of PIWCM: (a) measured; (b) calculated; (c) simulated.

(a)

```
                                                              f1    1   FFT
                                                                   10.0  dB/div
                                                              pos: -20.00  dBm
```

```
-25.000 us              0.000 s              25.000 us
                       5.00 us/div              realtime  Trigger Mode:
        y2(f1)  0.00000  dBm      x2(f1)  2.00000 MHz     Edge
        y1(f1)  0.00000  dBm      x1(f1)  1.00000 MHz
        delta y 0.00000  dB       delta x 1.00000 MHz     1  ⌐_  2.500  V
                                  1/delta x 1.00000 us
```
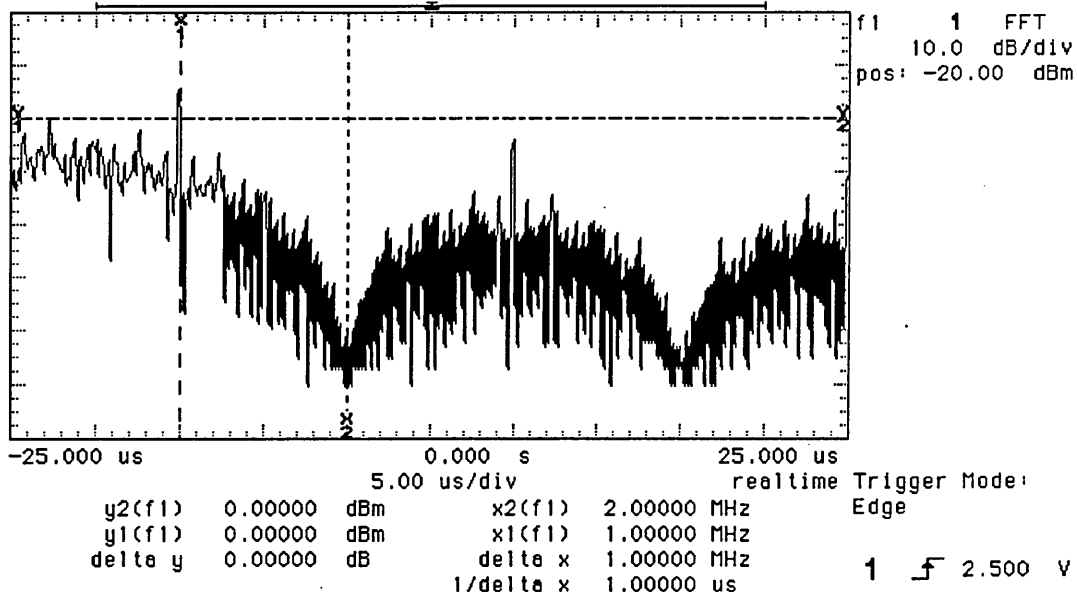
(b)
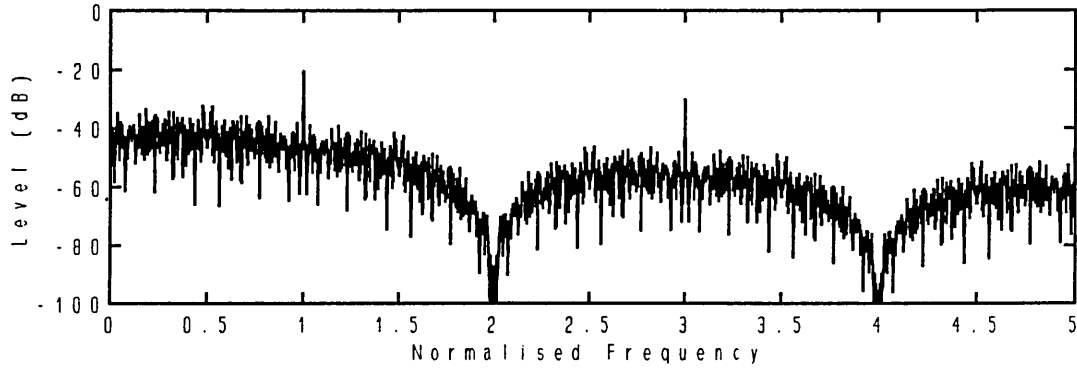
(c)
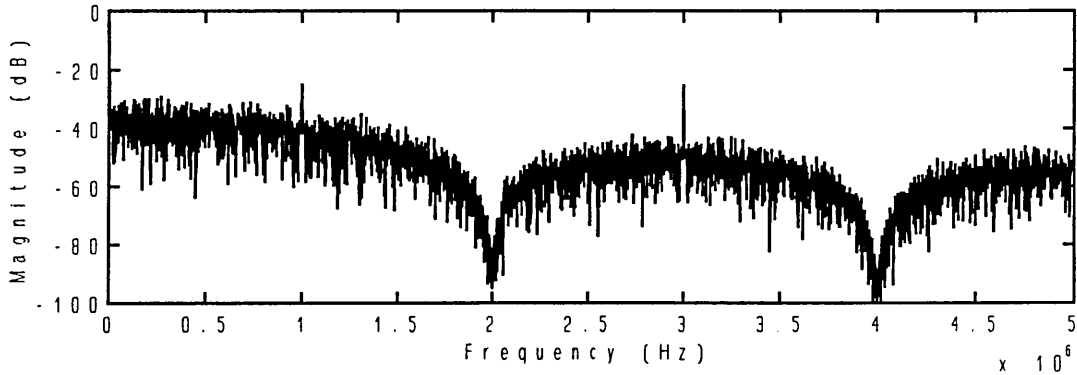
Figure 7.2 PSD of PICM: (a) measured; (b) calculated; (c) simulated.

109

7.2. Analogue Input versus Analogue Output

To demonstrate the functionality of the digital PTM system, the analogue input may be compared with the analogue output. This evidence has been obtained through hardware measurements and simulation using PIWCM and PICM. The analogue input signal was of sinusoidal or triangular shape. In the case of a sinusoidal signal, the recovered waveform will reflect on the purity of the transmitted information, whereas the triangular signal will display the linearity of the recovered waveform.

Using a sinusoidal signal input under noise free environment, the measured and simulated input and output waveforms are shown in Figures 7.3 and 7.4 respectively. In both cases the recovered signal faithfully resembles the original transmitted waveform. To test the overall linearity of the PIWCM and PICM systems, a low frequency ramp signal of 500 Hz is used. Figures 7.5 and 7.6 illustrate the measured and simulated waveforms respectively, showing very good linearity in both cases.

7.3. Harmonic Distortion

Another method of evaluating the system performance is to measure the harmonic distortion of a single tone sine wave at the output of the receiver. In this measurement, the frequency response of the recovered analogue signal, as shown in Figure 7.7, is evaluated. Ideally, the spectrum of a single tone sine wave should have only one frequency component — the fundamental frequency. However, the function generator used in this experiment produces harmonic components as shown in Figure 7.8 where the 2nd and 3rd harmonic components are 47 dB and 43 dB below the fundamental component. Using a single tone sinusoidal input signal of a frequency of 500 Hz, the spectrum of the output signal is shown in Figure 7.7. The 2nd and 3rd harmonic differences are measured

1	1.53 V/div
	pos: 2.552 V
	10.00:1 1MΩ dc

2	1.21 V/div
	pos: 1.976 V
	10.00:1 1MΩ dc

-2.5000 ms　　　　　　　　0.000 s　　　　　　2.5000 ms

500 us/div　　　　　　　　realtime Trigger Mode:

	current	minimum	maximum	average	Edge
.frequency (1)	500.275 Hz	499.278 Hz	502.307 Hz	500.533 Hz	

1 ⨍ 3.288 V
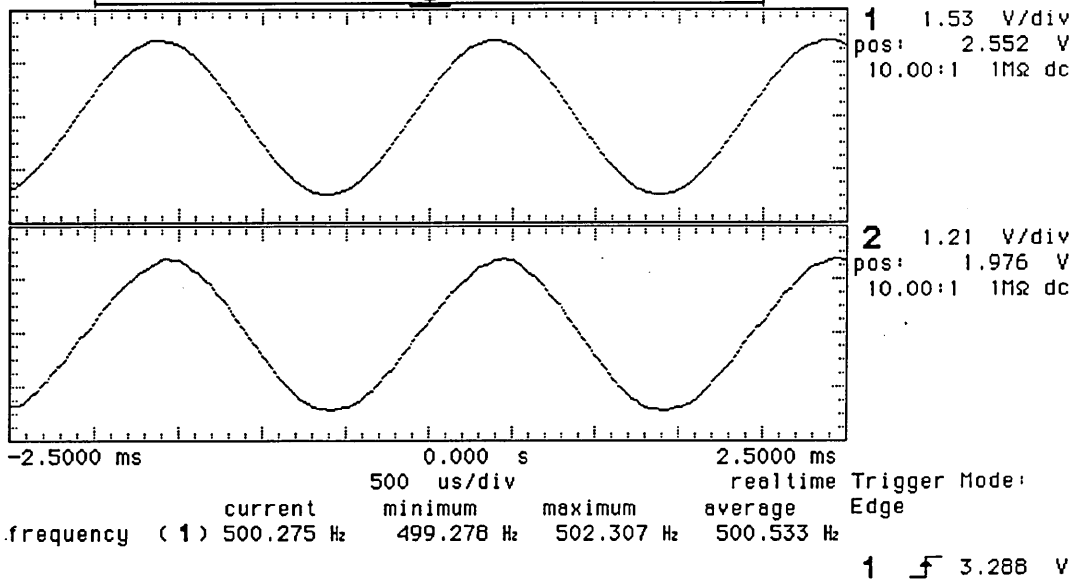
Figure 7.3 PIWCM (a) input and (b) output waveform.
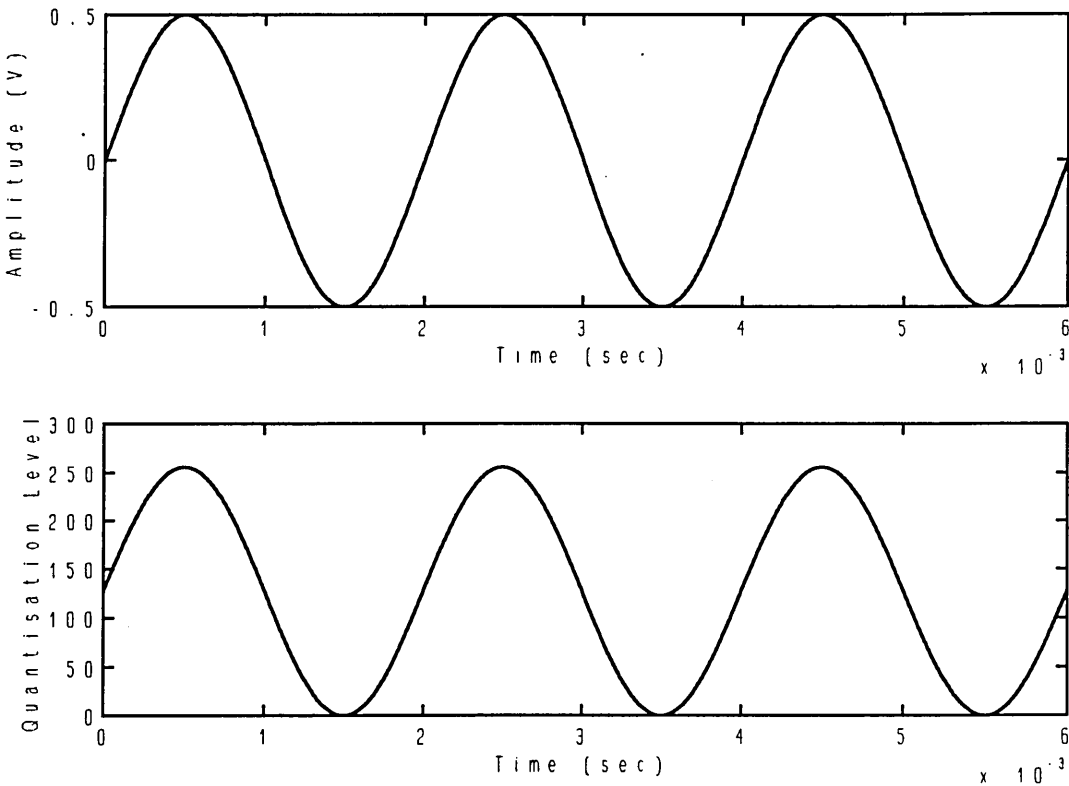
Figure 7.4 PIWCM (a) input and (b) output simulation.

111
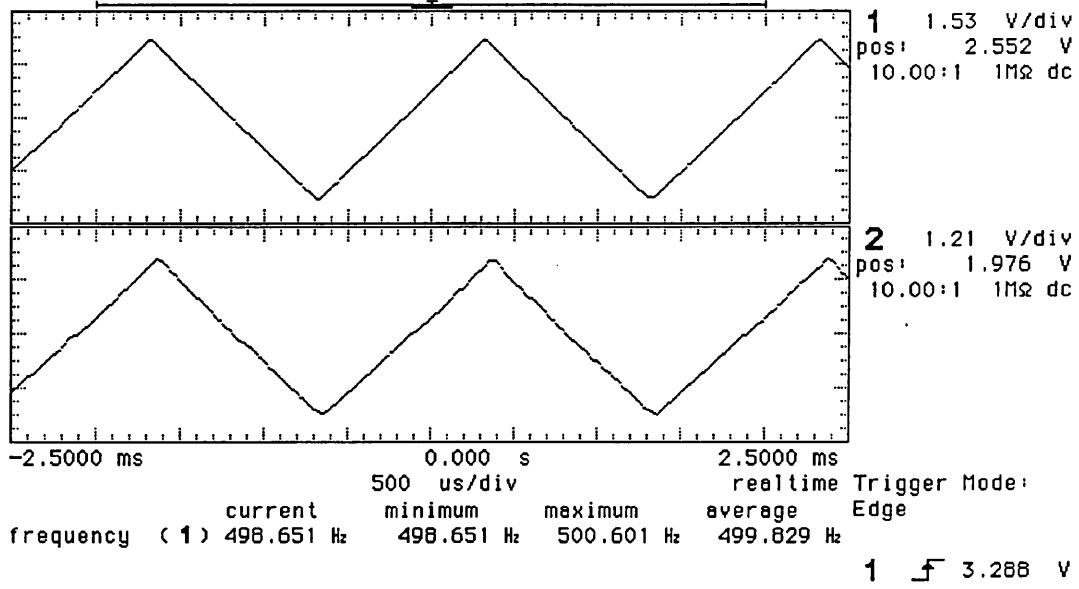
Figure 7.5 PICM (a) input and (b) output waveform.
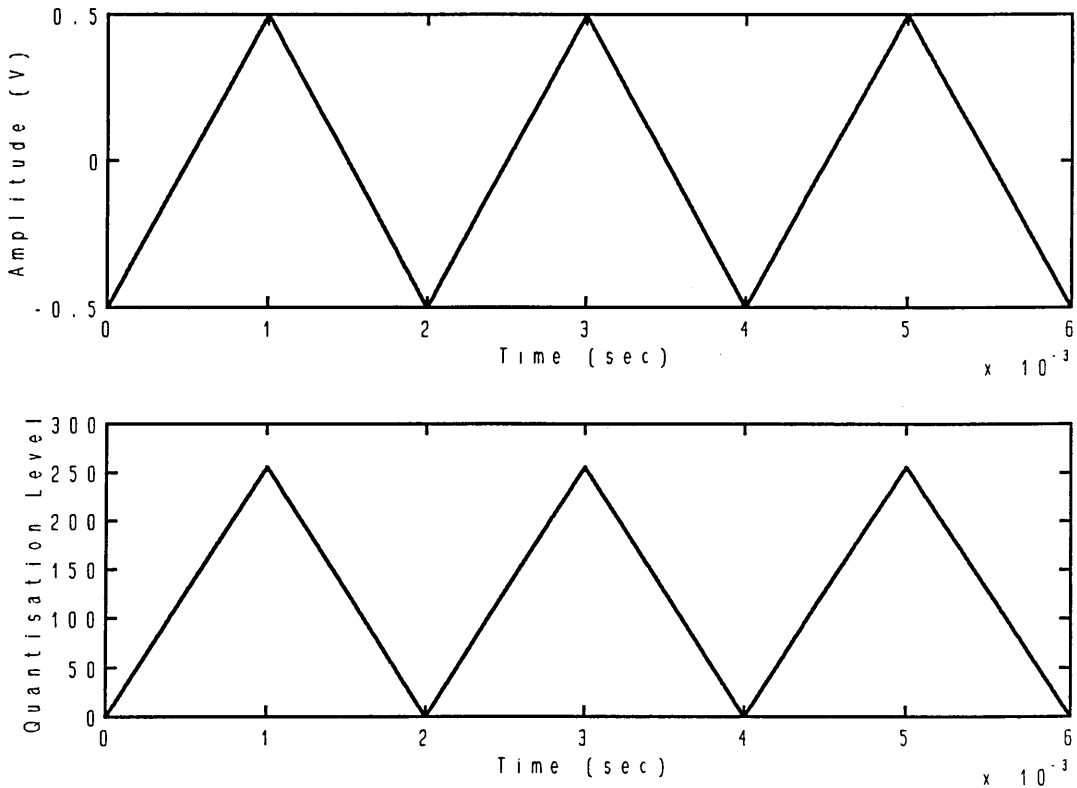
Figure 7.6 PIWM (a) input and (b) output simulation.
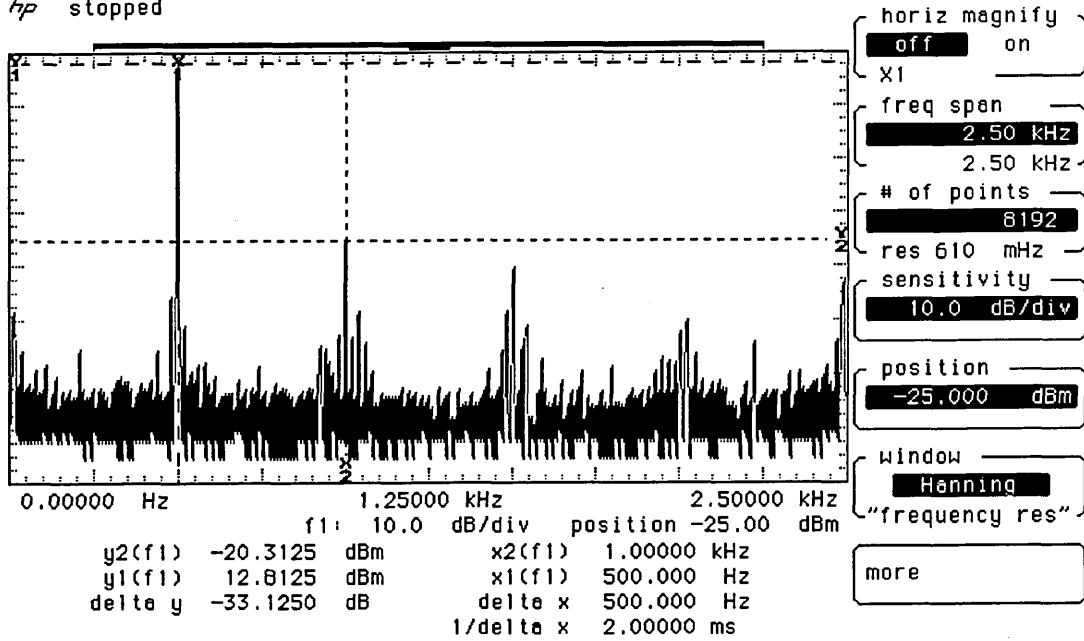
Figure 7.7 Harmonic content of sinusoidal output signal.
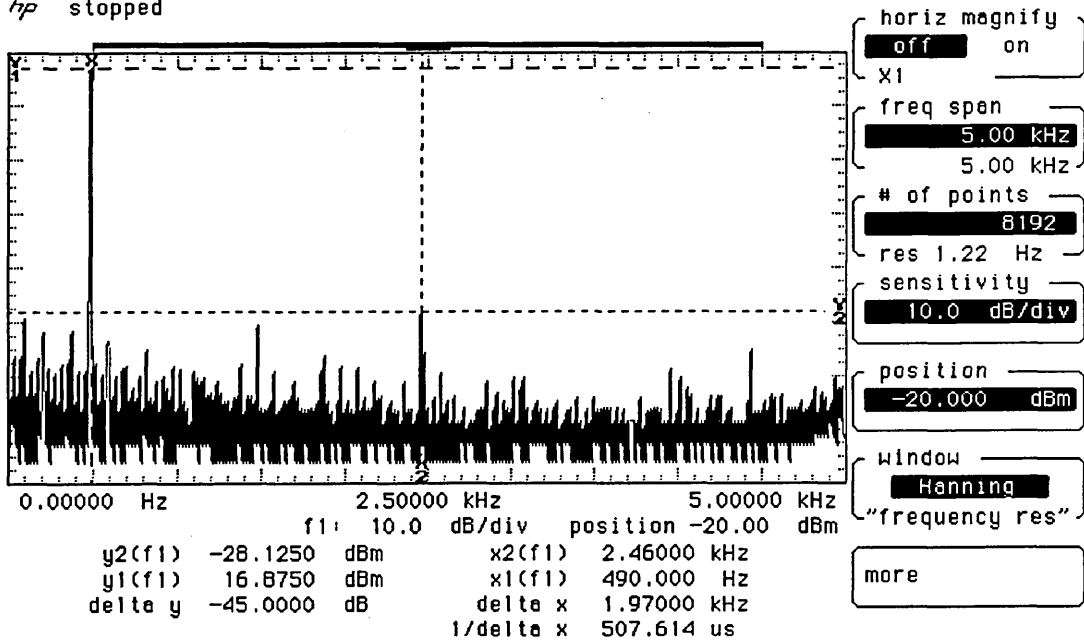
Figure 7.8 Harmonic content of sinusoidal input signal.

Input (V_{p-p})	Modulation Index (%)	Fundamental (dB)	2nd Harm. (dB)	1st - 2nd (dB)	3rd Harm. (dB)	1st - 3rd (dB)
4.8	96	14.0	-17.6	31.6	-24.1	38.1
4.5	90	13.4	-19.2	32.6	-24.3	37.7
4.0	80	12.5	-22.9	35.4	-24.5	37.0
3.5	70	11.2	-22.8	34.0	-24.6	35.8
3.0	60	9.7	-24.5	34.2	-24.8	34.5
2.5	50	8.1	-24.5	32.6	-25.0	33.1
2.0	40	6.0	-24.8	30.8	-25.0	31.0

Table 7.1 Harmonic components relative to the signal amplitude

at the output of the PIWCM system, are tabulated in Table 7.1 and graphically shown in Figure 7.9 This graph shows, that the system is best operated at higher amplitudes, i.e. at modulation indices greater than 50%.
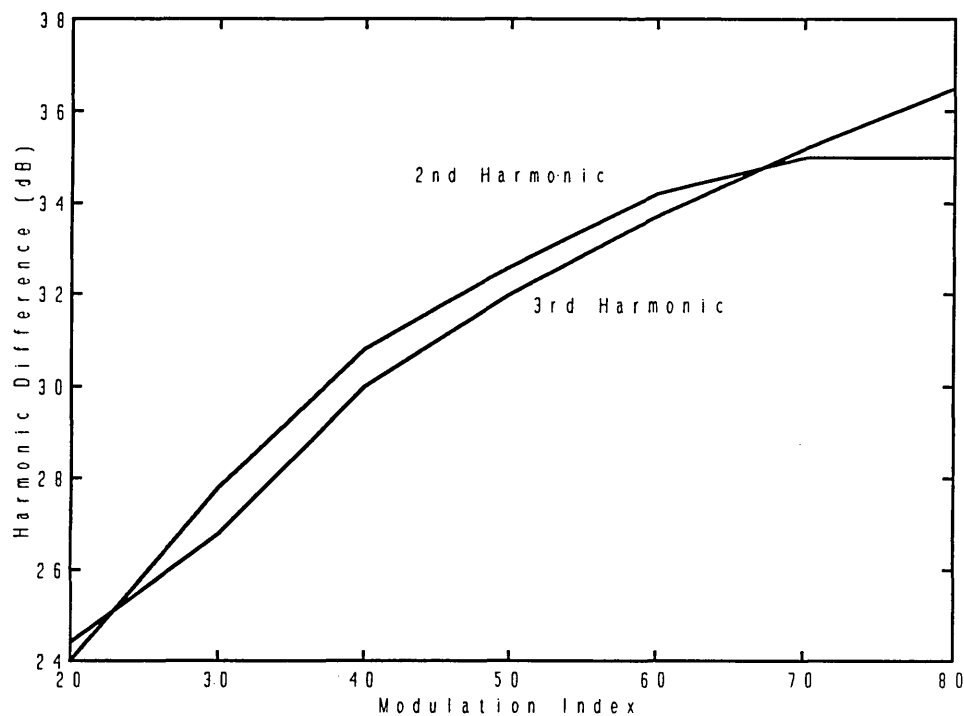
Figure 7.9 Harmonic difference of the output waveform relative to the signal amplitude.

7.4. Error Rate versus Carrier-to-Noise Ratio

In a binary transmission system, the probability of errors is a measure of the quality of the modulated waveforms in the transmission channel under noisy conditions. The error rate (for the three types of error: false alarm, erasure and wrong slot) is a function of carrier-to-noise ratio.

The regenerated wave trains were sampled at the centre (PIWCM), or the first quarter (PICM), of the bit period (see also Section 5.2.2). The period of the sampling pulse was selected as 100 ns and a time counter was used to account the number of errors. Along with the number of errors, the transmitted bits were counted and the error rate is defined as:

$$P_e = \frac{number\ of\ errors}{transmitted\ bits} \tag{7.1}$$

The channel bandwidth also contributes significantly to the quality of the signal. Figure 7.10 illustrates the frequency response of the electrical transmission channel, in
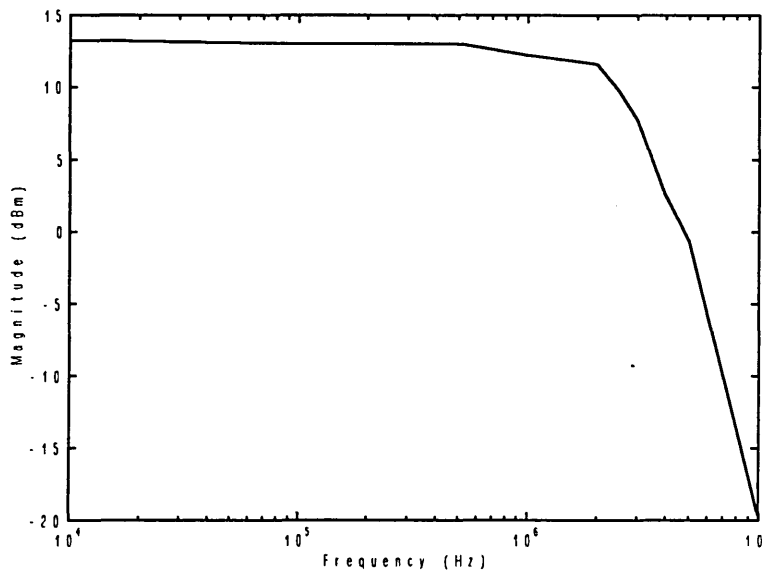
Figure 7.10 Frequency response of the electrical channel.

which the error rate is being measured. From the graph the channel has a bandwidth of 5.6 MHz and displays the behaviour of a 3rd order low-pass filter.

With this characteristic, the channel acts as a pre-detection device, such as a 3rd-order Butterworth low-pass filter with cut-off frequency of 5.6 MHz, filtering both signal and noise and hence distorting the frequency spectrum. However, the bandwidth limitation upon the noise rms value is not significant and the bandwidth equivalent noise margin may be neglected.

Using a single tone sine wave at amplitude of 4 V_{p-p} and a frequency of 1 kHz, the measured rms noise voltage, carrier-to-noise (C/N) and error rate (P_e) for both PIWCM and PICM are tabulated in Table 7.2. On average, the PIWCM C/N is 3.5 times that of PICM, hence the C/N margin between PIWCM and PICM is approx 10.7 dB. On the other hand, for the same noise level PICM has a larger P_e than PIWCM which is due to its pulse nature.

Noise level (Vrms)	C/N (PIWCM) (dB)	Pe (PIWCM)	C/N (PICM) (dB)	Pe (PICM)
0.25	19.1	0	8.3	0
0.26	18.5	3.2e-9	7.8	6.4e-9
0.27	18.2	2.0e-8	7.5	4.0e-8
0.3	17.3	3.2e-7	6.6	4.7e-7
0.33	16.5	8.9e-6	5.7	1.7e-5
0.38	15.3	1.4e-4	4.5	2.6e-4
0.43	14.2	8.1e-4	3.4	1.6e-3
0.48	13.2	2.6e-3	2.5	5.6e-3
0.57	11.7	1.3e-2	1.0	2.6e-2

Table 7.2 Error rate for PIWCM and PICM.

Figures 7.11 and 7.12 illustrate the measured and simulated error rate performance as a function of carrier-to-noise ratio for uncoded PIWCM and PICM respectively, showing

Pe vs. CNR: Slicer, PIWCM
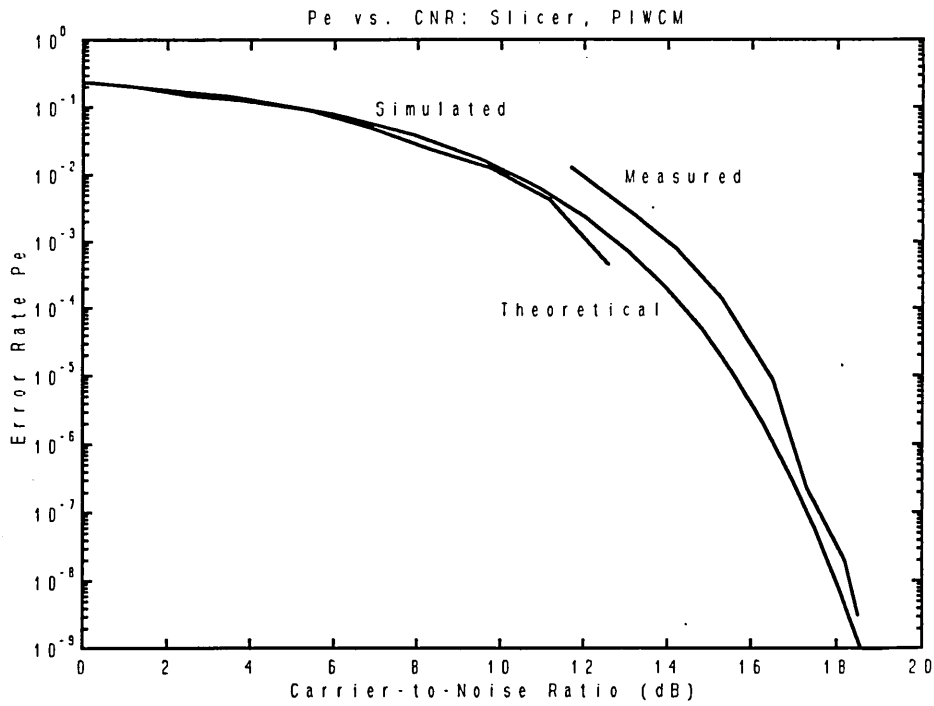
Figure 7.11 PIWCM: error rate versus carrier-to-noise ratio.

Pe vs. CNR: Slicer, PICM
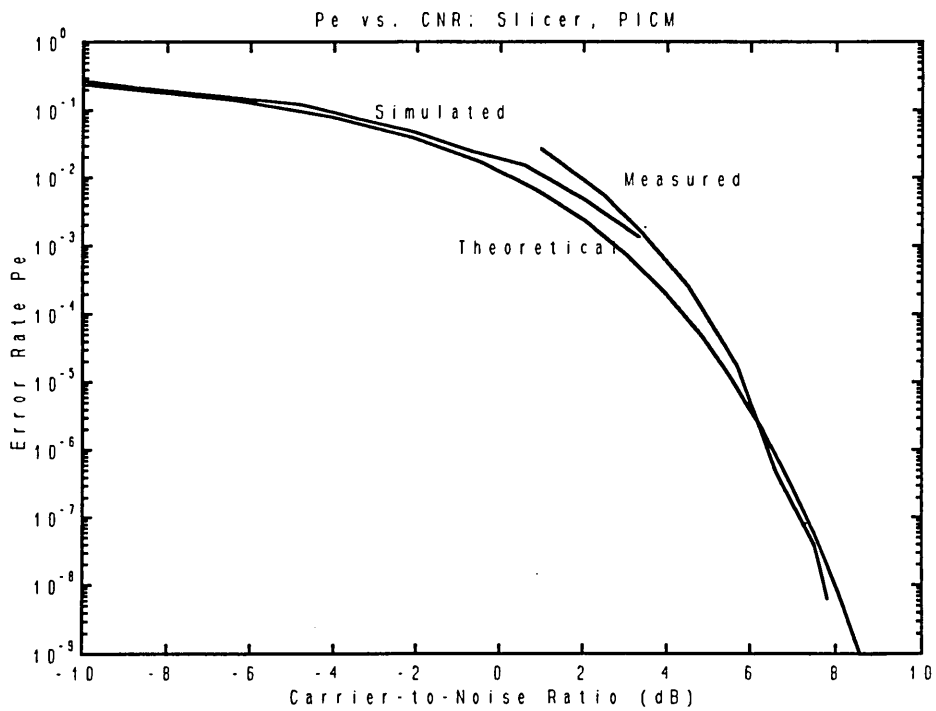
Figure 7.12 PICM: error rate versus carrier-to-noise ratio.

117

excellent agreement with the theoretical prediction based on Eq. (2.4). The discrepancy between the curves is probably due to uncertainties in actual values of noise voltages. At an error rate of 10e-9 the uncoded PIWCM offers a C/N of $\approx$ 18 dB whereas PICM offers a C/N of $\approx$ 8 dB. Thus the improvement is $\approx$ 10 dB in received C/N which can be used to increase the span in long-haul transmission links.

The error rate can be further reduced by employing a pre-detection filter prior to the demodulator. This is only carried out in the simulation and the results obtained indicate the validity of the idea. The two filter types being investigated are:

1) 3rd-order Butterworth low-pass filter and

2) matched filter.

The optimum cut-off frequency for a 1st-order low-pass filter with inter-symbol interference is equally applicable for a 3rd-order filter and can be obtained as follows [101]:

$$P_e = Q\left(\sqrt{C/N \frac{1}{v\,T_s}\left[\frac{1-e^{-v\,T_s/2}}{1+e^{-v\,T_s/2}}\right]^2}\right) \tag{7.2}$$

where $v = 1/RC$, T is the bit period of 1 μs and 0.5 μs for PIWCM and PICM respectively and Q is the complementary error function. Plotting P_e against the cut-off frequency $f_{co} = v/2\pi$, shows that a minimum P_e appears at a cut-off frequency of 700 kHz and 1.4 MHz for PIWCM and PICM respectively, see Figure 7.13.

Figures 7.14 and 7.15 illustrate the simulated error rate as a function of C/N for PIWCM and PICM respectively. It can be seenthat for the same C/N the P_e for a matched filter is much lower than that for the 3rd-order Butterworth filter and the basic slicer with

118
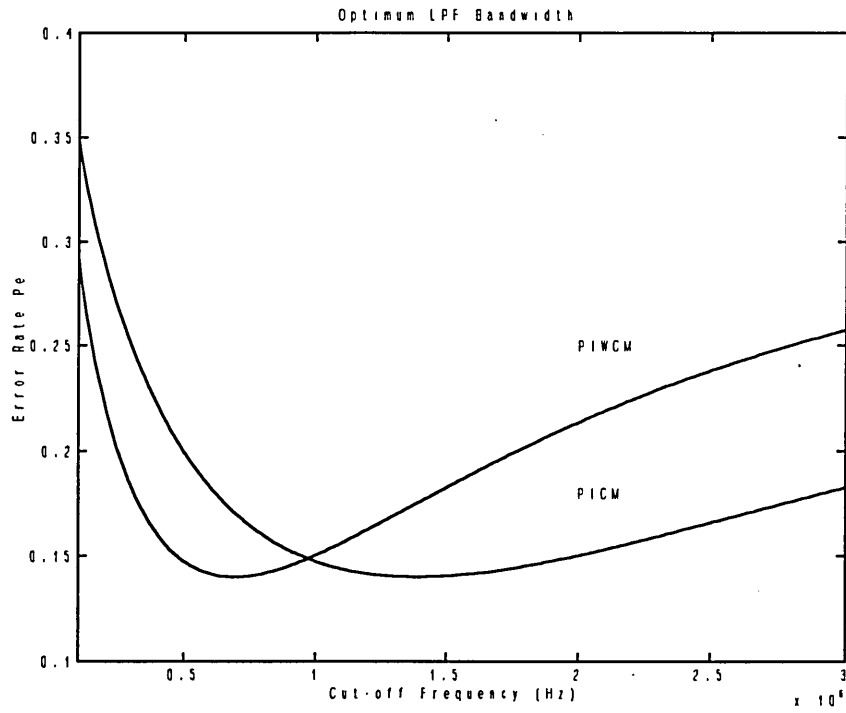
Figure 7.13 Error rate versus RC pre-detection filter cut-off frequency.
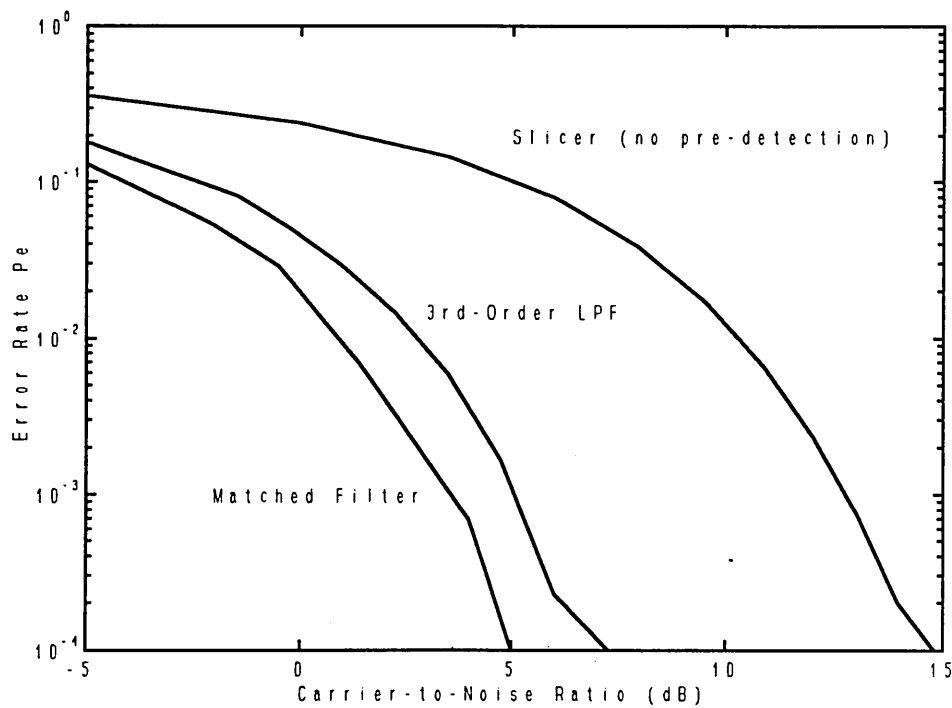
Figure 7.14 PIWCM: error rate versus carrier-to-noise ratio with pre-detection filter.

119
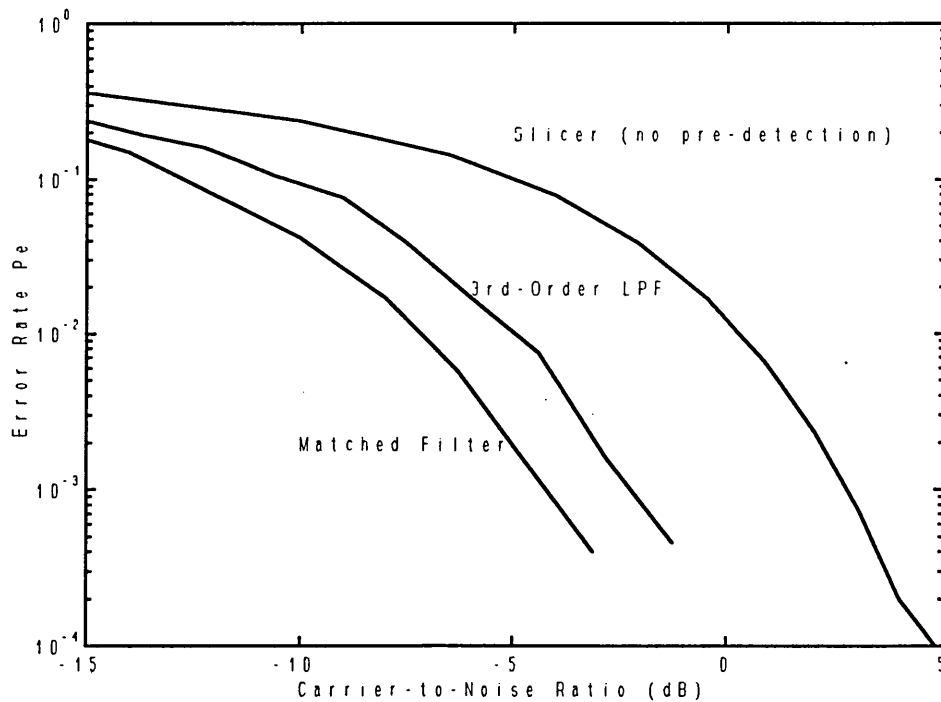
- **Figure 7.15** PICM: error rate versus carrier-to-noise ratio with pre-detection filter.

no pre-detection filter. These results indicate that the system performance can be further improved and the saving gained in the received C/N can be used to increase the length of the transmission link.

7.5. Signal-to-noise Ratio versus Carrier-to-Noise Ratio

Figure 7.16 illustrates the measured signal-to-noise ratio performance at the output of the system as a function of the carrier-to-noise ratio with simulated results, it is seen to be good [102], because it approches PCM. The results display a threshold effect below which the signal pulses become indistinguishable from the noise pulses. For PIWCM, the measured threshold point for C/N is 16.5 dB corresponding to the lowest S/N margin of 40 dB which is slightly worse than 8-bit PCM, see Figure 7.16.
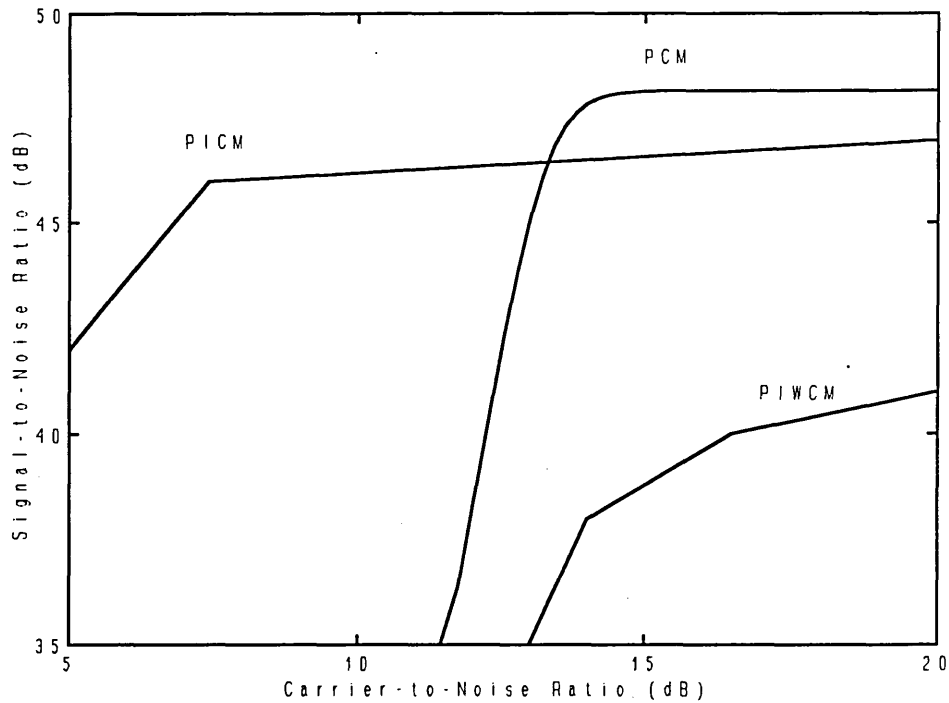
Figure 7.16 Signal-to-noise ratio versus carrier-to-noise ratio.

In the case of PICM, the threshold point for C/N is at 7.4 dB corresponding to S/N of 46 dB — an improvement of 6 dB to PIWCM. Thus measured and simulated results have indicated that high quality analogue outputs can be developed with PICM.

7.6. Summary

The theoretical spectral prediction obtained for both PIWCM and PICM waveforms showed close agreement with the measured and simulated results. The spectral components at the slot rate can be used for receiver synchronisation. Measured error rate performances match reasonably well the predicted and simulated results. For the same C/N, PICM has a lower P_e than PIWCM. Furthermore, it was shown that the error rate can be reduced by employing pre-detection filtering. Finally, S/N measurements indicated the good quality transmission capability of the system.

CHAPTER 8

CONCLUSIONS

8. CONCLUSIONS

This thesis has presented the design, analysis, simulation, implementation and results of an investigation into digital PTM systems, namely PIWCM and PICM. The primary objective of this study was to investigate the potential of two new digital modulation methods for use in electrical and/or optical fibre transmission systems.

In both PIWCM and PICM the message signal is digitally encoded and the generated frame lengths are different and determined only by the sampled value of the message signal. In PIWCM information is represented by the number of time slots associated with mark and space in a given frame, whereas in PICM it is represented by the number of time slots between two successive constant width pulses.

The main advantage of PICM is its narrow pulse width, providing high peak power levels and reduced average power, ideal for optical sources. On the other hand the average power content of PIWCM is higher. In general PICM will require much larger transmission bandwidth compared to PIWCM. However, this bandwidth expansion may be well traded for signal-to-noise performance in wide bandwidth channels (such as optical fibre). PIWCM, has frame synchronisation capability, since each frame is initiated with a mark followed by a space, whereas in PICM frame synchronisation is essential. PIWCM and PICM have a higher transmission capacity compared to PCM and PPM and on average, this capacity is increased by a factor of two.

To simulate the complete system, the Matlab engineering software package has been utilised to produce a complex software tool which was found to be very useful in

implementing the system in hardware. The simulation package incorporates a graphical user interface through which the user can look at all aspect-functions of the digital PTM system. Furthermore, simulation results indicate that the system measurements were carried out effectively and accurately.

Programmable logic devices have been used to implement the modulator and demodulator where the PTM pulse train and associated control signals are being generated in one device. With this approach, the complete system is implemented with just three transmitter and receiver modules: input/output buffer, data converter, modulator/ demodulator. Thus resulting in compact and more reliable system layout.

Original expressions were given for channel capacity, code characteristics and power spectral density. The predicted results for the power spectral density are in good agreement with the simulated and measured data, thus indicating the validity of the expressions.

At the optimum modulation index of 70% the second and third harmonic distortion levels measured at the output of the receiver are 34 dB and 36 dB respectively for PIWCM. This shows that the signal can be reproduced faithfully by the system.

For an error rate of 10^{-7}, the measured carrier-to-noise ratios for PIWCM and PICM are 17.4 dB and 7.4 dB respectively, agreeing well with the predicted and simulated values within ± 1 dB. This improvement of 10 dB (for PICM) can be used to increase the overall span of the transmission link.

The simulation results indicate that the error rate can be further reduced by employing pre-

detection filters. For a carrier-to-noise ratio of 5 dB, the error rate is reduced from 0.1 for a slicer to 10^{-2} and 10^{-4} for RC and matched filter respectively. However, this needs to be investigated in future.

Like all PTMs, the signal-to-noise ratio performance exhibits a threshold level beyond which the signal-to-noise ratio deteriorates rapidly. For PIWCM and PICM these threshold values are at 40 dB and 46 dB respectively (compared with 48 dB for PCM). The extra 6 dB gain in PICM can be used to extend the distance of transmission.

Both systems are suitable for high quality signal transmission over coaxial or fibre cables. Results indicate that PICM has further potential in long distance wide bandwidth transmission systems.

CHAPTER 9

FUTURE WORK

9. FUTURE WORK

Inclusion of an anti aliasing filter at the input and the output of the system may be made to be of high order to reduce the sampling ratio and to remove unwanted high frequency components at the output.

For more efficient coding, a companding scheme may be adapted which maps the small signal amplitudes to short frame combinations and refers large amplitudes to long frame combinations. In other words, the aim is to add higher resolution and to increase the quality of information without increasing the transmission bandwidth or the sampling ratio. A companding input/output has already been implemented in the digital PTM system which is catered for by the displacement (Disp7..0) input/output in the PLD devices. Companding may be accomplished either with a static device, such as a look up table or with an intelligent device such as a micro controller. The look up table may be programmed according to the distribution of data whereas the micro controller adds a higher degree of freedom, thus providing additional flexibility for variable data distribution changes.

One area that needs further development is the system synchronisation. This may be best achieved by employing phase locked loops at the receiver in order to lock onto the incoming pulse train and to extract the frequency component. Up to this point it is not clear if any line coding needs to be implemented. Due to the strong frequency components in the PICM spectrum, the PLL might still be able to regenerate reliable timing information even with rare pulse occurrences under noisy conditions. In the PIWCM case, this cannot be foreseen.

. Error detection and correction techniques may be implemented using neural networks.

Soliton optical fibre communication is intended for ultra high speed data transmission, relying on transmission of short pulses. Thus PICM, because of its pulse nature, may be used for this application.

CHAPTER 10

APPENDIX

10. APPENDIX

10.1. Listing of PIWCM and PICM PSD Calculation with Matlab

```
%codepsd.m generates the PSD of PIWCM/PICM for random data
fm=5;                      %normalised mod. frequency
sr=2;                      %min. sampling rate
p=8;                       %bit resolution
mors= 2^(p/2);             %maximum length for mark or space
Lmax=2*(mors);             %maximum frame length
comb =2^(p);               %total combinations
f=1:5*fm*(Lmax)*sr;        %frequency
slotrate=(Lmax)*fm*sr;     %slot rate
Ts=1/(slotrate);           %time slot
totalframes=1:4000;        %total number of frames

%random data
data=rand(1,length(totalframes));
p10=10^(ceil(log10(comb)));
data=ceil((data*comb/p10)*p10);

%account all generated frames
displacement=zeros(1,length(data));
pulsewidth=fix(data./mors)+1;     %convert data into pulse width
pulseinterval=rem(data,mors)+1;   %conv data into pulse interval
exponent=zeros(1,length(data));   %hexponent of PIWCM pulse width
highexponent=zeros(1,length(data));%high-word exponent
lowexponent=zeros(1,length(data)); %low-word exponent
finalpiwcm=zeros(1,length(f));    %final PIWCM spectrum
finalpicm=zeros(1,length(f));     %final PICM spectrum
dutycycle=0.5;                    %duty cycle for PICM

%prepare first frame
exponent(1)=0;
highexponent(1)=0;
lowexponent(1)=pulsewidth(1)*(-j*2)*pi*Ts;
displacement(1)=pulsewidth(1)+pulseinterval(1);
totalperiod=pulsewidth(1)+pulseinterval(1);

%take single frequency components and multiply each element in
%the exponent matrix to obtain exp, find displacement of every
%component
for sample=2:length(totalframes)
    exponent(sample)=displacement(sample-1)*(-j*2)*pi*Ts;
    highexponent(sample)=displacement(sample-1)*(-j*2)*pi*Ts;
    lowexponent(sample)=(displacement(sample-1)+...
        pulsewidth(sample))*(-j*2)*pi*Ts;
    displacement(sample)=displacement(sample-1)+...
        pulsewidth(sample)+pulseinterval(sample);
    totalperiod=totalperiod+pulsewidth(sample)+...
        pulseinterval(sample);
end
```

127

```
%generate spectrum
fcountpiwcm=0;                          %componets at particular frequency
fcountpicm=0;
angle=pi*Ts;                            %phase angle
fpicm=sin(Ts*dutycycle*pi*f); %PICM frequency components
denpicm=pi*f;
fden=0;

c=length(f);
for a=1:c
    fcountpiwcm=0;
    fcountpicm=0;
    spec=0;
    den=a*pi;
    fden(a)=fpicm(a)/denpicm(a);
    for b=1:length(data)
        spec=(1/den)*sin(angle*a*pulsewidth(b));
        fcountpiwcm=fcountpiwcm+spec*(exp(a*exponent(b)));
        fcountpicm=fcountpicm+exp(a*highexponent(b))+...
            exp(a*lowexponent(b));
    end
    finalpiwcm(a)=fcountpiwcm;
    finalpicm(a)=fcountpicm;
end

finalpicm=fden.*finalpicm;
finalpiwcm=abs(finalpiwcm).^2;          %remove complex parts
finalpicm=abs(finalpicm).^2;
finalpiwcm=finalpiwcm/(Ts*totalperiod); %perform truncation
finalpicm=finalpicm/(Ts*totalperiod);

plot(f*Ts,10*log10(finalpiwcm));
xlabel('Normalised frequency');
ylabel('level  dB');
axis([0 4 -100 0])

figure
plot(f*Ts,10*log10(finalpicm));
xlabel('Normalised frequency');
ylabel('level  dB');
axis([0 4 -100 0])
```

10.2. Listing of Matlab File Content

```
Digital PTM System
    code        initialises Digital PTM System and opens initial
                screen and initial menu
    codegen     initialises Digital PTM System and opens initial
                menu
    codemenu    initial menu for the Digital PTM System

Data Conversion
    adc12       12-bit analogue digital converter
    adc8        analogue digital converter
    bin256      samples the analogue wave form at 256 equally
                spaced intervals
    bin2dec     convert binary code to decimal number
    dec256      recovers original waveform at 256 equally spaced
                intervals
```

128

```
        dec2bin      is the decimal to binary conversion of a given
                     decimal value
GUI Items
    adcgen      adc GUI
    channel     introduction of channel properties via GUI
    demgen      GUI for demodulator, recovers the original analogue
                signal.
    fungen      function generator, GUI
    recgen      receiver user inteface

Transmitter and Receiver Items
    amp         set amplitude of wave form
    bininput    input of various digital bit pattern combinations
    dcshift     set DC off-set
    time        generate time vector
    wave        generate analogue wave form
    demod       demodulator reconstituting the pulse train into
                8-bit parrallel
    demtext     displays transmitted and demodulated text string
    mod         modulator generating PICM and PIWCM
    errbwn      test routine to run measurements for Pe vs CNR at
                variable bandwidth
    errcnr      test routine to run measurements for Pe vs CNR at
                constant bandwidth
    errcomp     error detection for pre-detection method
    errtest     demonstration of Pe vs SNR
    match       matched filter simulation
    receive     error detection through comparator
    signr       signal-to-noise ratio
    sncn        SNR vs CNR

Display
    about       about the simulation and programmer
    chplot      plots channel traces in time and frequency domain
    eyecode     plots the eye pattern of the transmitted code
    loadscr     load initial screen
    modplot     plot of PICM & PIWCM
    plots       opens new figure and assigns 'ok' push button
    scope       continious time simulation

Other
    bmp256      convert 256-colour bitmap into *.mat-file
    cmenu       generate a menu of choices for user input
    contents    content of Digital PTM simulation package
    frame       code construction according to dec.-equiv. value
    lddeflt     loads default workspace
    loadwsp     loads specified workspace variables
    savewsp     saves default/specified workspace variables
```

10.3. Listing of Modulator PLD Programming with Snap

```
@PINLIST
datain[7..0]          i;
disp[7..0]            i;
clock                 i;
reset                 i;
picm                  o;
piwcm                 o;
sof                   o;
```

```
init                o;

@LOGIC EQUATIONS
data[7..0]          = datain[7..0] :+: disp[7..0];
mux[3..0]           = (outbuf*dlatch[3..0]) + (/outbuf *
                      dlatch[7..4]);
dlatch[7..0].d      = data[7..0];
dlatch[7..0].clk    = sof;
dlatch[7..0].rst    = reset;
ff[4..0].clk        = clock;
ff[3..0].rst        = reset;
ff4.set             = reset;
outbuf.d            = /outbuf;
outbuf.rst          = reset + init;
outbuf.clk          = tpicm * /clock;
picm                = tpicm * /clock;
piwcm               = outbuf;
sof                 = clock * /outbuf * ff[4..0] == 08h;
init                = (ff[4..0] == 10h) * reset;

@INPUT VECTORS
[outbuf, mux[3..0]]
   h0 = 00h; h1 = 01h; h2 = 02h; h3 = 03h;
   h4 = 04h; h5 = 05h; h6 = 06h; h7 = 07h;
   h8 = 08h; h9 = 09h; ha = 0ah; hb = 0bh;
   hc = 0ch; hd = 0dh; he = 0eh; hf = 0fh;
   10 = 10h; 11 = 11h; 12 = 12h; 13 = 13h;
   14 = 14h; 15 = 15h; 16 = 16h; 17 = 17h;
   18 = 18h; 19 = 19h; 1a = 1ah; 1b = 1bh;
   1c = 1ch; 1d = 1dh; 1e = 1eh; 1f = 1fh;

@OUTPUT VECTORS
[tpicm]
   picm0 = 0b; picm1 = 1b;

@STATE VECTORS
[ff[4..0]] jkffsr
   s0  = 08h; s1  = 00h; s2  = 01h; s3  = 03h;
   s4  = 02h; s5  = 06h; s6  = 07h; s7  = 05h;
   s8  = 04h; s9  = 0ch; s10 = 0dh; s11 = 0fh;
   s12 = 0eh; s13 = 0ah; s14 = 0bh; s15 = 09h;
   s16 = 18h; ini = 10h;

@TRANSITIONS
while [ini] with  [picm0] if []   then [s0]
while [s0]  with  [picm1] if [10] then [s16]
while [s0]  with  [picm1] if [11] then [s1]
while [s0]  with  [picm1] if [12] then [s2]
while [s0]  with  [picm1] if [13] then [s3]
while [s0]  with  [picm1] if [14] then [s4]
while [s0]  with  [picm1] if [15] then [s5]
while [s0]  with  [picm1] if [16] then [s6]
while [s0]  with  [picm1] if [17] then [s7]
while [s0]  with  [picm1] if [18] then [s8]
while [s0]  with  [picm1] if [19] then [s9]
while [s0]  with  [picm1] if [1a] then [s10]
while [s0]  with  [picm1] if [1b] then [s11]
while [s0]  with  [picm1] if [1c] then [s12]
while [s0]  with  [picm1] if [1d] then [s13]
while [s0]  with  [picm1] if [1e] then [s14]
while [s0]  with  [picm1] if [1f] then [s15]
```

```
while [s16] with [picm1] if [h0] then [s0]
while [s16] with [picm1] if [h1] then [s1]
while [s16] with [picm1] if [h2] then [s2]
while [s16] with [picm1] if [h3] then [s3]
while [s16] with [picm1] if [h4] then [s4]
while [s16] with [picm1] if [h5] then [s5]
while [s16] with [picm1] if [h6] then [s6]
while [s16] with [picm1] if [h7] then [s7]
while [s16] with [picm1] if [h8] then [s8]
while [s16] with [picm1] if [h9] then [s9]
while [s16] with [picm1] if [ha] then [s10]
while [s16] with [picm1] if [hb] then [s11]
while [s16] with [picm1] if [hc] then [s12]
while [s16] with [picm1] if [hd] then [s13]
while [s16] with [picm1] if [he] then [s14]
while [s16] with [picm1] if [hf] then [s15]
while [s1]  with [picm0] if [l0+l1+l2+l3+l4+l5+l6+l7+
                            l8+l9+la+lb+lc+ld+le+lf] then [s16]
while [s1]  with [picm0] if [h0+h1+h2+h3+h4+h5+h6+h7+
                            h8+h9+ha+hb+hc+hd+he+hf] then [s0]
while [s2]  with [picm0] if []   then [s1]
while [s3]  with [picm0] if []   then [s2]
while [s4]  with [picm0] if []   then [s3]
while [s5]  with [picm0] if []   then [s4]
while [s6]  with [picm0] if []   then [s5]
while [s7]  with [picm0] if []   then [s6]
while [s8]  with [picm0] if []   then [s7]
while [s9]  with [picm0] if []   then [s8]
while [s10] with [picm0] if []   then [s9]
while [s11] with [picm0] if []   then [s10]
while [s12] with [picm0] if []   then [s11]
while [s13] with [picm0] if []   then [s12]
while [s14] with [picm0] if []   then [s13]
while [s15] with [picm0] if []   then [s14]
while [s16] with [picm0] if []   then [s0]
```

10.4. Listing of Modulator Pin Assignment

```
Device = PML2552-35
Pin8    = RESET
Pin9    = DATAIN0
Pin10   = DATAIN1
Pin11   = DATAIN2
Pin12   = DATAIN3
Pin13   = DATAIN4
Pin14   = DATAIN5
Pin16   = DATAIN6
Pin17   = DATAIN7
Pin20   = CLOCK
Pin22   = DISP0
Pin23   = DISP1
Pin40   = DISP7
Pin41   = DISP6
Pin42   = DISP5
Pin43   = DISP4
Pin44   = DISP3
Pin45   = DISP2
Pin46   = SOF
Pin47   = PICM
```

```
Pin48   = PIWCM
Pin50   = INIT
```

10.5. Listing of Demodulator PLD Programming with Snap

```
@PINLIST
piwcm_in                i;
picm_in                 i;
disp[7..0]              i;
reset                   i;
clock                   i;
dataout[7..0]           o;
error                   o;
valid                   o;
n_valid                 o;

@LOGIC EQUATIONS
ff[5..0].clk        = clock;
ff[4..0].set        = reset;
ff5.rst             = reset;
inbuf.rst           = reset;
inbuf.clk           = picm_in;
inbuf.d             = /inbuf;
piwcm               = piwcm_in + inbuf;
dataout[7..0]       = outbuf[7..0] :+: disp[7..0];
outbuf[7..0].rst  ` = reset;
outbuf[7..4].d      = ff[3..0];
outbuf[3..0].d      = ff[3..0];
outbuf[3..0].clk    = /(piwcm * clock);
outbuf[7..4].clk    = /(/piwcm * clock);
error               = ff5;
valid               = piwcm * ff4;
n_valid             = /(piwcm * ff4);

@INPUT VECTORS
[piwcm ]
    piwcm0 = 0b; piwcm1 = 1b;

@STATE VECTORS
[ff[5..0]] jkffsr
    ds0  = 00h; ds1  = 01h; ds2  = 02h; ds3  = 03h; ds4  = 04h;
    ds5  = 05h; ds6  = 06h; ds7  = 07h; ds8  = 08h; ds9  = 09h;
    ds10 = 0ah; ds11 = 0bh; ds12 = 0ch; ds13 = 0dh; ds14 = 0eh;
    ds15 = 0fh; ds16 = 10h; ds17 = 11h; ds18 = 12h; ds19 = 13h;
    ds20 = 14h; ds21 = 15h; ds22 = 16h; ds23 = 17h; ds24 = 18h;
    ds25 = 19h; ds26 = 1ah; ds27 = 1bh; ds28 = 1ch; ds29 = 1dh;
    ds30 = 1eh; ds31 = 1fh; ds32 = 20h;

@TRANSITIONS
while [ds0]  if [piwcm1] then [ds1]  else [ds16]
while [ds1]  if [piwcm1] then [ds2]  else [ds16]
while [ds2]  if [piwcm1] then [ds3]  else [ds16]
while [ds3]  if [piwcm1] then [ds4]  else [ds16]
while [ds4]  if [piwcm1] then [ds5]  else [ds16]
while [ds5]  if [piwcm1] then [ds6]  else [ds16]
while [ds6]  if [piwcm1] then [ds7]  else [ds16]
while [ds7]  if [piwcm1] then [ds8]  else [ds16]
while [ds8]  if [piwcm1] then [ds9]  else [ds16]
while [ds9]  if [piwcm1] then [ds10] else [ds16]
```

```
while [ds10] if [piwcm1] then [ds11] else [ds16]
while [ds11] if [piwcm1] then [ds12] else [ds16]
while [ds12] if [piwcm1] then [ds13] else [ds16]
while [ds13] if [piwcm1] then [ds14] else [ds16]
while [ds14] if [piwcm1] then [ds15] else [ds16]
while [ds15] if [piwcm1] then [ds32] else [ds16]
while [ds16] if [piwcm0] then [ds17] else [ds0]
while [ds17] if [piwcm0] then [ds18] else [ds0]
while [ds18] if [piwcm0] then [ds19] else [ds0]
while [ds19] if [piwcm0] then [ds20] else [ds0]
while [ds20] if [piwcm0] then [ds21] else [ds0]
while [ds21] if [piwcm0] then [ds22] else [ds0]
while [ds22] if [piwcm0] then [ds23] else [ds0]
while [ds23] if [piwcm0] then [ds24] else [ds0]
while [ds24] if [piwcm0] then [ds25] else [ds0]
while [ds25] if [piwcm0] then [ds26] else [ds0]
while [ds26] if [piwcm0] then [ds27] else [ds0]
while [ds27] if [piwcm0] then [ds28] else [ds0]
while [ds28] if [piwcm0] then [ds29] else [ds0]
while [ds29] if [piwcm0] then [ds30] else [ds0]
while [ds30] if [piwcm0] then [ds31] else [ds0]
while [ds31] if [piwcm0] then [ds32] else [ds0]
```

10.6. Listing of Demodulator Pin Assignment

```
Device = PML2552-35
Pin1   = ERROR
Pin8   = RESET
Pin9   = DISP0
Pin10  = DISP1
Pin11  = DISP2
Pin12  = DISP3
Pin13  = DISP4
Pin14  = DISP5
Pin16  = DISP6
Pin17  = DISP7
Pin20  = CLOCK
Pin22  = PIWCM_IN
Pin23  = PICM_IN
Pin46  = DATAOUT0
Pin47  = DATAOUT1
Pin48  = DATAOUT2
Pin50  = DATAOUT3
Pin51  = DATAOUT4
Pin52  = DATAOUT5
Pin53  = DATAOUT6
Pin54  = DATAOUT7
Pin67  = N_VALID
Pin68  = VALID
```

CHAPTER 11

REFERENCES

11. REFERENCES

[1]. W.W. WU and A. LIVINE: 'ISDN: a snapshot', *Proc. of the IEEE*, Vol. 79, No. 2, 1991, pp. 103-111.

[2]. A. MILLER: 'From here to ATM', *IEEE Spectrum*, Vol. 94, No. 6,1994, pp. 20-24.

[3]. J. CHESNOY, B. CLESCA, R. HEIDEMANN and B. WEDDING: 'Ultra-high bit rate transmission for the years 2000', *Alcatel Electrical Communication*, 3rd Quarter, 1994, pp. 241-250.

[4]. D. LARGE:, 'Creating a network for interactivity', *IEEE Spectrum*, Vol. 95, April,1995, pp. 58-63.

[5]. M. SCHWARTZ: 'Information transmission, modulation and noise', McGraw-Hill, 4th Ed., New York, 1990, Chs. 1, 6.3, 7.7.

[6]. C.E. SHANNON: 'A mathematical theory of communications', *The Bell System Technical Journal*, 1948, Vol 27. (a) July, pp. 379-423 (b) Oct., pp. 623-656.

[7]. R.J. SCHOENBECK: 'Electronic communications modulation and transmission, Macmillian Publishing Company, 2nd Ed., New York, 1992, Ch. 14.

[8]. J.M. SENIOR: 'Optical fiber communications - principles and practice', Prentice Hall, 2nd Ed., Cambridge, 1992, Ch. 4.6.

[9]. W.M. HUBBARD: 'Utilization of optical frequency carriers for low- and moderate bandwidth', *The Bell System Technical Journal*, Vol. 52, No. 5, 1973, pp. 731-765.

[10]. E. B. CHAMPAGNE, 'Optimization of optical systems', *Appl. Opt.*, Vol. 5, Nov 1966, pp. 1843-1845.

[11]. J.J. REFI: 'Fibre bandwidth and its relation to system design', *J. of Opt. Sensors*, Vol. 2, No. 2, 1987, pp. 89-105.

[12]. P.E. BARNSLEY: 'Future-proofing the core network using novel but simple optical technology', *BT Technol. J.*, Vol. 11, No. 2, 1993, pp. 19-34.

[13]. B.Z. KOBB: 'Telecommunications', *IEEE Spectrum*, Vol. 95, No. 1,1995, pp. 30-34.

[14]. 'The U.S. HDTV standard -the Grand Alliance', *IEEE Spectrum*, April 1995, pp. 36-45.

[15]. K.W. CATTERMOLE, 'Principles of pulse code modulation', Illiffe Books Ltd., London, 1969.

[16]. F.R. CONNOR: 'Introductory topics in electronics and telecommunication modulation', Edward Arnold, 2nd Ed., London, 1982, Ch. 5.

[17]. F.G. STREMLER: 'Introduction to communication systems', Addison Wesley, 3rd Ed., New York, Chs. 7, 9.

[18]. W. STALLINGS: 'Digital signalling techniques', *IEEE Comms Magazine*, Vol. 22, No. 12, 1984, pp. 21-25.

[19]. P. COCHRANE, D.J.T. HEATLEY, P.P. SMYTH, and I.D. PEARSON: 'Optical telecommunications - future prospects', *Electron. and Commun. Eng. J.*, Aug 1993, pp. 221-232.

[20]. T.S. KINSEL: 'Wide-band optical communication systems: part 1 - time division multiplexing', *Proc. IEEE*, Vol. 58, No. 10, Oct 1970, pp.1666-1683.

[21]. R.A. CRYAN, R.T. UNWIN, A.J. MASSARELLA, M.J.N. SIBLEY, and I. GARRETT: 'A comparison of coherent digital PPM with PCM', *European Trans. on Telecom.*, Vol. 3, No. 4, 1992, pp. 331-341.

[22]. I. GARRETT: 'Pulse position modulation for transmission over optical fibers with direct or heterodyne detection', *IEEE Trans on Communications*, Vol. COM 31, No. 4, 1983, pp. 518-527.

[23]. I. GARRETT: 'Digital pulse position modulation over dispersive optical fibre channels', *Record of Globecom 83*, IEEE Global Communications Conference 1983, pp 733-737.

[24]. T. VAN LANDGEM, M. DE PRYCKER and F. Van De BRANDE: '2005: A vision of the network of the future', *Alcatel Electr. Commun.*, 3rd Quarter, 1994, pp. 231-240.

[25]. B. WILSON and Z. GHASSEMLOOY: 'Pulse time modulation techniques for optical communications: a review', *IEE Proc.-J*, Vol. 140, No. 6, Dec 1993, pp.346-357.

[26]. J.M. ARNOLD: 'Soliton pulse position modulation', *IEE Proc.-J*, Vol. 140, No. 6, Dec 1993, pp. 359-366.

[27]. M. SATO, M. MURATA, and T. NAMEKAWA, 'Pulse interval and width modulation for video transmission', *IEEE Trans. on Cable Television*, Vol. 3, No. 4, 1978, pp. 165-173.

[28]. B. WILSON and Z. GHASSEMLOOY: 'Optical fibre transmission of multiplexed video signals using pulse width modulation', *Int. Journal of Optoelectronics*, 1989, Vol. 4, No. 1, pp 3-7.

[29]. S.Y. SUH: 'Pulse width modulation for analog fiber-optic communications', *Journal of Lightwave Technology*, 1987, LT-5, pp 102-112.

[30]. B. WILSON, Z. GHASSEMLOOY, and J.C.S. CHEUNG: 'Optical pulse interval and width modulation for analogue fibre communications', *IEE Proc. - J*, Dec 1992, Vol. 139, No. 6, pp 376-382.

[31]. B. WILSON and Z. GHASSEMLOOY: 'Present theoretical development in pulse time modulation', Int Symposium on Comms, Theory and Apps. 1993.

[32]. B. WILSON, Z. GHASSEMLOOY, and L. CHAO: 'High-speed PTM techniques', SPIE Multigigabit Fiber Comms; Vol. 1787, 1992, pp. 292-302.

[33]. V. Di BIASE, P. PASSERI, and R. PIETROIUSTI: 'Pulse analogue transmission of TV signal on optical fiber', *Alta Frequenza*, Vol. 56, No. 4, 1987, pp. 195-203.

[34]. Z. JELONEK: 'Noise problems in pulse communications', *Journal IEE Pt. III-A*; Vol. 94, 1947, pp. 533-545.

[35]. B. WILSON, Z. GHASSEMLOOY, and A. LOK, 'Spectral structure of multitone PWM', *Electronic Letters*; Vol. 27, No. 9, 1991, pp. 702-704.

[36]. B. WILSON and Z. GHASSEMLOOY: 'Multiple sidetone structure in pulse width modulation', *Electronic Letters*, Vol. 24, No. 9, 1988, pp. 516-518.

[37]. H.S. BLACK; Modulation Theory; Van Nostrand Company, London, Ch. 17.

[38]. R.D. STUART: 'An introduction to fourier analysis', University Press Cambridge, 1961.

[39]. Z. GHASSEMLOOY and B. WILSON: 'Optical fibre communications (part II)', Sheffield, Sheffield City Polytechnic, 1991.

[40]. M.C. BERRY and J.M ARNOLD: 'Pulse width modulation for optical fibre transmission of video', *IEE Conf. of: The Impact of High-Speed and VLSI Technology on Communication Systems*, 1983, pp. 14-18.

[41]. W.S. HOLDEN, 'An optical pulse position modulation experiment', *The Bell System Technical Journal*, 1975, pp. 285-296.

[42]. D.J.T. HEATLEY: 'Video transmission in optical fibre networks using PPM', *ECOC 83 - 9th Europ. Conf. on Optical Comms.*, 1983, pp 343-346.

[43]. W.M. HUBBARD: 'Utilization of optical frequency carries for low- and moderate bandwidth', *The Bell System Technical Journal*, No. 5/6, 1973, pp. 731-765.

[44]. Z. GHASSEMLOOY: 'Pulse position modulation spectral investigation', *Int. J. Electronics*, Vol. 74, No. 1, 1993, pp. 153-158.

[45]. Z. GHASSEMLOOY, B. WILSON, and B. BETTERIDGE: 'Pulse position modulation baseband spectral investigation, *Fourth Bangor Symposium on Communications*, 1992, pp 221-225.

[46]. F.R. CONNOR: 'Introductory topics in electronics and telecommunication noise', Edward Arnold, 2nd Ed., London, 1982, Ch. 6.2.

[47]. J. DAS and P.D. SHARMA: 'Pulse interval modulation', *Electronic Letters*, June 1967, Vol. 3, No. 6, pp. 288-289.

[48]. J.N. TRIPATHI: 'Spectrum measurements of pulse interval modulation', *Int. J. Electronics*, Vol. 49, No. 5, 1980, pp. 415-419.

[49]. R.S. FYATH, S.A. ABDULLAH, and A.M. GLASS: 'Spectrum investigation of pulse interval modulation', *Int. J. Electronics*, Vol. 59, No. 5, 1985, pp. 597-601.

[50]. Y. UENO and T. YASUGI: 'Optical fibre communication systems using pulse interval modulation', *NEC Research and Development*, Vol. 48, 1978, pp. 45-51.

[51]. Y. UENO, Y. OHGUSHI, and T. YASUGI: 'An optical fiber communications system using pulse-interval modulation', *IEE 1st Europ. Conf on Optical Fibre Comms.*, 1975, pp 156-158.

[52]. B. WILSON, Z. GHASSEMLOOY, and J.C.S. CHEUNG: 'Spectral prediction for pulse interval and width modulation', *Electronic Letters*, Vol. 27, No. 7, 1991, pp. 580-581.

[53]. S.D. MAROUGHI and K.H. SAYHOOD: 'Signal-to-noise performance of the PIWM system', *Electronic Letters*, Vol. 19, No. 14, 1983, pp. 528-530.

[54]. B. WILSON, Z. GHASSEMLOOY and L. CHAO: 'Square wave frequency modulation techniques', *IEEE Trans. on Comms.*, Vol 43, No. 2/3/4, Feb-April 1995, pp.1505-1512.

[55]. L. CHAO: 'Optical transmission of wide-band video signal using SWFM', PhD thesis, University of Manchester Inst. of Science and Technology, 1990.

[56]. J.H. CHIO: 'Optical fibre data link employing SWFM', MSc thesis, University of Manchester Inst. of Science and Technology, 1991.

[57]. I. GARRETT, N.M. CALVERT, M.J.N. SIBLEY, R.T. UNWIN and R.A. CRYAN: 'Optical fibre pulse position modulation', *BT Technolol. J.*, Vol. 7, No. 3, July 1989, pp 5-11.

[58]. J. D. MARTIN and H.H. HAUSIEN: 'PPM versus PCM for optical local area networks', *IEE Proc. I*, Vol. 193, No. 3, June 1992, pp 241-250.

[59]. J.J.O. PIRES and J.R.F. Da ROCHA: 'Digital pulse position modulation over optical fibres with avalanche photo diodes receivers', *IEE Proc.*, Vol. 133, pt. J, No. 5, Oct 1986; pp 309-313.

[60]. M.J.N. SIBLEY and A.J. MASSARELLA: 'Detection of digital pulse position modulation over highly / slightly dispersive optical channels', SPIE, Vol. 1974, 1993, pp 99-110.

[61]. R.A. CRYAN, R.T. UNWIN, I. GARRETT, M.J.N. SIBLEY, and N. CALVERT: 'Optical fibre digital pulse-position-modulation assuming a gaussian received pulse shape', *IEE Proc.-J*, Vol. 137, No. 2, 1990, pp. 89-96.

[62]. N.M. CALVERT, M.J.N. SIBLEY, and R.T. UNWIN: 'Experimental optical fibre digital pulse position modulation system', *Electronic Letters*, Vol. 24, No. 2, 1988, pp. 129-131.

[63]. R.A. CRYAN, R.T. UNWIN, A.J. MASSARELLA, M.J.N. SIBLEY, I. GARRETT and N. CALVERT: 'Optical fibre digital PPM: theoretical and experimental results', *Int. Symposium on Comms, Theory and Apps.*, July 1993.

137

[64]. R.A. CRYAN and R.T. UNWIN: 'Design of a bipolar receiver for optical fibre digital PPM', *Third Bangor Symposium on Comms.*, 1992, pp 309-312.

[65]. J.M.H. ELMIRGHANI and R.A. CRYAN: 'Analytic and numeric modelling of optical fibre PPM slot and frame spectral properties with application to timing extraction', IEE Proc - Commun., Vol. 141, No. 6, 1994, pp. 379-389.

[66]. R.A. CRYAN: 'High sensitivity optical digital pulse position modulation systems', PhD thesis, University of Huddersfield, 1992.

[67]. M.J.N. SIBLEY: 'Design implications for high-speed PPM', *SPIE Multigigabit Fibre Communication Systems*, Vol. 2024, 1993, pp. 324-353.

[68]. J.J. O'REILLY and W. YICHAO: 'Line code design for digital PPM', *IEE Proc.-F*, Vol. 132, No. 6, 1985, pp. 441-446.

[69]. H. SUGIYAMA: 'Method for block synchronisation in optical PPM', *IEE Proc.-J*, Vol. 140, No. 6, 1993, pp. 377-384.

[70]. J.M.H. ELMIRGHANI, R.A. CRYAN, and F.M. CLAYTON: 'Theoretical characterisation and practical implementation of optical fibre PPM self synchronisation sequences', *European Trans. on Telecom.*, Vol. 5, No. 3, 1994, pp. 97-103.

[71]. Z. GHASSEMLOOY, B. WILSON, and L. CHAO: 'Digitally generated pulse width modulation over optical fibre', *Int. J. Electronics*, Vol. 75, No. 3, 1993, pp. 433-436.

[72]. K. NANVAZADEH: 'Digital pulse width modulation', MSc thesis, Sheffield City Polytechnic, Jan. 1991.

[73]. M. SATO, M. MURATA and T. NAMEKAWA: 'A new optical communication system using pulse interval and width modulated code', *IEEE Trans. on Cable Television*, Vol. CATV-4, 1979, pp. 1-9.

[74]. L.W. COUCH: 'Digital and analog communication systems', Macmillan, 4th Ed., New York, 1987, Ch. 6.2.

[75]. C.J.J. ROTH: 'Fundamentals of logic design', West Publishing Company, 4th Ed., St Paul, 1992, Chs. 13, 22, 26.

[76]. GEC Plessey Semiconductors: 'Application note AN72: SP973T8 - an 8-bit wide-band Flash ADC with TTL outputs', Data Converters & Datacoms - IC Handbook, July 1991, pp. 4-74 to 4-79.

[77]. Texas Instruments: '74LS04 Hex inverter', The TTL Data Book, Texas Instruments 1982, pp. 5-11 to 5-12.

[78]. Texas Instruments: '74LS00 Hex inverter', The TTL Data Book, Texas Instruments 1982, pp. 5-3 to 5-4.

[79]. GEC Plessey Semiconductors: 'SL560, 300 MHz low noise amplifier and line driver', Personal Communications - IC Handbook, May 1992, pp. 62-66.

[80]. Analog Devices: 'LC^{2}MOS high speed, μp-compatible 8-bit ADC with track/hold function', Data Converters Reference Manual Vol II, 1992, pp. 2-521 to 532.

[81]. Maxim Integrated Products: 'Dual micropower, single supply rail-to-rail op-amp', Data sheet no. 19-0265, June 1994.

[82]. Philips Semiconductors - NAPC / Signetics: 'CMOS high density programmable logic PML2552', Product Specification, April 1991.

[83]. Texas Instruments, '74LS08 quad 2-input positive And gates', The TTL Data Book, Texas Instruments 1982, pp. 5-15 to 5-16.

[84]. Maxim Integrated Products: 'Single, dual and quad 10 MHz single-supply op-amp', Product Specification 19-0260, Jun 1994.

[85]. Maxim Integrated Products: 'Single ULTRA-FAST, LOW-POWER, PRECISION TTL comparator', Product Specification 19-0157, Jan 1994.

[86]. Texas Instruments: 'SN74121 monostable multivibrators with schmitt-trigger inputs', Standard TTL Data Book Vol. 1, Texas Instruments 1983, pp. 3-245 to 3-250.

[87]. Hewlett Packard: 'HFBR-14X2 high-speed low-cost fibre optic transmitter', Optoelectronics Designer's Catalogue, 1993, pp. 5-23 to 5-30.

[88]. Hewlett Packard: 'HFBR-24X4 high-speed low-cost fibre optic receiver', Optoelectronics Designer's Catalogue, 1993, pp. 5-31 to 5-30 to 5-34.

[89]. GEC Plessey Semiconductors: 'ZN428E8 8-bit latched input D-A converter', Data Converters & Datacoms - IC Handbook, July 1991, pp. 1-155 to 1-163.

[90]. GEC Plessey Semiconductors: 'TAB1043 quad op-amp', Professional Products- IC Handbook, May 1991, pp. 1-75 to 1-77.

[91]. J. MIDDLEHURST: 'Practical filter design', Prentice Hall, Sidney, 1993, Ch. 2, pp.1.

[92]. P. HORROWITZ and W. HILL: 'The art of electronics', Cambridge University Press, Cambridge, 2nd Ed. 1989, Ch. 8.27.

[93]. Philips Semiconductors: 'SNAP: synthesis netlist analysis and program software', User Manual; Sunnyvale, Philips North American Company, 1993.

[94]. A. SCHATORJÉ: 'PLC42VA12 used as an I^{2}C-bus remote n-bit i/o expander controller', Report No. EIE/AN93004; Product Concept & Application Laboratory Eindhoven (NL), March 1993.

[95]. U. KRÜGER and J. MEIXNER: 'Coder and decoder for wire encoded signals with PML2552', Philips Application Note; Ingenieurhochschule Mittweida (Ger), June 1993.

[96]. M. KRUG: 'Modelling and simulation of a sub-carrier multiplexed system using Matlab', Final year project, Fachhochschule fur Technik Esslingen (Ger) & Sheffield Hallam University, 1994.

[97].   The Mathworks Inc.: 'Matlab reference guide', Natick MA 1993.

[98].   The Mathworks Inc.: 'Matlab user's guide', Natick MA 1993.

[99].   Z. GHASSEMLOOY, R.U. REYHER, A.J. SIMMONDS and E.D KALUARACHCHI: 'Digital pulse interval width modulation', *Microwave and Electronic Letters*, submitted: August 1995.

[100].   Z. GHASSEMLOOY, E.D. KALUARACHCHI, R.U. REYHER and A.J. SIMMONDS: 'A new modulation technique based on digital pulse interval modulation (DPIM) for optical-fiber communication', *Microwave and Optical Technology Letters*, Vol. 10, No. 1, Sep. 1995, pp. 1-4.

[101].   U. SCHILLER, R.U. REYHER, Z. GHASSEMLOOY, A.J. SIMMONDS and J.M. HOLDING: 'Modelling of a baseband data transmission system in hardware and software', *IEEE Transactions on Education*, submitted: July 1993, reviewed: Feb. 1994, scheduled for publication: autumn 1996.

[102].   R. U. REYHER, Z. GHASSEMLOOY, A.J. SIMMONDS and E.D. KALUARACHCHI: 'Digital pulse interval width code modulation (PIWCM) for optical fibre communication', *SPIE Photonics East: 1st International Symposium on Photonics Technologies and Systems for Voice, Video and Data Communications*, 23-26 Oct 1995, Philadelphia USA, SPIE 2641-08.

CHAPTER 12

PUBLISHED PAPERS

Pulse Interval and Width Code Modulation

Z. Ghassemlooy, R. Reyher, E. D. Kaluarachchi, A. J. Simmonds and R. Saatchi

Electronics & communication Engineering Research Group, School Of Engineering

Information Technology, Sheffield Hallam University, Sheffield, U.K.

Abstract

This paper investigates both theoretical and practical aspects of implementation of a new digital pulse time modulation technique based on pulse interval and width code modulation (PIWCM) scheme for transmission of analogue/digital signal. Original expression is presented for power spectral density and the results obtained closely match with simulated and practiacl results. The developed system will have applications in point-to-point fibre optic transmission links and fibre optic broaband networks.

Introduction

Pulse time modulation (PTM) techniques have been proposed for transmission of analogue signals over short to medium haul point-to-point optical fibre communication links. In this type of modulation the transmitted carrier is a binary pulse amplitude, where the pulse width, pulse position, pulse interval, pulse frequency is modulated by an incoming modulating signal. PTM schemes have the advantage that the information can be transmitted at a reduced bandwidth than that required by pule code modulation (PCM) at much reduced cost and complexity. They also have the ability to trade bandwidth overhead for signal-to-noise ratio performance[1-4]

Recently, a digital PTM scheme, known as digital pulse position modulation (DPPM) has been suggested for long-haul point-to-point links over mono-mode fibre, showing substantial improvement in receiver sensitivity compared to PCM under conditions that the fibre bandwidth is not limited. The scheme under consideration utilises the pulse position

modulation (PPM) [5-7] format where the time interval of M bits of PCM is subdivided into n = 2^M time slots and the information is conveyed by positioning a single pulse in one of the n time slots. In contrast to its analogue equivalent, digital PPM actually consumes more bandwidth than that required by PCM. It has been shown that digital PPM can offer improvements of between 5-11 dB [8-10] (depending on the coding level , bandwidth and detection technique) in receiver sensitivity when compared to PCM. This represents an increase in point-to-point transmission of between 25-55 km. However, DPPM timing requirements are exceptionally critical to the system performance and far exceed the equivalent PCM timing requirements[11]. This paper proposes a new digital PTM scheme known as pulse interval and width code modulation (PIWCM) (also known as digital PIWM) offering simplicity and ease of frame synchronisation.

Theoretical

PIWCM is closely related to PIWM in that it employs a waveform in which both mark and space represent the sampled data [3], but with PIWCM these mark and space time interval slots are made discrete. PIWCM is anisochronous PTM technique in which each successive frame length is different and determined only by the sampled value of the modulating signal, not by the choice of the predetermined clock (sampling) period. As a consequence, receiver design complexity is substantially reduced since there is no requirement to extract frame frequency and phase for synchronisation in order to correctly interpret the encoded sampled value. Depending on source connection, PIWCM can carry encoded PCM data or directly sampled signals.

The digital signal converted from analogue signal is coded into PIWCM code by an M bit coder and applied to the modulator, Fig. 1. An M bits digital signal is divided into two sets of k bits (here, k is chosen to be equal to half the M bits). The decimal equivalent of binary combination in a given set determines the number of time slots for mark (m) and space (s). At time t equal to zero conversion first takes place for mark followed by conversion for space. To represent zero one is added to each code words. Finally, time slots for mark and space are combined together to produce the desired PIWCM signal. Differentiating the PIWCM

142

waveform will result in a constant width narrow pulse train known as pulse interval code modulation (PICM), see Fig. 2. This modulation scheme is suitable for long-haul fibre optic communication system where high peak optical power and low average optical power is required. At the demodulator the process is reversed, where the transmitted frame length is determined by simply counting the number of time slots for mark and space, a process which requires frame synchronisation, and converting them to binary digit. PIWCM modulator and demodulator designs can be formulated around state machines. This new scheme offers higher transmission capacity by virtue of fully utilising the time slots for a given frame and illuminating unused time slots. Synchronisation is simply achieved by initiating each frame with marks followed by spaces.

PIWCM frame length will be given by:

$$L = \left[\text{Mod}\left(\frac{x}{2^k}\right) + 1 \right] + \left[\text{Rem}\left(\frac{x}{2^k}\right) + 1 \right] \tag{1}$$

where the first and second term represent the number of time slot for mark and space respectively, x is the decimal equivalent of each k bit binary set. The longest and shortest PIWCM frame lengths will be are 2^{k+1} and 2 time slots T_s, resulting in average frame length of $2^k + 1$ time slots. The maximum total time occupied by a PIWCM frame is T_f which is therefore $2^{k+1} T_s$ seconds. The expression for time slot duration in PIWCM and PCM in terms of sampling frequency f_s can be written as:

$$T_{PIWCM} = \frac{1}{2^{k+1} f_s}$$
$$T_{PCM} = \frac{1}{M f_s} \tag{2}$$

PIWCM displays shorter time slot duration compared to PCM (and wider time slot duration compared to DPPM) and hence higher channel bandwidth requirement for values of M greater than 2. For a signal of bandwidth f_m Hertz sampled at the minimum Nyquist rate the maximum slot rate will reduce to $f_r = 2 f_m 2^{k+1}$. Owing to its anisochronous nature resulting in

different frame lengths, the instantaneous sampling frequency (slot rate) of PIWCM changes according to the amplitude of the modulating signal.

The transmission capacity for PCM and PIWCM systems are:

$$C_T = \frac{Maximum\ code\ length}{Average\ code\ length} 2f_m Log_2\ (Possible\ number\ of\ valid\ codes)$$

Thus: $C_{PCM} = 2Mf_m$ and $C_{PIWCM} = \frac{2^{k+1}}{2^k+1} 2f_m M$ (3)

For large values of M the transmission capacity of PIWCM (and PICM) is twice that of the PCM, see Fig 3. This is as we expected, since on average a PIWCM frame will be only half the length of a PCM frame, enabling two-times the sampling frequency rate to be employed, thus permitting a signal of two-times the bandwidth to be adequately sampled.

In DPPM guard space is required at the end of each frame to cater for pulse dispersion and hence to avoid interframe interference. However, in PIWCM this guard space is redundant, since each frame is started off with a mark followed by a space.

Mathematically PIWCM wave train consisting of frames of different lengths and mark-space patterns could be represented as:

$$x(t) = \sum_{i=-\infty}^{\infty} P_{(m,s)_i} \left[t - T_s \left(\sum_{a=-\infty}^{i-1} (m_a + s_a) \right) \right]$$ (4)

where $P_{(m,s)_i}$ represents the ith PIWCM sample with m_i time-slots of mark and s_i time-slots of space and m_a and s_a are the number of time-slots for mark and space at the a th sample respectively and T_s is the slot duration.

The Equation (4) indicates that PIWCM does not display a regular periodic frame structure in the manner of PCM and DPPM, except in the absence of any incoming data where the results is an alternating mark and space pattern.

To be able to characterise the process practically it is beneficial to evaluate the power spectral density of a truncated realisation. Following a process similar to that obtained in Reference 11, we have obtained a numeric spectral model for digital PIWCM given by

$$S(f) = \frac{1}{T_S \sum\limits_{i=0}^{N}(m_i + s_i)} \left| \sum\limits_{i=0}^{N} G_{(m,s)_i}(f) e^{-j2\pi f T_s \sum\limits_{a=0}^{i-1}(m_a + s_b)} \right|^2 \tag{5}$$

where: $G_{(m,s)_i}(f)$ is the PIWCM pulse shape transform of the ith sample, m_i and s_i are the number of time slots for mark and space in the ith sample respectively, a random number 1, 2 ...2^k for M bit resolution. N gives the length of the truncated data frame sequence

A typical PIWCM spectrum evaluated using Equation (5) for a random data taken over 1000 frames evaluated at 320 frequency points for 8 bit resolution is shown in Fig. 4.a with the frequency axis normalised to the slot frequency and power level over the frequency span to 0 dBm. Confirmation of the Equation (5) is provided by the close match obtained with the results from the simulated spectral analysis and practical system , Fig.4.b & c. In all cases the digital PIWCM provides distinctive spectral components at the slot frequency and its harmonics.

Conclusions

In this paper a new digital PTM scheme know as PIWCM has been presented examined as a possible alternative to conventional PCM. It has shown to have a much higher transmission capacity and requires no complex frame synchronisation in the receiver in contrast to PCM and DPPM. These features have been obtained at the expense of increased transmission bandwidth. Original expressions have been presented to characterise the scheme in the frequency and time domains, showing excellent agreement with results obtained from software simulation. The signal format appears to be, at this time, an attractive possibility for medium to high speed point-to-point optical communication links.

Acknowledgements

References

1   Sato, M., et al,: 'A New Optical Communication System Using the Pulse Interval and Width Modulation Code', IEEE Trans. Cable TV, Vol. CATV-4, No. 1, 1979, pp. 1-10.

2   Wilson B and Ghassemlooy Z: 'Pulse Time Modulation Techniques for Optical Communications: a Review', IEE Proceedings J, Vol. 140, No. 6, Dec. 1993, pp. 346-357.

3   Wilson B, Ghassemlooy Z and Cheung J C S: ' Optical Pulse Interval and Width Modulation Systems', IEE Proceedings J, Vol. 39, No. 6, 1992, pp. 376-382.

4   Heatley, D J T,: 'Video Transmission in Optical Local Area Network using Pulse Time Modulation', 9th European Conference on Optical Communications, Geneva, 1983, pp. 343-345.

5   Garrett I.: 'Digital PPM over Dispersive Optical Fibre Channels', International Workshop on Digital Communications', Tirrenia, Italy, Aug. 1983, pp. 15-19.

6   Pires J T O, et al.: 'Digital PPM over Optical Fibers with Avalanched Photodiodes Receivers', IEE Proc. J. Optoelectronics, 1986, Vol. 133, pp. 309-313.

7   Calvert MN, et al,: 'Experimental Optical Fibre Digital Pulse Position Modulation System', Electronic Lett., 1988, Vol. 24, pp. 129-131.

8   Garrett I.: 'Pulse Position Modulation for Transmission over Optical Fibers with Direct or Heterodyne Detection ', IEEE Trans. on Commun., 1983, COM-31, pp. 518-527.

9   Garrett I, 'Pulse Position Modulation for Transmission over Optical Fibres with Direct or Heterodyne Detection', 1983, IEEE Tran., COM-31, (4), pp. 518-527.

10   Cryan R A, et al.: 'Optical Fibre Digital Pulse-Position-Modulation Assuming a Gaussian Received Pulse Shape', IEE Proc. J, 1990, 137, (4), pp. 89-96.

11   Elmirghani, J.M.H and Cryan, R.A.: 'Analytical and numeric modelling of optical fibre PPM slots and frame spectral properties with application to timing extraction', IEE. Proce.-Comms, 1994, 141, pp. 379-389.
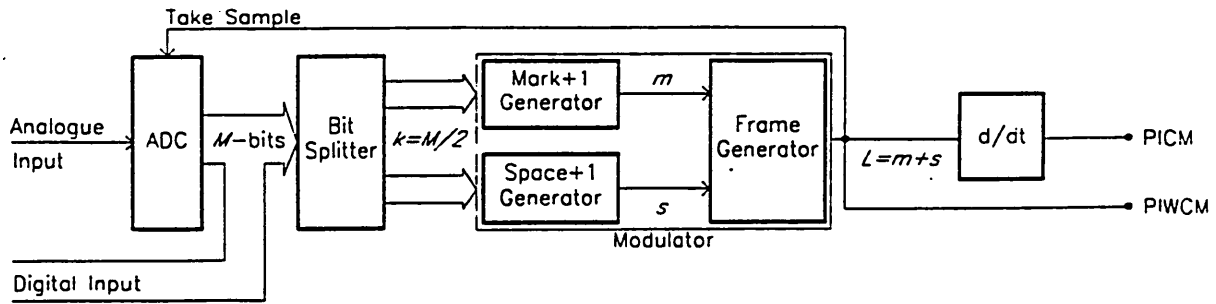
Figure 1 Modulator block diagram
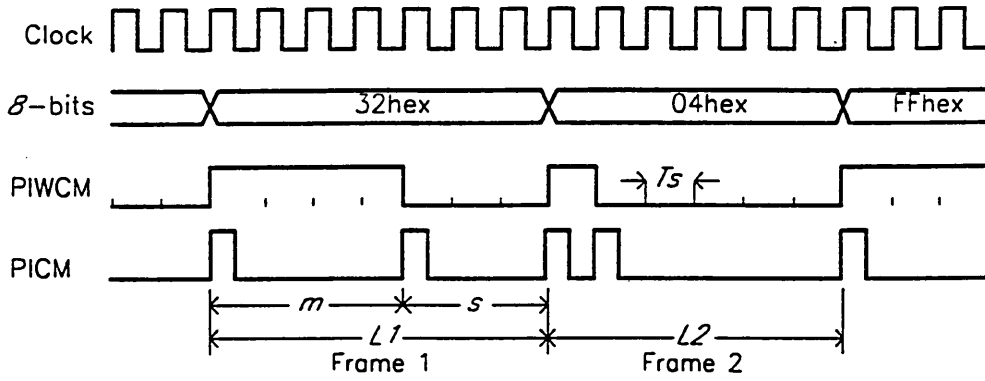
Figure 2 Typical PIWCM and PICM waveform
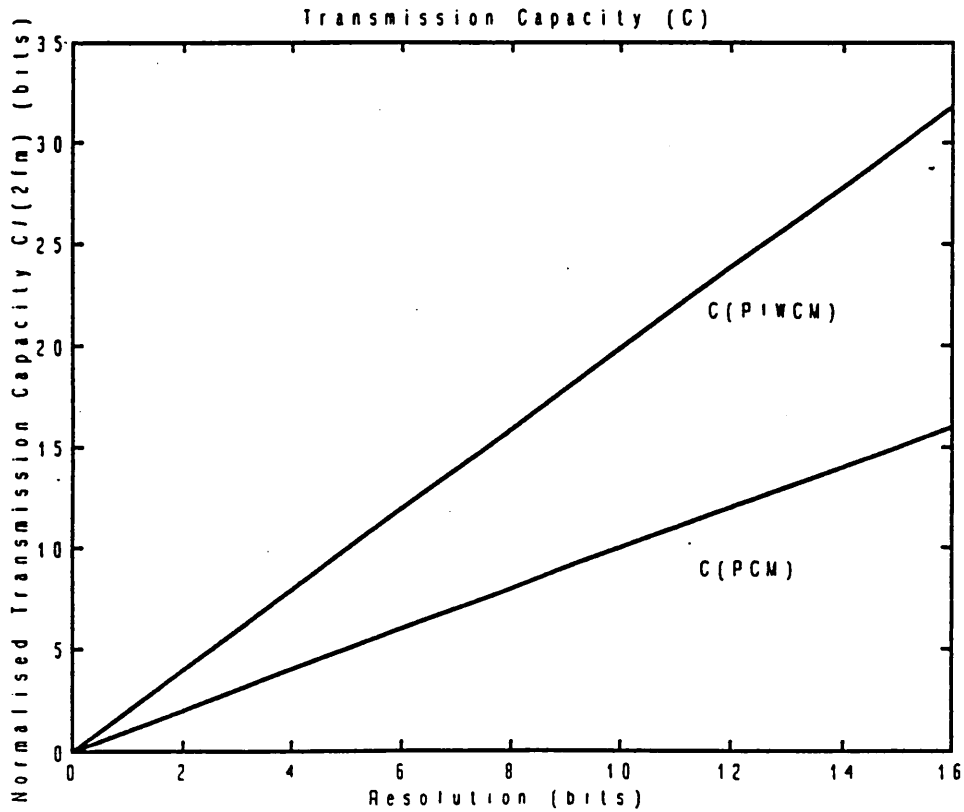
Figure 3 Transmission capacity versus bit resolution

147

(a)

(b)

Normalised Frequency

hp   stopped

horiz magnify
off   on
X1

freq span
5.00 MHz
5.00 MHz

# of points
8192
res 1.22 kHz

sensitivity
10.0 dB/div

position
0.00000   dBm

window
Hanning
"frequency res"

0.00000   Hz   2.50000 MHz   5.00000 MHz
                f1:   10.0   dB/div   position   0.000   dBm

y2(f1)   0.00000   dBm   x2(f1)   2.00000 MHz
y1(f1)   0.00000   dBm   x1(f1)   1.00000 MHz
delta y 0.00000   dB   delta x 1.00000 MHz
                           1/delta x 1.00000 us

more

Figure 4 Power spectral density for PIWCM (a) theoretical (b) simulated (c) measured

148

A Novel Digital Modulation System using Pulse Interval Code Modulation (PICM) and Pulse Interval Width Code Modulation (PIWCM)

R.U. Reyher, Z. Ghassemlooy, A.J. Simmonds and R. Saatchi
Sheffield Hallam University, School of EIT, Pond Street, Sheffield S1 1WB
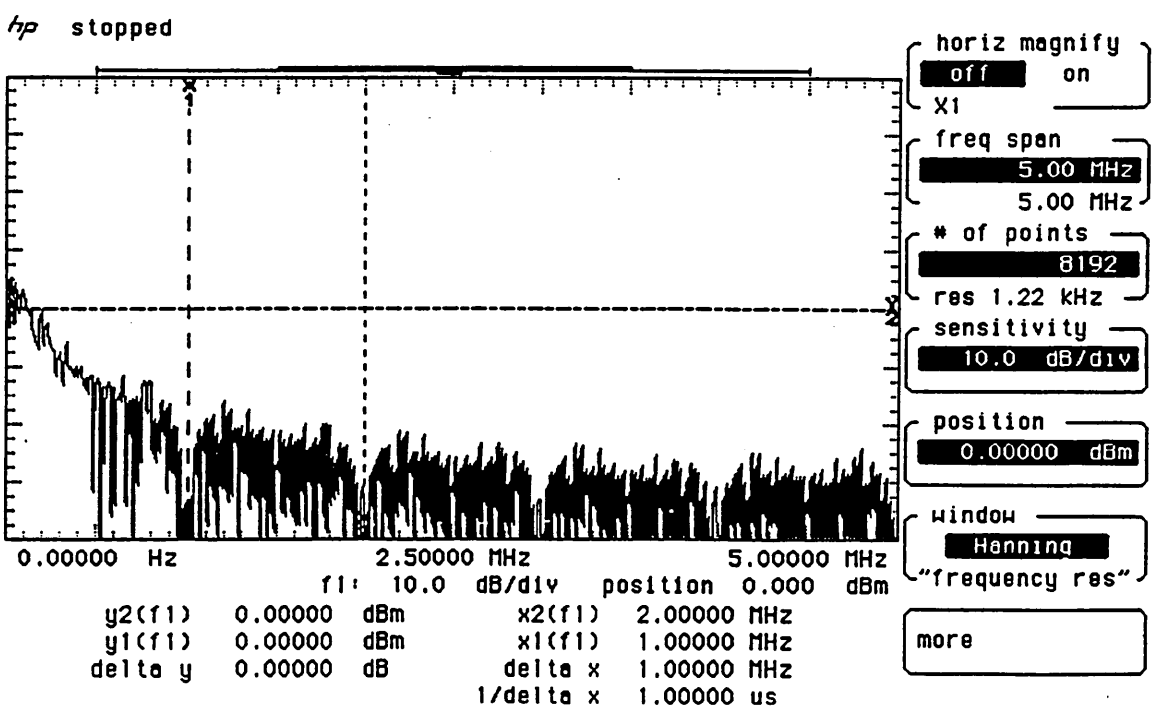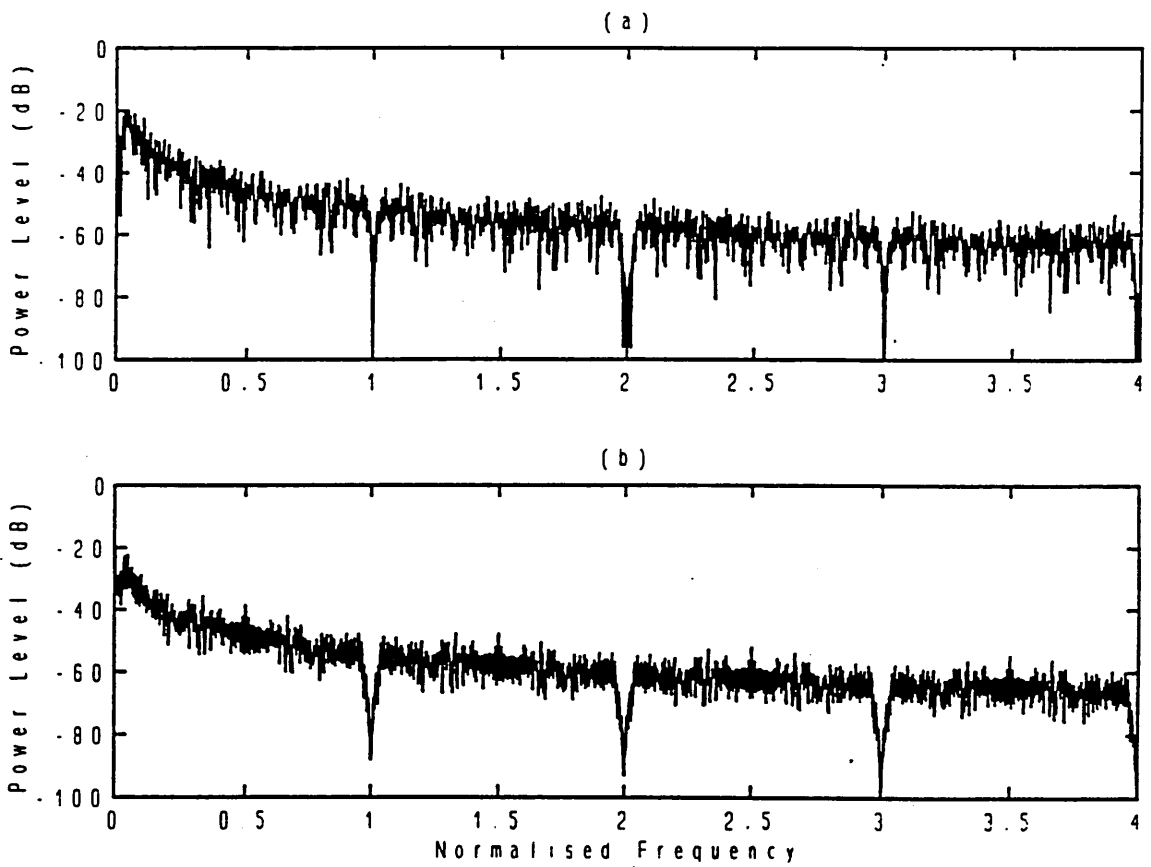
There are two types of pulse modulation methods, digital and pulse analogue modulation. Digital modulation (e.g. Pulse Code Modulation PCM) is widely accepted and is suitable for switching and routing through communications networks. The main advantages of digital networking are efficiency, flexibility, reliability and multiple application orientated services. Pulse analogue modulation techniques (in particular Pulse Time Modulation, PTM) are predominantly used for optical point-to-point transmission and are also employed in Local Area Networks (LANs).

Models of digital Pulse Position Modulation (PPM) have been discussed by a number of authors. It is shown that digital PPM has a clear operating advantage over PCM for conventional data rates due to its high peak optical power which is substantially greater than its mean power; this leads to an increase of receiver sensitivity, a greater signal-to-noise ratio and consequently to a smaller bit-error-rate compared to PCM. Discrete code generation with the Pulse Interval Width format was presented in 1979. This code shows advantages in synchronisation and bandwidth requirement over the PPM and PCM codes.

Two new modulation schemes, Pulse Interval Code Modulation and Pulse Interval Code Width Modulation are proposed. Both codes vary the pulse and frame length according to the modulating signal and can accommodate more information than similar schemes with a fixed frame length (PPM, PWM). PICM and PIWCM are closely related and can be converted easily from one form to the other, but they exhibit different characteristics and are therefore suitable for different applications. Attention is drawn to PIWCM because of its self synchronising code recognition. Code properties of PICM and PIWCM are presented to gain high resource utilisation and the coding scheme is described, suitable for digital communication over wire or optical fibre links.

PICM and PIWCM are derivatives of anisochronous PTM techniques where the pulse duration and the frame length varies with the amplitude of the modulating signal. However with PICM and PIWCM the output is a digital signal, consisting of time slots within a variable frame, not a continuous signal as is the case with existing Pulse Interval Modulation (PIM) and Pulse Interval Width Modulation (PIWM). The transmission capacity is found to be higher than in PPM or PWM, but less than in PCM.

In PIWCM each frame consists of two transitions with the low-high transition indicating the start of frame, and the high-low transition associated with the end of mark. Therefore, with a single channel system, there is no requirement for the transmission of an additional frame synchronisation pulse, which is necessary when using PCM. The average pulse period (mark) of a PIWCM pattern is greater than that of a corresponding PCM pulse pattern assuming the same data rate, thus requiring less average transmission bandwidth.

Every transition in PIWCM is indicated with a short pulse in PIWCM. The pulses, with fixed duration, and the low duty cycle compared to PIWCM and PCM will require higher transmission bandwidth. But the gain is that high peak optical power output is provided compared to a low average optical power budged. This allows a very high signal-to-noise ratio to be achieved, therefore reducing the bit-error rate and increasing the reliability of the system.

A practical 8-bit word system is designed and built. Analogue to digital conversion provides a parallel 8-bit stream that is transformed by the modulator into PICM and PIWCM at the modulator output simultaneously. The receiver uses the demodulator to transform either of the transmitted pulse trains back into a parallel bit stream which is then converted by the digital-to-analogue converter in order to recover the original message.

Basic elements in modulator and demodulator are state machines that guarantee synchronous code generation and recognition. Their task is to count out the provided discrete information. It is assumed that the ADC converts data at every clock interval. Sampling in the modulator is achieved with an internal D-latch that only takes data from the ADC when the last time slot of a frame is issued. The modulator is then fed with a multiplexed split code, consisting of low-word and high-word, four bits each. Using the parallel bit stream of each word, translates their value into the relevant number of time slots for mark and space, triggered at every clock interval. With the received frame, the demodulator state machine translates marks and spaces, at every clock interval, into low-word and high-word respectively which are than stored in buffers to built up the discrete 8-bit code. The DAC is then ready to sample that information.

Transmitter-receiver synchronisation is achieved by locking the demodulator onto the rising edges of the received PIWCM frames, assuming the same clock speed for both devices. No guard band is required, as in PCM or PPM. Synchronisation is more critical with PICM because having two pulses per frame may lead to the inversion of mark and space. At this stage of implementation it is assumed that the first received PICM pulse is also the start of frame. Additional time slots are introduced for mark and space, one each, to make sure that a zero level has still marks and spaces. To increase the signal-to-noise performance of the system a matched filter at the receiver input is proposed to maximise the peak pulse signal in the presence of additive noise. Multiplexing potential of the modulation system is also identified.

The process of code generation and detection is examined along with coding rules, and the associated system requirements. Simulation and experimental results are compared with the theoretical prediction and placed along with equivalent PCM and PPM systems.

A NEW MODULATION TECHNIQUE BASED ON DIGITAL PULSE INTERVAL MODULATION (DPIM) FOR OPTICAL-FIBER COMMUNICATION

Z. Ghassemlooy, E. D. Kaluarachchi, R. U. Reyher, and A. J. Simmonds
Electronics & Communication Engineering Research Group
School of Engineering Information Technology
Sheffield Hallam University
Sheffield, United Kingdom

ABSTRACT

A novel digital pulse time modulation (PTM) technique called digital pulse interval modulation (DPIM) is presented, in which the input signal information is transmitted by the time intervals between two succeeding pulses. DPIM has simplicity of circuit configuration combined with other attractive features of digital pulse position modulation (DPPM) for optical-fiber communications. This article derives theoretical expressions for transmission capacity, code characteristics, and power spectral density (PSD), and the analytical results are compared with experimental data. © 1995 John Wiley & Sons, Inc.

1. INTRODUCTION

Today, commonly available optical fiber links have bandwidths an order of magnitude greater than required for the data rates transmitted over them. The availability of this wider bandwidth may be used to achieve a high information capacity with low system complexity by using suitable modulation techniques. It is well known that PTM techniques may be used to trade bandwidth for signal-to-noise ratio; such systems have been explored for video transmission over optical fibers [1–7]. Recently, a discrete PTM scheme called digital pulse position modulation (DPPM) has been suggested for long-haul point-to-point links over single-mode fiber [9–13]. Garrett [9] and Calvert, Sibley, and Unwin [10] have shown substantial improvements of receiver sensitivity for DPPM over an equivalent binary pulse code modulation (PCM) system when the fiber bandwidth was several times that required by PCM. Martin and Hausien [11] show DPPM as a possible alternative to conventional signaling in local area networks. However Cryar and Elmirghani [12] point out the necessity of introducing special circuitry for synchronization. Thus, DPPM does need special provision to ensure synchronization at the receiver end.

This article introduces a new asynchronous digital PTM system called digital pulse interval modulation DPIM. In this modulation technique each frame starts with a pulse of one time slot duration and the information to be transmitted is represented by the number of time slots between two successive pulses; thus the name pulse interval modulation. No synchronization is required at the demodulator, unlike DPPM, as this modulating technique has synchronization imbedded. Due to the average code length of DPIM being less than that of PCM and DPPM, DPIM has a higher transmission capacity. In this article analytical results for transmission capacity, time slot duration, and power spectral density are presented, and, where appropriate, compared with DPPM and PCM.

2. SYSTEM DESCRIPTION

In DPIM, the sampled input is transmitted by a mark of one time slot followed by a space of $n + 1$ time slots, where n is the modulating signal amplitude (instead of displacement of pulse position from equally spaced reference time positions as utilized in DPPM). An M-bit PCM word with magnitude n is input to the DPIM coder. In order to transmit zero, 1 is added to ensure there is always an interval. The DPIM coder thus generates one time slot of mark followed by $n + 1$ time slots of space, hence the DPIM signal frame length is dependent on the magnitude of the PCM code word; see Figures 1 and 2. This means the sampling frequency of the system will vary accordingly.

At the receiver, the occurrence of a short pulse (mark) indicates the start of a new frame. The demodulator then determines the transmitted frame length by counting the number of time slots between two pulses. Hence no synchronization of reference time positions between the transmitter and receiver is required. The slot clock can be simply extracted from the incoming data stream; see the spectral model. The spectral component of the slot clock can be optimized by varying the duty cycle of the DPIM pulse. Therefore, this scheme has a simplicity of circuit configuration together with the well-known attractive features of DPPM for optical communications systems [12].

With M slot PCM let the interval between samples (i.e., the frame length in seconds) be T_f. The frame length of DPPM with 2^M slots is also T_f. When DPIM transmits the highest magnitude signal (all M bits high) the DPIM frame length is also T_f. The time slots for PCM, DPPM, and DPIM can be given as

$$Ts_{PCM} = \frac{1}{Mf_f},$$

$$Ts_{PPM} = \frac{m}{2^M f_f},$$

$$Ts_{DPIM} = \frac{1}{(2^M + 1)f_f} \tag{1}$$

where

$$f_f = \frac{1}{T_f} \text{ is the minimum sampling frequency.}$$

M is the PCM word length and m is the modulation index ($0 \leq m \leq 1$) of DPPM. From Eq. 1 DPIM has a longer time slot duration than DPPM at $m < 1$. This results in a reduced worst-case transmission bandwidth for DPIM compared to DPPM ($m < 1$).

Due to the asynchronous nature of the DPIM code the sampling frequency f_s varies; that is,

$$\frac{(2^M + 1)f_f}{2} \geq f_s \geq f_f, \tag{2}$$

where M is the PCM word length.

To show that DPIM code has a higher transmission capacity than with DPPM and PCM assume the modulating signal occupies the full range of the A/D, in another words 100% modulation. For M-bit PCM the possible code combinations for DPIM may be given as 2^M and the shortest and longest duration of DPIM codes are $2Ts$ and $(2^M + 1)Ts$, respec-

tively. Thus with 100% modulation the average code length of DPIM, assuming a ramp signal, can be given by

$$C_{avg} = \frac{\sum_{l=2}^{2^M+1} l}{2^M} = \frac{2^M + 3}{2}. \tag{3}$$

The transmission capacity is given by [8] as

$$C_{cap} = \frac{\text{longest code length}}{\text{average code length}} \log_2(\text{valid code combinations}).$$

Thus for M-bit PCM and for DPPM $C_{cap} = M$, while for DPIM,

$$C_{cap} = \frac{2M(2^M + 1)}{2^M + 3}. \tag{4}$$

Transmission capacity of DPIM is compared with PCM in Figure 3, where transmission capacity is normalized to the PCM sampling frequency.

3. CODE CHARACTERISTICS

When all M bits in the PCM word are high the DPIM code has its frame duration (T_A) equal to the PCM frame duration
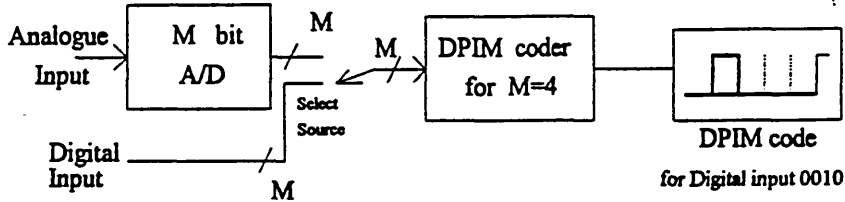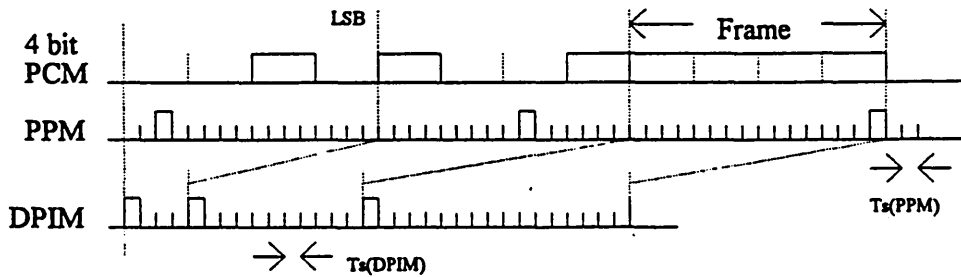

Figure 1 DPIM code generation

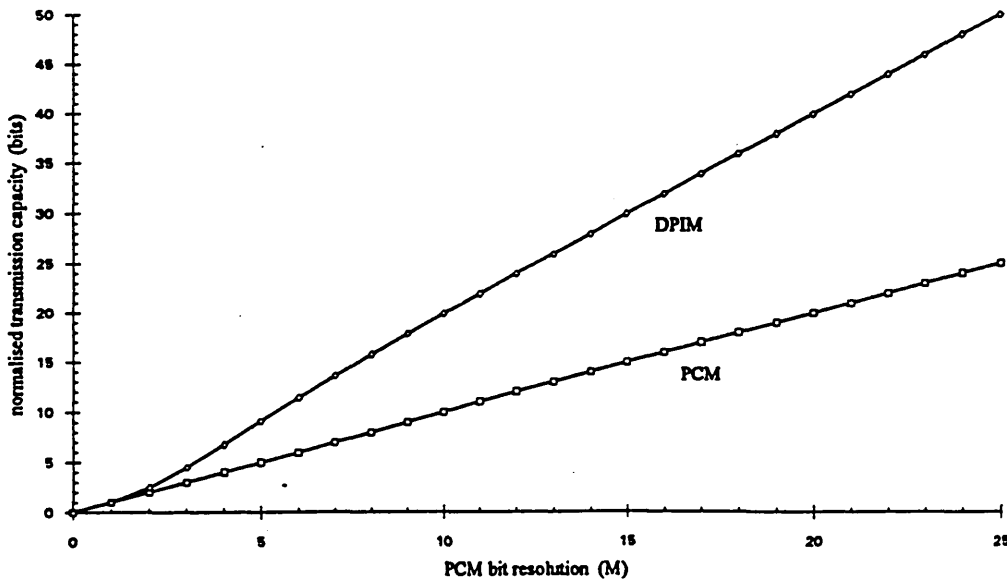Figure 2 PCM, DPPM, and DPIM code patterns

Figure 3 Transmission capacity versus PCM bit resolution

(T_f). Time slot duration is evaluated taking the maximum modulating signal amplitude and the sampling frequency into account, as given in Eq. (1). Due to the nature of DPIM frames, as the modulating signal amplitude increases the pulse displacement between two samples increases, and as the amplitude decreases the pulse displacement reduces. Thus the higher the signal amplitude, the lower the sampling frequency and vice versa. The DPIM pulse stream can be represented by

$$x(t) = \sum_{k=-\infty}^{\infty} P\left(t - T_s\left(k + \sum_{m=-\infty}^{k-1} S_m\right)\right),\qquad (5)$$

where $P(t)$ is the DPIM pulse wave form, S_m is the number of time slots for space for the mth sample and T_s is the DPIM time slot. The kth sample includes the pulse $P(t)$ and S_k time slots of spaces.

4. SPECTRAL MODEL

The power spectral density function (PSD) $S_{DPIM}(\omega)$ describes the distribution of power versus frequency and hence is an important measurement of the system. Elmirghani and Cryan [13] consider the DPPM spectrum as being composed of the sum of contributions from a set of delayed pulses. Considering a random number of DPIM samples, this approach is equally valid with DPIM. The PSD function for DPIM has been modeled and compared with the DPIM spectrum obtained from the prototype. Equation (6) gives the PSD model of the DPIM system:

$$S_{DPIM}(f) = \frac{1}{T_s\left(L + \sum_{k=0}^{L} S_k\right)}$$

$$\times \left\{\left|G(f) \sum_{k=0}^{L} e^{-j2\pi f T_s(k + \sum_{m=0}^{k-1} S_m)}\right|^2\right\},\qquad (6)$$

where L is the number of frames, $G(f)$ is the DPIM pulse transform. S_k is the number of time slots of spaces in the kth sample, and T_s is the DPIM time slot.

Using Eq. (6), a digital spectrum was evaluated for a random data sample of 4000 frames (L) and 9000 frequency points. Results are given in Figure 4. The frequency axis is normalized to the slot frequency, and the power levels of the above frequency span are normalized to 1 dB. Compare this with the prototype system spectrum Figure 5 and clearly the theory is accurate.

From Figures 4 and 5 it can be seen that DPIM gives distinctive frequency components at odd harmonics of the slot frequency. Thus, with this modulating technique. the slot rate can be extracted from the incoming data stream at the receiver. Variation of this component with respect to the duty
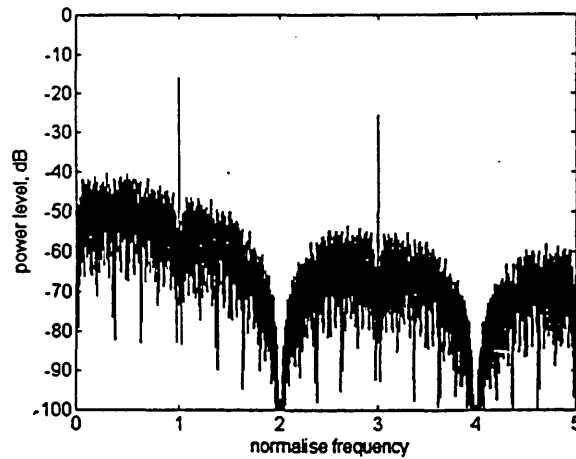

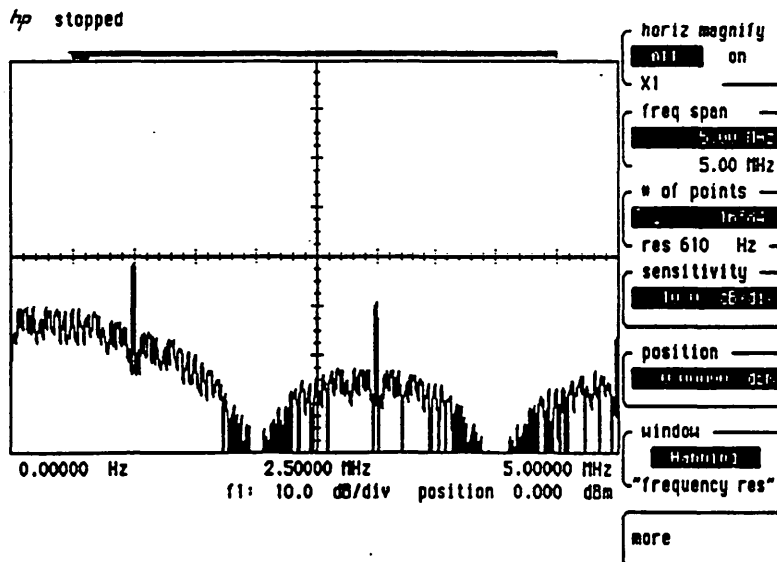**Figure 4** Predicted spectrum for DPIM with $M = 4$ and 50% duration pulses

Figure 5 The measured slot rate spectrum with $M = 4$, slot frequency $= 1$ MHz, 50% duration pulses

cycle of the DPIM pulse has been analyzed, and it was observed that a 50% duty cycle of the pulse at the start of a DPIM frame is suitable for optimum timing extraction.

5. CONCLUSIONS

We have presented a novel digital pulse time modulation technique for optical fiber transmission called digital pulse interval modulation (DPIM). Original analytical and experimental results for power spectral density and information capacity are presented and compared with the predicted performance. The technique is simple to implement, requires no special synchronization techniques, and offers bandwidth savings over DPPM.

REFERENCES

1. Wilson, Z. Ghassemlooy, and J. C. S. Cheung, "Optical Pulse Interval and Width Modulation for Analogue Fibre Communications," *IEE Proc. Pt. J*, Vol. 139 No. 6, 1992, pp. 376–382.
2. B. Wilson and Z. Ghassemlooy, "Pulse Time Modulation Techniques for Optical Communications: A Review," *IEE Proc. Pt. J*, Vol. 140 No. 6.
3. M. Sato, M. Murata, and T. Namakawa, "Pulse Interval and Width Modulation for Video Transmission," *IEEE Trans. Cable Television*, vol. CATV-3 No. 4, 1978, pp. 165–173.
4. A. Okazaki, "Still Picture Transmission by Pulse-Interval Modulation," *IEEE Trans. Cable Television*, Vol. CATV-4, No. 1, pp. 17–22.
5. A. Okazaki, "Pulse Interval Modulation Applicable to Narrow Band Transmission," *IEEE Trans. Cable Television*, Vol. CATV-3, No. 4, 1978, pp. 155–164.
6. Y. Ueno, T. Yasugi, and Y. Ohgushi, "Optical Fibre Communication Systems Using Pulse-Interval Modulation," *NEC Res. Devel.*, Vol. 48, Jan. 1978, pp. 45–52.
7. Y. Ueno, T. Yasugi, and Y. Ohgushi: "Optical Fibre Communication Systems Using Pulse-Interval Modulation," In *Proceedings of the IEE First European Conference on Optical Fibre Communication*, 1975, pp. 156–158.
8. M. Sato, M. Murata, and T. Namakawa, "A New Optical Communication System Using the Pulse Interval and Width Modulation Code," *IEEE Trans. Cable Television*, Vol. CATV-4, No. 1, 1979, pp. 1–9.
9. I. Garrett, "Pulse-Position Modulation for Transmission Over Optical Fibre with Direct or Heterodyne Detection," *IEEE Trans. Commun.*, Vol. COM-31, No. 4, 1983, pp. 518–527.
10. N. M. Calvert, M. J. N. Sibley, and R. T. Unwin: "Experimental Optical Fibre Digital Pulse-Position Modulation System," *Electron. Lett.*, Vol. 24, No. 2, 1988, pp. 129–131.
11. J. D. Martin and H. H. Hausien, "PPM Versus PCM for Optical Local-Area Networks," *IEE Proc. Pt. I*, Vol. 139, No. 3, 1992, pp. 241–250.
12. J. M. H. Elmirghani and R. A. Cryan, "Implementation and Performance Considerations for a PPM Correlator-Synchroniser," In *IEEE International Symposium on Circuits and Systems London, 1994*, Vol. 3, No. 3, 1994, pp. 157–160.
13. J. M. H. Elmirghani and R. A. Cryan, "Analytic and Numeric Modelling of Optical Fibre PPM Slots and Frame Spectral Properties with Application to Timing Extraction," *IEE Proc. Commun.*, Vol. 141, No. 6, pp. 379–389.

Digital pulse interval and width modulation for optical fibre communications

Z. Ghassemlooy, R.U. Reyher, E.D. Kaluarachchi and A.J. Simmonds

Sheffield Hallam University, School of Engineering Information Technology,
Electronics & Communications Engineering Research Group,
Pond Street, Sheffield S1 1WB, UK

ABSTRACT

This paper investigates the implementation of a new digital pulse time modulation (PTM) technique based on digital pulse interval and width modulation (DPIWM) scheme. Original expressions are presented for power spectral density, code characterisation and channel capacity, illustrating the advantages of this technique compared with conventional pulse code modulation (PCM). Both theoretical and practical results are given showing close agreement.

Keywords: optical fibre communications, digital pulse time modulation, self synchronised code

1. INTRODUCTION

Fibre optic communication networks have the potential of providing wide-band telecommunication services that utilise multiplexes of video, audio and data channels. The choice of the modulation scheme on the optical carrier is therefore a major factor in realising a bandwidth efficient and high-performance system at an acceptable cost. In this context, PTM techniques offer simplicity and performance comparable to existing digital techniques and can be employed to trade signal-to-noise performance with bandwidth overhead (a particularly exploitable feature in fibre optic systems, in particular high-speed communication networks). Continuous PTM techniques have been widely used for transmission of video, data and audio signals over optical fibre[1-4].

In recent literature a discrete PTM scheme has been shown to be an effective modulation format for transmission of high bit data rate over monomode fibre. This modulation scheme utilises the pulse position modulation (PPM)[5-7] format where the time interval of M bits of PCM frame is divided into $n = 2^M$ time slots, plus a guard interval of a few time slot duration. The information is conveyed by positioning a single pulse in one of the n time slots, Fig. 1. It has reported that digital PPM can offer improvements of between 5-11 dB[8-9] (depending on the coding level, bandwidth and detection technique) in receiver sensitivity when compared to PCM. This corresponds to an increase in point-to-point transmission distance of between 25-55 km. However, DPPM timing requirements are exceptionally critical to the system performance and far exceed the equivalent PCM timing requirements[10]. This paper introduces

a new digital PTM scheme known as digital pulse interval and width modulation (also known as pulse interval and width modulated code) offering simplicity and ease of frame synchronisation. It is constructed as a combination of pulse width and pulse interval that have discrete time length forming a frame. The frame length, which is a sum of a pulse width and pulse interval, depends on the amplitude of the information signal. Original expressions are presented for code characterisation, channel capacity and power spectral density together with results obtained from hardware implementation of the DPIWM system.

2. THEORY

DPIWM is closely related to PIWM in that it employs a waveform in which both mark and space represent the sampled data[3], but with DPIWM this mark and space time slots are made discrete. DPIWM is an anisochronous PTM technique in which each successive frame length is different, see Fig. 1, being determined only by the sampled
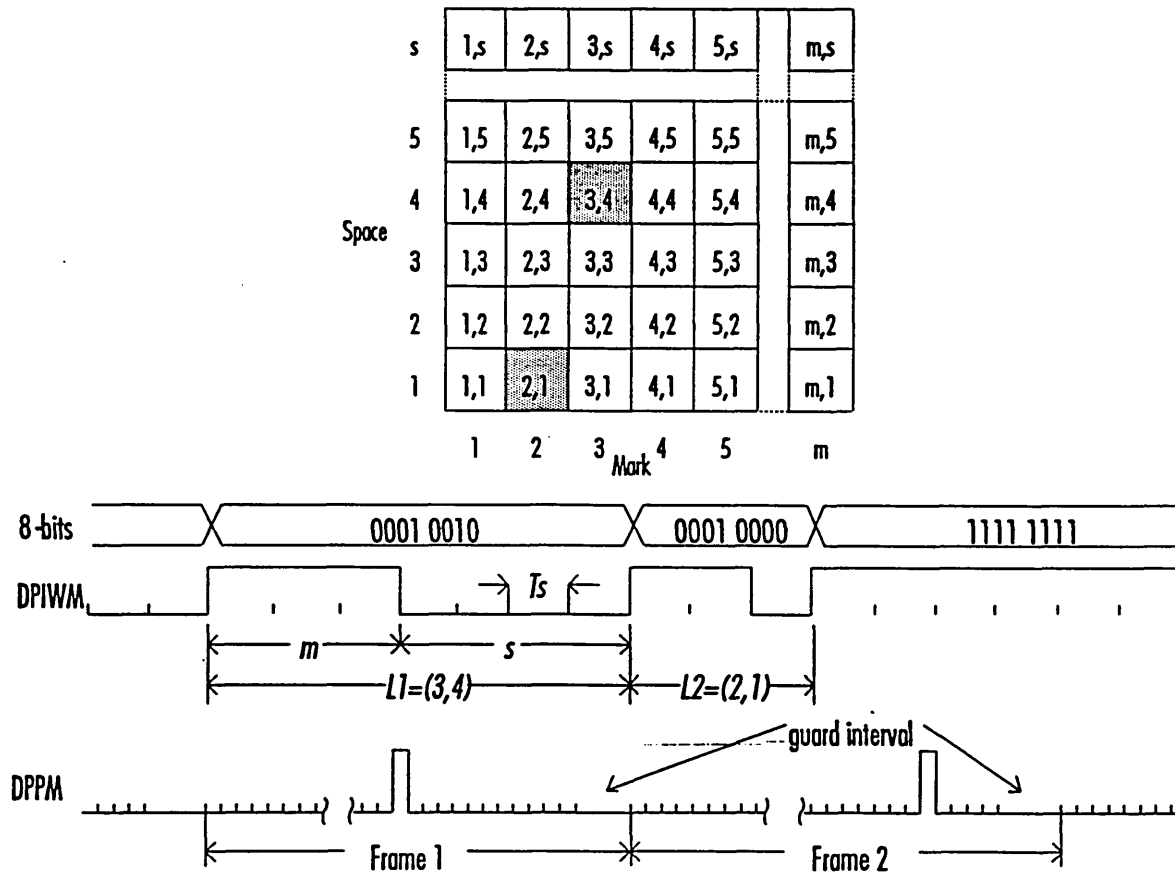

Figure 1 Example of a DPIWM wave train

156

value of the modulating signal not by the choice of the predetermined clock (sampling) period. As a consequence, receiver design problems are substantially reduced since there is no requirement to extract frame frequency and phase for synchronisation in order to correctly interpret the encoded sampled value. PIWM code has varying frame length. In this new scheme more combinations of pulse width and interval are possible than those of the other systems such as DPPM. This means that DPIWM has higher transmission capacity by fully utilising the time slots for a given frame and eliminating unused time slots. Frame synchronisation is simply achieved by detecting the rising edge of each frame, where each frame is initiated by a mark followed by space, see Fig. 1. Depending on source connection, the DPIWM code can carry encoded PCM data or directly sampled signals.

M bits digital data (PCM data or converted analogue signal) is split into two sets of k bits (k is chosen to be equal to half the M bits), where the decimal equivalent of the binary combination in a given set determines the number of time slots for mark (m) and space (s) in a given frame. To represent zero, one time slot is added to each k set. At time $t = 0$ conversion first takes place for mark followed by conversion for space. Finally, time slots for mark and space are combined together to produce the desired digital PIWM signal, Fig. 2. At the demodulator after threshold detection the number of time slots for mark and space is counted and their corresponding equivalent binary numbers are generated and added together to reproduce an M bit binary data. Digital to analogue converter followed by a low pass filter recovers the information signal, Fig. 2.

DPIWM modulator and demodulator designs may be formulated around analogue to digital (ADC) and digital to analogue (DAC) converters and state machine structures.
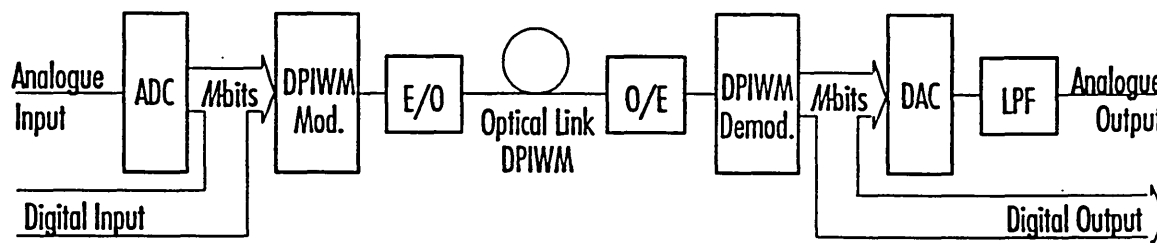

Figure 2 DPIWM system block diagram

157

2.1. Code properties

DPIWM (or PIWM code) frame length, $L = m + s$, may be given as:

$$L = \left[\text{Mod}\left(\frac{x}{2^k}\right) + 1 \right] + \left[\text{Rem}\left(\frac{x}{2^k}\right) + 1 \right]$$

(1)

where x is the decimal equivalent of an M bit binary data and $k = M/2$ bits. The longest and shortest DPIWM frame lengths are 2^{k+1} and 2 time slots T_s respectively, resulting in an average frame length of $2^k + 1$ time slots. The maximum total time occupied by a DPIWM frame is $T_f = 2^{k+1} T_s$ seconds. The expression for time slot duration in DPIWM and PCM in terms sampling frequency f_s can be written as:

$$T_{PIWM} = \frac{1}{2^{k+1} f_s} \quad \text{and} \quad T_{PCM} = \frac{1}{M f_s}$$

(2)

DPIWM displays shorter time slot duration compared to PCM (and wider time slot duration compared to digital PPM and digital pulse interval modulation) and hence higher channel bandwidth requirement. Owing to its anisochronous nature resulting in different frame lengths, the instantaneous frame rate of DPIWM signal changes according to the amplitude of the input signal. DPIWM also display a higher transmission capacity compared to PCM and DPPM by virtue of its anisochronous nature as the frame length is variable. For a modulating signal of bandwidth f_m Hertz sampled at the minimum Nyquist rate the transmission capacity for PCM and DPIWM are:

$$C_T = \frac{Maximum\ code\ length}{Average\ code\ length} 2 f_m Log_2 \ (Possible\ number\ of\ valid\ codes)$$

Thus:

$$C_{PCM} = 2 f_m M$$

(3.a)

and

$$C_{DPIWM} = \frac{2^{\frac{M}{2}+1}}{2^{\frac{M}{2}} + 1} 2 f_m M$$

(3.b)

For large values of M the transmission capacity of DPIWM is twice that of the PCM, see Fig. 3. This is as expected, since on average a DPIWM frame will be only half the length of a PCM frame, enabling twice the sampling frequency rate to be employed and thus permitting a signal of two times the bandwidth to be adequately sampled.

In DPPM a guard interval, a few time slots long, is included at the end of each frame to cater for pulse dispersion and hence to avoid interframe interference. However, in DPIWM this guard interval is redundant, since each frame is started with a mark followed by a space, see Fig. 1.
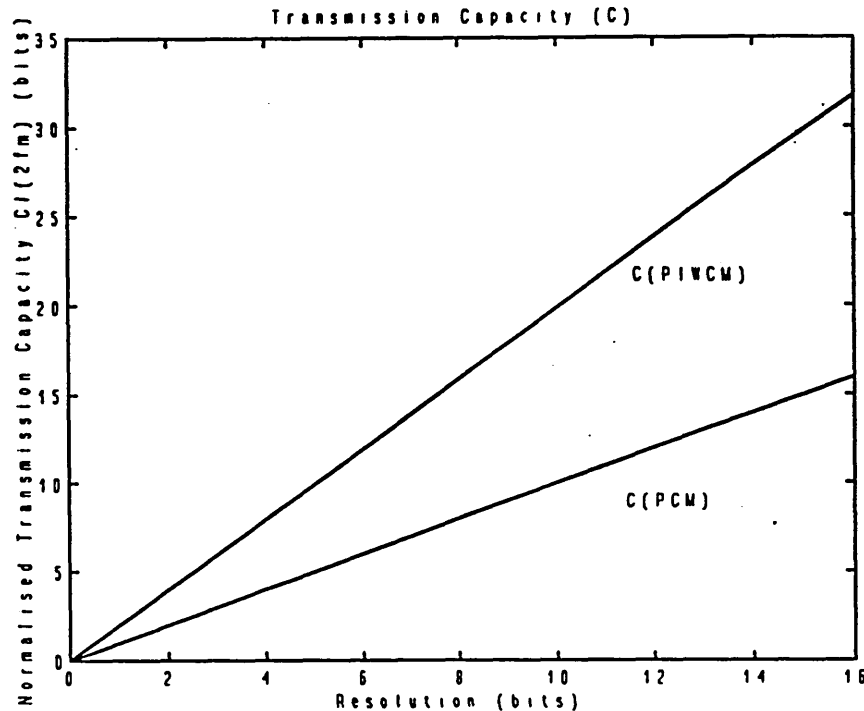

Figure 3 Resolution vs. transmission capacity

2.2. Power spectral density

Mathematically, a DPIWM wave train consisting of frame of different lengths and mark-space patterns could be represented as:

$$x(t) = \sum_{i=-\infty}^{\infty} P_{(m,s)_i}\left[t - T_s\left(\sum_{a=0}^{i-1}(m_a + s_a) \right) \right] \tag{4}$$

where $P_{(m,s)_i}$ represents the i-th DPIWM sample with m_i time-slots of mark and s_i time-slots of space and m_a and s_a are the number of time-slots for mark and space at the a-th sample respectively and T_s is the slot duration. The equation indicates that DPIWM does not display a fixed periodic frame structure in the manner of PCM and DPPM, except in the absence of any incoming data where the result is an alternating mark and space pattern.

To be able to characterise the process practically it is beneficial to evaluate the power spectral density of a truncated realisation. Following a process similar to that obtained in Reference 10, we have obtained a numeric spectral model for DPIWM given by:

$$S(f) = \frac{1}{T_s \sum\limits_{i=0}^{N}(m_i + s_i)} \left| \sum_{i=0}^{N} G_{(m,s)_i}(f) e^{-j2\pi f T_s \sum\limits_{a=0}^{i-1}(m_a + s_a)} \right|^2 \tag{5}$$

where: $G_{(m,s)_i}(f)$ = is the DPIWM pulse transform of the i-th sample, m_i, and s_i are the number of time slots for mark and space in the i-th sample respectively (random numbers 1, 2 ...2^k for M bit resolution) and N gives the length of the truncated data frame sequence.

3. RESULTS

A typical digital PIWM spectrum evaluated using Equation (5) for random data taken over 4000 frames evaluated at 320 frequency points for 8 bit resolution is shown in Fig. 4.a, with the frequency axis normalised to the slot frequency and power level over the frequency span to 0 dBm. To confirm our predicted results a practical model was developed for DPIWM system. The measured spectrum of the DPIWM waveform for slot rate and input frequency of 1 MHz and 1 kHz respectively is illustrated in Fig. 4.b showing close agreement with the predicted results. In both cases the DPIWM provides distinctive spectral components at the slot frequency and its harmonics. As can be seen from Fig. 4 the power spectral distribution is mainly concentrated at frequencies lower than the slot rate, decaying rapidly at frequencies above the slot rate indicating that DPIWM signal may be transmitted over a channel having bandwidth less than the slot rate.

In order to quantify the detected baseband signal-to-noise ratio (SNR) performance of the DPIWM system, simulation of the complete system was carried out for a single tone input signal of 5 kHz bandwidth, average sampling frequency of 15 kHz and with additive white Gaussian noise introduced at the channel, see Fig. 5. Simulation result obtained for 10000 time slots clearly indicate that the DPIWM exhibits a noise threshold, as in accordance with all PTM schemes beyond which signal pulses become indistinguishable from the noise pulses. At the threshold for carrier-to-noise ratio of 14.2 dB the baseband SNR is at 44 dB clearly showing the inherent improvement that such a system has.

Finally, Fig. 6 illustrates low distortion behaviour in the time domain by comparing input and output signals.
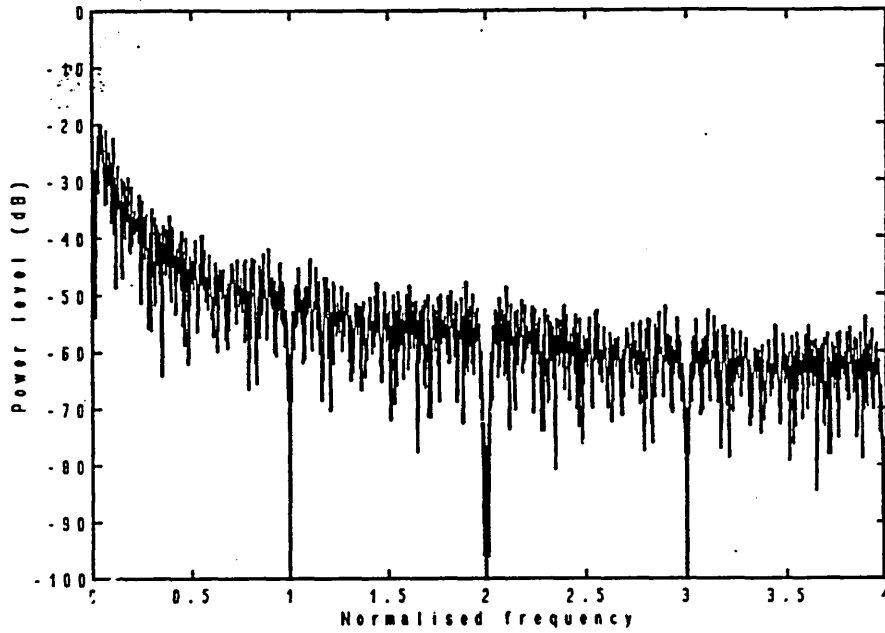
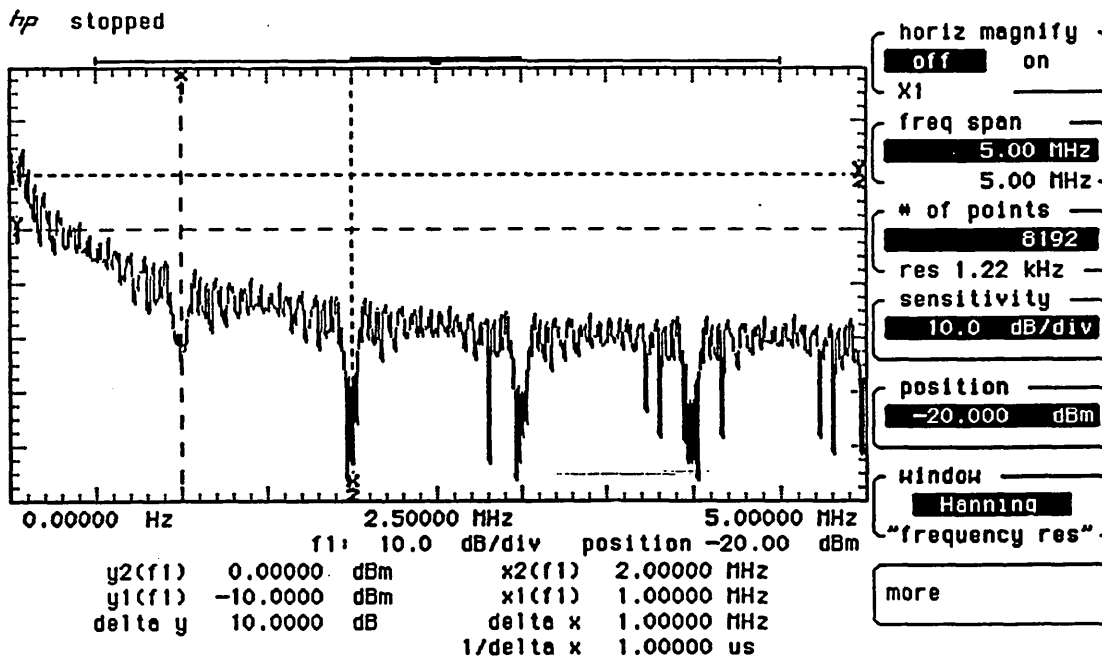**Figure 4. a** Predicted DPIWM power spectral density with $M = 8$

hp stopped

horiz magnify
off   on
X1

freq span
5.00 MHz
5.00 MHz

# of points
8192
res 1.22 kHz

sensitivity
10.0 dB/div

position
-20.000   dBm

window
Hanning
"frequency res"

more

0.00000 Hz   2.50000 MHz   5.00000 MHz
f1: 10.0 dB/div position -20.00 dBm

y2(f1)	0.00000 dBm	x2(f1)	2.00000 MHz
y1(f1)	-10.0000 dBm	x1(f1)	1.00000 MHz
delta y	10.0000 dB	delta x	1.00000 MHz
		1/delta x	1.00000 us

Figure 4. b Measured PSD for DPIWM with clock frequency of 1 MHz

161
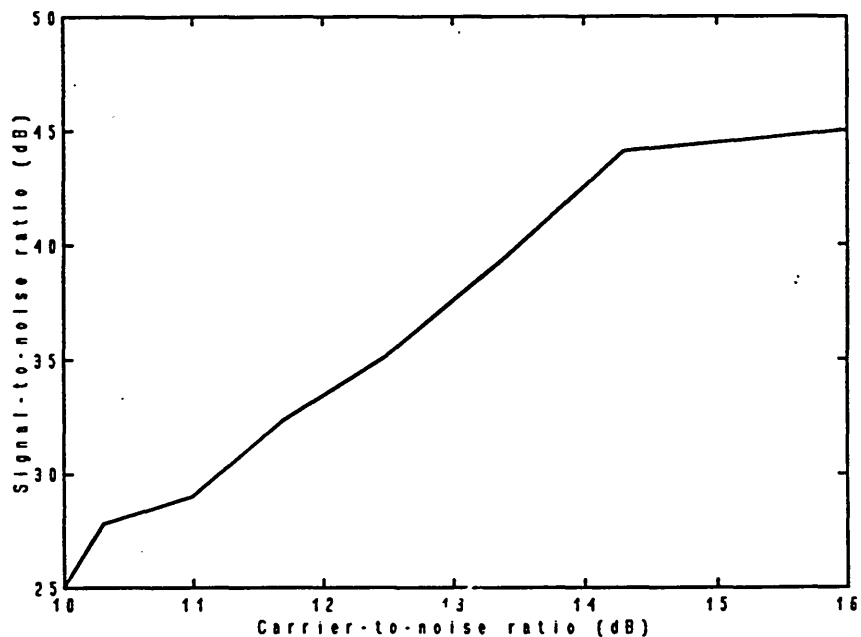
Figure 5 Noise performance of the DPIWM system

hp stopped

```
1   400  mV/div
pos:    0.000  V
10.00:1   1MΩ dc


2   400  mV/div
pos:    3.000  V
10.00:1   1MΩ dc
```

-990.00 us   10.00 us   1.01000 ms
                      200 us/div   realtime Trigger Mode:
Vp-p   (1) 1.17500 V   Vp-p   (2) 1.20000 V   Edge
frequency   (1) 1.01659kHz   frequency   (2) 1.04307kHz

1   ⌐ 50.00 mV
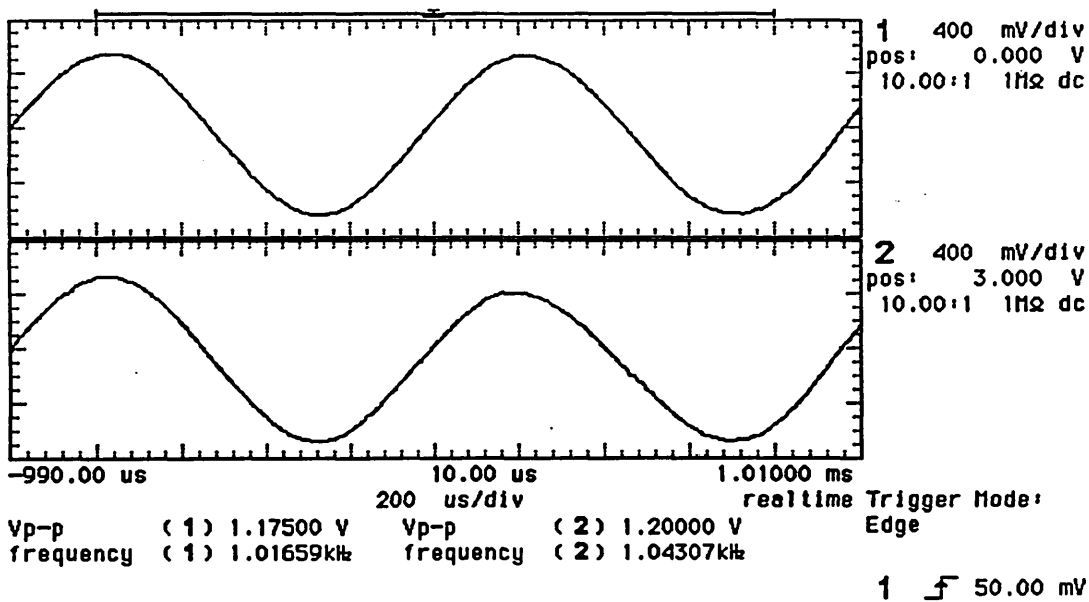
Figure 6 System response to 1 KHz sine wave signal at transmitter input (upper trace)
and receiver output (lower trace)

162

4. CONCLUSIONS

In this paper a new digital PTM scheme knows as DPIWM has been presented. It is shown to have a much higher transmission capacity and requires no complex frame synchronisation in the receiver in contrast to PCM and DPPM. These advantages have been obtained at the expense of increased transmission bandwidth. Original expressions have been presented to characterise the scheme in the frequency and time domains, showing excellent agreement with results obtained from a practical system. The baseband SNR performance obtained from simulation shows characteristic distinctive to all PTM schemes. The signal format appears to be, at this time, an attractive possibility for medium to high speed point-to-point optical communication links.

ACKNOWLEDGEMENTS

REFERENCES

1. M. Sato, et al,: 'A New Optical Communication System Using the Pulse Interval and Width Modulation Code', IEEE Trans. Cable TV, CATV-4, 1979 pp. 1-10.
2. B. Wilson and Z. Ghassemlooy : 'Pulse Time Modulation Techniques for Optical Communications: a Review', IEE Proceedings J, 140, DEC. 1993, pp. 346-357.
3. B. Wilson, Z. Ghassemlooy and Cheung J C S: ' Optical Pulse Interval and Width Modulation Systems', IEE Proceedings J, 39, 1992, pp. 376-382.
4. D. J. T. Heatley,: 'Video Transmission in Optical Local Area Network using Pulse Time Modulation', 9th European Conference on Optical Communications, Geneva, 1983, pp. 343-345.
5. I. Garrett, : 'Digital PPM over Dispersive Optical Fibre Channels', International Workshop on Digital Communications', Tirrenia, Italy, Aug. 1983, pp. 15-19.
6. J. T. O. Pires, et al.: 'Digital PPM over Optical Fibers with Avalanched Photodiodes Receivers', IEE Proc. J. Optoelectronic, 133, 1986, pp. 309-313.
7. M. N. Calvert, et al,: 'Experimental Optical Fibre Digital Pulse Position Modulation System', Electronic Lett., 24, 1988, pp. 129-131.
8. I. Garrett,: 'Pulse Position Modulation for Transmission over Optical Fibers with Direct or Heterodyne Detection ', IEEE Trans. on Commun., COM-31, 1983, pp. 518-527.
9. R. A. Cryan, et al.: 'Optical Fibre Digital Pulse-Position-Modulation Assuming a Gaussian Received Pulse Shape', IEE Proc. J, 137, 1990, pp. 89-96.
10. J. M. H. Elmirghani, and R. A. Cryan,: 'Analytical and numeric modelling of optical fibre PPM slots and frame spectral properties with application to timing extraction', IEE. Proce.-Comms, 141, 1994, pp. 379-389.